LEABHARLANN CHOLÁISTE NA TRÍONÓIDE, BAILE ÁTHA CLIATH | TRINITY COLLEGE LIBRARY DUBLIN
Ollscoil Átha Cliath | The University of Dublin

Terms and Conditions of Use of Digitised Theses from Trinity College Library Dublin

Copyright statement

All material supplied by Trinity College Library is protected by copyright (under the Copyright and Related Rights Act, 2000 as amended) and other relevant Intellectual Property Rights. By accessing and using a Digitised Thesis from Trinity College Library you acknowledge that all Intellectual Property Rights in any Works supplied are the sole and exclusive property of the copyright and/or other IPR holder. Specific copyright holders may not be explicitly identified. Use of materials from other sources within a thesis should not be construed as a claim over them.

A non-exclusive, non-transferable licence is hereby granted to those using or reproducing, in whole or in part, the material for valid purposes, providing the copyright owners are acknowledged using the normal conventions. Where specific permission to use material is required, this is identified and such permission must be sought from the copyright holder or agency cited.

Liability statement

By using a Digitised Thesis, I accept that Trinity College Dublin bears no legal responsibility for the accuracy, legality or comprehensiveness of materials contained within the thesis, and that Trinity College Dublin accepts no liability for indirect, consequential, or incidental, damages or losses arising from use of the thesis for whatever reason. Information located in a thesis may be subject to specific use constraints, details of which may not be explicitly described. It is the responsibility of potential and actual users to be aware of such constraints and to abide by them. By making use of material from a digitised thesis, you accept these copyright and disclaimer provisions. Where it is brought to the attention of Trinity College Library that there may be a breach of copyright or other restraint, it is the policy to withdraw or take down access to a thesis while the issue is being resolved.

Access Agreement

By using a Digitised Thesis from Trinity College Library you are bound by the following Terms & Conditions. Please read them carefully.

I have read and I understand the following statement: All material supplied via a Digitised Thesis from Trinity College Library is protected by copyright and other intellectual property rights, and duplication or sale of all or part of any of a thesis is not permitted, except that material may be duplicated by you for your research use or for educational purposes in electronic or print form providing the copyright owners are acknowledged using the normal conventions. You must obtain permission for any other use. Electronic or print copies may not be offered, whether for sale or otherwise to anyone. This copy has been supplied on the understanding that it is copyright material and that no quotation from the thesis may be published without proper acknowledgement.

The role of activated RET in papillary tumour morphogenesis

A thesis submitted for the Degree of Doctor of Medicine

By

Dr. Richard Flavin
BMedSc, MB, PhD, FRCPath

Trinity College
University of Dublin

2011

Supervisor: Prof. Orla Sheils MA (Dub) MA Med Law and Ethics (Lond) PhD FAMLS FRCPath FTCD

Declaration

I declare that this thesis is my own work, and has not been submitted previously for an MD degree at this or any other university. I agree that the library may lend or copy this thesis on request.

Richard Flavin

Richard Flavin

TRINITY COLLEGE
2 6 JUL 2011
LIBRARY DUBLIN
THESIS
9230

To My Family

Contents

Chapter 2 MATERIALS AND METHODS

Chapter 3 RET/PTC REARRANGEMENT OCCURRING IN PRIMARY PERITONEAL CARCINOMA

Chapter 4 BRAF (T1799A) MUTATIONS ARE NOT A GENOTYPIC LINK IN THE PAPILLARY PHENOTYPE

Chapter 5 GENERAL DISCUSSION

Figures

Tables

Acknowledgements

It's been a long road since I first set out on this 'RET' journey and there are many people to thank! First and foremost I have to say a big heartfelt thanks to my mentor Prof. Sheils. She first took me under my wing when I was a molecular novice not knowing my DNAs from RNAs! Not only was she a mentor but she is also a friend with whom I've had many lunchtime and barstool chats on the merits of Munster (and the not so may merits of Leinster!), pucas, 'focussing', ethics and the more serious joys of histopathology! A big thank you Orla for everything and all the hours of help, laughter and encouragement.

So to my original lab bedfellows: Paul, Steve, Esther (and later Susanne and Amanda) well what can I say? Paul thank you first and foremost for all the countless hours of advice and help, not to mention the many zany 'Conference' nights abroad! Don't forget us mate. Steve you've worn many hats for me: a good friend, and colleague, a wise counsellor, a fellow lover of Planxty, Munster rugby, Cork hurling (with Frank McCarthy) but also a neighbour from the 'Collig township of Corcaigh! Doubt' ya boyo and go raibh mile maith agat do gach rud eigin. Is suil go bheimid cairde I bhfad nios mo bliana. Esther, Susanne and Amanda thank ye all so much for the advice and all the lunch time laughs. Esther thanks for letting us stay with you in the US and best of luck with the Final Med exams.

To the newer additions in the lab: Sinead, Karen, Jinghuan and Ciara (not forgetting our honorary lunchtime member Therese Murphy): lads its been a great and fun last few years- from the whacky nights out, to the trips abroad and not forgetting our lunchtime chats. A heartfelt thanks for your friendship and help. Good luck to all of ye in your careers and if ye ever decide to open up that lab on the beach make sure ye offer me a job! To all my friends in the Coombe Women's Hospital (Cara Martin, Mick Gallagher, Cynthia Heffron and old timers Richie Shattock, Niamh Murphy and Ivan 'Yo Flayvan' Silva) a big thank

you. I'll never forget that first Christmas party up in Wicklow! A special big hug and thanks to Martina Ring a friend and enormous help through the 'immuno' wilderness!

To all the lab and clinical staff in the histology department in the CPL a big thank you. Special thanks to Ronan Ward, Susan Russell, Eoin Gaffney and Sean O'Briain. To Prof. John O'Leary: from the first time I meet you, I have never been so amazed by your enthusiasm, knowledge and cerebration and especially your ability to think outside of the box. The infrastructure that you have laid our for the department is second to none and surely has firmly established the department as the leading academic pathology unit in these islands. As a friend and mentor I really appreciate all your advice and encouragement and a big heartfelt thanks for everything. To Horst Ziztzelsberger, Dr. Jackl and everyone at the Institute for Radiobiology in Munich also a big thank you.

And finally to my family. Philly and Johnny (my mum and dad), Caroline and Bryan thanks for all your help and encouragement down through the years. To my lovely wife, Maeve thank you so much pet for all your patience and support. Thank you for all the sacrifices that you've made for my career. I love you and Aaron and Luke (and soon the new baby!) very much.

List of Abbreviations

°C	Degrees centigrade
3D	3 Dimensional
ABC	avidin:biotinylated enzyme complex
ATP	Adenosine TriPhosphate
BM	Basement Membrane
BSA	Bovine Serum Albumin
CA.	Carcinoma
CCND1	Cyclin D1
CRD	Cysteine Rich Domain
Ct	Threshold cycle
C-terminal	Carboxy Terminal
Cy3	Cyanine 3
DAB	diaminobenzidene
DNA	Deoxyribonucleic acid
dNTP	Deoxynucleoside triphosphate
dUTP	Deoxyuracil Triphosphate
EC	Extracellular
ECM	Extracellular Matrix
EOC	Epithelial Ovarian Cancer
ERK	Extracellular Signal-Related Kinase
FA	Follicular Adenoma
FAM	6-carboxyfluorescein
FFPE	Formalin Fixed Parrafin Embedded
FIGO	The International Federation of Gynaecologists and Obstetricans
FISH	Flourescent in-situ Hybridization

FITC	Fluorescein isothiocyanate
FSH	Follicle Stimulating Hormone
FTC	Follicular thyroid carcinoma
FVPTC	Follicular variant papillary thyroid carcinoma
GAPDH	Glyceraldehyde-3-phosphate dehydrogenase
GDNF	Glial cell line-derived neurotrophic factor
GDP	Guanosine diphosphate
GNRH	Gonadotrophin Releasing Hormone
GOG	Gynaecological Oncology Group
Grb2	Growth factor receptor binding protein 2
GTP	Guanosine triphosphate
H&E	Haematoxylin and Eosin
IGFBP7	Insulin-like growth factor binding protein 7
IHC	Immunohistochemistry
IPC	Internal Positive Control
IPMN	Intra-Ductal Papillary Mucinous Neoplasia
JOE	6-carboxy-4,5-dichloro-2,7-dimethoxyfluorescein
KSR	Kinase Suppressor of RAS
LCM	Laser Capture Microdissection
LH	Luteinizing Hormone
MAPK	Mitogen activated protein kinase
MDCK	Madin-Darby Canine Kidney Cells
MEK1/2	MAPK/ERK kinase 1/2
MEN	Multiple Endocrine Neoplasia
MGB	Minor groove binder
MiRNA	Micro Ribonucleic acid

MITF	Microphthalmia-associated Transcription Factor
mRNA	Messsanger RNA
N/A	Not Applicable
ND	Not Detected
NEG	Negative
NFQ	non-fluorescent quencher
NIH	National Institute of Health
NTC	No Template control
N-terminal	Amino Terminal
PAKs	p21 Activated Kinases
PBS	Phosphate Buffered Saline
PCR	Polymerase Chain Reaction
PI3K	Phosphatidylinositol-3-kinase
POS	Positive
PP2A	Protein Phosphatase 2
PPC	Primary Peritoneal Carcinoma
PRCC	Papillary Renal Cell Carcinoma
PTC	Papillary thyroid Carcinoma
ret	Rearranged during Transfection
Rn	Normalised Reporter Signal
RNA	Ribonucleic acid
ROCK	Rho Kinase
RT	Reverse transcription
SBT	Serous Borderline Tumour
SE	Standard Error
shRNA	Short hairpin Ribonucleic acid

siRNA	Small interfering Ribonucleic acid
SNPs	Single Nucleotide Polymorphisms
SOS	Son of Sevenless
SP	Signal Peptide
SSCP	Single Strand Conformation Analysis
SV40	Simian virus 40
TAE	Tris Acetate EDTA Buffer
TAMARA	6-carboxy-N,N,N′,N′-tetramethylrhodamine
TBS	Tris Buffered Saline
TET	6-carboxy-4,7,2′,7′-tetrachlorofluorescein
TGF-β	Transforming Growth Factor- Beta
TK	Tyrosine Kinase
TM	Transmembrane Domain
TMA	Tissue MicroArray
TPA	Tissue Plasminogen Activator
TTF-1	Thyroid Transcription Factor-1
UNG	Uracil-DNA glycosylase
WHO	World Health Organisation
x	Mean
YAC	Yeast Artificial Clones
Δ	Delta

Publications

Array comparative genomic hybridisation analysis of gamma-irradiated human thyrocytes.
SP Finn, P Symth, E. O'Regan, S. Cahill, **R Flavin,** J O'Leary, O Sheils.
V Archiv 2004 Oct; 445(4):396-404.
PMID: 15258756

ret/PTC and BRAF act as distinct molecular, time-dependant triggers in a sporadic Irish cohort of papillary thyroid carcinomas.
P Symth, S Finn, S Cahill, E O'Regan, **R Flavin**, J O'Leary, O Sheils.
Int Journal of Surgical Pathology 2005 Jan; 13(1):1-8.
PMID: 15735849

Effect of ret/PTC 1 rearrangement on transcription and post-transcriptional regulation in a papillary thyroid carcinoma model.
S Cahill, P Smyth, SP Finn, K Denning, **R Flavin**, EM O'Regan, JH Li, A Potratz, SM Guenther, R Henfrey, J O'Leary, O Sheils.
Mol Cancer. 2006 Dec 11; 5(1):70.
PMID: 17156473

Low level genomic instability is a feature of Papillary Thyroid Carcinoma: An array CGH study of laser capture microdissected Papillary Thyroid Carcinoma tumours and clonal cell lines.
S Finn, P Smyth, S Cahill, E O'Regan, **R Flavin**, M Toner, C Timon, J O'Leary and O Sheils.
Arch Pathol Lab Med. 2007 Jan;131(1):65-73.
PMID: 17227125

Expression microarray analysis of papillary thyroid carcinoma and benign thyroid tissue: emphasis on the follicular variant and potential markers of malignancy.
S Finn, P Smyth, S Cahill, C Streck, E O'Regan, **R Flavin**, J Sherlock, D Howells, R Henfrey, M Cullen, M Toner, C Timon, J O'Leary and O Sheils.
Virchows Arch. 2007 Jan 25; 450(3):249-60.
PMID: 17252232

Effect of BRAFV600E mutation on transcription and post-transcriptional regulation in a papillary thyroid carcinoma model.

S Cahill, P Smyth, K Denning, **R Flavin**, J Li, A Potratz, SM Guenther, R Henfrey, JJ O'Leary and O Sheils.

Mol Cancer 2007 Mar 13; 6(1):21.

PMID: 17355635

BRAF T1799A mutation occurring in a case of malignant struma ovarii.

R Flavin, P Symth, S Finn, P Crotty, M Ring, S Cahill, EM O'Regan, JJ O'Leary, O Sheils.

Int J Surg Pathol. 2007 Apr; 15(2):116-20.

PMID: 17478764

A Molecular Expression Signature distinguishes Follicular Variant of PTC and Follicular Thyroid Carcinoma from Follicular Adenoma using Pre-Amp RT-PCR in archival samples.

K Denning, P Smyth, S Cahill, S Finn, Conlon E, JH Li, **R Flavin**, S Aherne, S Guenther, A Ferlinz, JJ O'Leary, O Shiels.

Modern Pathology 2007 Oct; 20(10):1095-102.

PMID: 17660800

ret/PTC-1 expression alters the immunoprofile of thyroid follicular cells.

K Denning, P Smyth, Cahill S, JH Li, **R Flavin**, S Aherne, JJ O'Leary, O Shiels.

Molecular Cancer 2008, 7:44.

PMID: 18505566

Geographical Mapping of a Multifocal Thyroid Tumour using Genetic Alteration Analysis and miRNA Profiling.

S Aherne, P Smyth, **R Flavin**, K Denning, JH Li, JJ O'Leary, O Sheils.

Mol Cancer 2008, 7:89.

PMID: 19055826

RET/PTC rearrangement occurring in primary peritoneal carcinoma.

R Flavin, G Jackl, S Finn, P Smyth, M Ring, K Unger, S Cahill, EM O'Regan, K Denning, E Gaffney, G Tallini, JJ O'Leary, H Zitzelsberger, O Sheils.

Int J Surg Path 2009 Jun; 17(3):187-97

PMID: 19147513

SUMMARY

RET/PTC rearrangements are initiating events in the development of a significant proportion of papillary thyroid carcinomas. Activated *RET/PTC* mutations are thought to be restricted to thyroid disease, but in this study we propose that these events maybe features of papillary morphology. 57 non-thyroid papillary tumours were examined for *RET/PTC* rearrangements using interphase FISH, Taqman™ RT-PCR and immunohistochemistry. 20% (3/15) of primary peritoneal carcinoma had detectable *RET/PTC*1 rearrangements by all three methodologies. A further case of similar histotype had an alternate *RET/PTC* rearrangement. No *RET/PTC*1 rearrangements were detected in the remaining tumour cohort. Our results indicate that *RET/PTC* rearrangements occur in a small subset of non-thyroid papillary tumours. These rearrangements may not be directly implicated in tumour growth; rather representing 'passenger' mutations reflecting *RET* instability in secondary tumour subclones.

The Ras/Raf/MEK/ERK signalling pathway has been implicated in a variety of human neoplasms, with BRAF mutations having been detected in tumours such as melanoma, low grade serous papillary carcinomas of the ovary and papillary carcinoma of the thyroid (PTC). A missense mutation of thymine to adenine at nucleotide position 1799, results in a valine to glutamic acid change at codon 600 (V600E), which can be found in approximately 80% of BRAF mutations. This BRAF mutation is highly prevalent in PTC's with a papillary or mixed papillary-follicular growth pattern. We investigated the hypothesis that BRAFV600E mutations might be expressed in non-thyroid papillary tumours.

57 non-thyroid papillary tumours (15 primary peritoneal carcinoma, 10 serous carcinoma of the ovary (including 2 borderline tumours), 10 papillary renal cell carcinoma, 10 urothelial cell carcinoma, 5 serous carcinoma of the endometrium, and 7 carcinomas with mixed phenotypes) were analyzed for expression of mutated BRAF T1799A by Taqman™ SNP detection. All 57 tumours were homozygous for wild type BRAF. BRAF V600E mutations are restricted to certain subgroups of papillary tumours (PTC, low grade serous carcinoma of the ovary) and do not serve as a molecular link between tumours with a papillary phenotype.

In conclusion, we demonstrate for the first time, ret rearrangements in papillary tumours from outside the thyroid thereby breaking traditional dogma. These rearrangements may be indirectly implicating in the morphogenesis of the papillary phenotype through interactions with the E-cadherin complex and the actin-myosin cytoskeleton.

Chapter 1

General Introduction

1.1 Introduction

This thesis is a study of ret/PTC and BRAF expression in a cohort of papillary tumours of urogenital tract origin. To date ret rearrangements have been synonymous with papillary thyroid carcinoma however in this thesis we propose that they may have a role in papillary tumour morphogenesis.

1.2 The History of Histology

In 1665, Robert Hooke (1635-1703), an English microscopist, when examining a piece of cork with a rudimentary microscope, saw an abundance of empty small compartments which he called "cells". Hooke derived the designation from the Latin, cellula; i.e., small compartment, having in mind a comparison with a honeycomb. (Espinasse, 1962) Almost two hundred years later a definition of cell was achieved; according to Max Schultze (1861): Cell is a small mass of nucleated protoplasm.

The first description of the nucleus (from the Latin, nucleus = almond) was carried out by Leeuwenhoek in 1700. (Ford, 1991) The first description of the nuclear envelope was made by Jan Evangelista Purkinje (1787-1869), a Czech biologist, in 1830. Robert Brown (1773-1858), a Scottish botanist, introduced the term nucleus in microscopy after the examination, in 1831, of epidermal cell of some orchids and some Asclepiadacea. (Brown, 1827) Wolff (1759), Brisseau-Mirbel (1802), Oken (1805) and Lamarck (1809) seemed to have recognized that the cellular organization is a characteristic of all living beings they studied; however, Matthias Schleiden (1804-1881), a German botanist, in 1838, had the merit of understanding the true importance of

the cells. He saw, under the microscope, thousands of plant specimens, and inferred that all the vegetables are made of cells. By extension, similar studies carried out on animals, by Theodor Schwann (1810-1882), a German zoologist and physiologist, came to the conclusion that all the then known living beings were composed of cells. Thus, the dogma called the ***cell theory*** became established. According to it, the living beings may grow and reproduce themselves because, in fact, the cells may in turn multiply. In addition, it assumed that it is only possible to form new cells from other pre-existing ones.

Rudolf Virchow (1821-1902), a German pathologist, embellished the theory, when he demonstrated that pathological injuries also had a cellular structure; thus, he is considered to be the pioneer of cellular pathology. Virchow saw that all the cells of the pathological tissues derived from healthy ones and that all living cells originated from pre-existing ones. This discovery was known as the ***Law of Virchow (or Fundamental Law of Biology).*** Indeed, Virchow edified the bases of modern Pathology, being the author of the famous fundamental aphorism: Omnis cellula e cellula ; that is, each cell comes from another cell. Marie François Bichat, a French pathologist (1771-1802), described the 21 textures. A texture was a "tissue" (i.e., a body component) as perceived by its macroscopic physical properties. Owing to the importance of his works, Bichat is considered, by some authors, to be the founder of Animal Histology. Marcello Malpighi (1628-1694), an Italian anatomist, is in fact considered the true "Father of Histology". His textures were described based on dissections, and in the subsequent analyses of the macroscopic physical characteristics of the different structures that form the human organism. By using a rudminetary microscope Malpighi described a series of microscopic structures never seen until then e.g. capillaries.

17 years after the death of Bichat, A. Mayer created the term Histology. The term histos meant originally any woven material. In 1844, it was recommended for large usage by Sir Richard Owen (1804-1892), an English palaeontologist. Rudolph von Kölliker (1817-1905), a Swiss professor of Anatomy — published in 1852, Handbuch der Gewebelehre (i.e., The book for teaching tissues), so some authors considered him the true founder of Histology.

1.3 Embryology of the Urogenital system

The development of the renal and genital systems are closely related. The paired primitive kidney (mesonephros) develops from the intermediate mesoderm on either side of the gut tube (Figure 1.1) The mesonephros is connected to a specialized midline region of the caudal gut (cloaca) via the metamerically patterened mesonephric (Wolffian) ducts. The caudal end of the ureteric bud induces the surrounding mesenchyme to form the mature kidney (metanephros). The primitive gonad develops at the rostral end of the mesonephric duct at the level of the stomach.

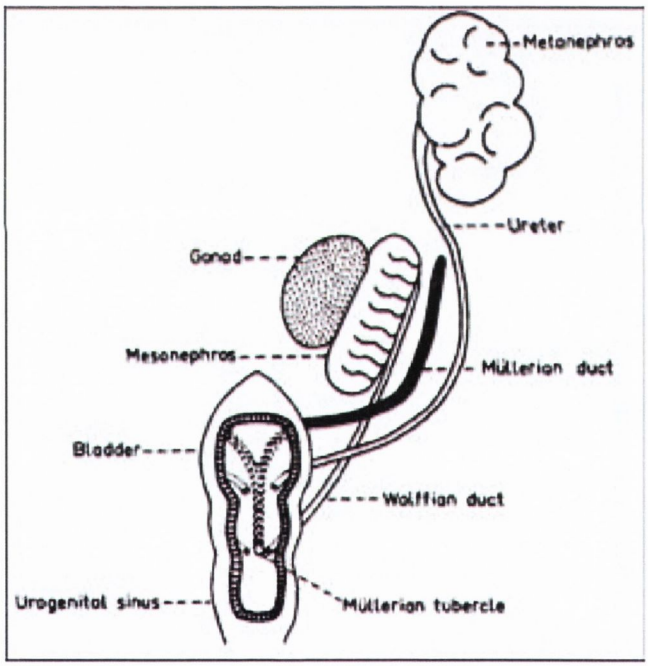

Figure 1.1: The developing urogenital system.

Subsequently, a paired duct system, the paramesonephric (Mullerian) duct forms parallel to the mesonephric duct. In male embryos the primitive gonad develops into the testis and the mesonephric duct forms the vas deferens; the paramesonephric duct regresses. In females, the primitive gonad becomes the ovary, the mesonephric duct regresses and the paramesonephric ducts form the fallopian tubes, uterus and upper vagina. The mesonephros regresses in both cases. The cloaca separates dorsally to form the rectum and ventrally to form the bladder, urethra and lower part of the vagina. (Drife J, 2004)

1.4 Anatomy, histology and function of the urogenital system

The kidneys are solid, bean shaped organs lying high on the posterior abdominal wall beneath the peritoneum. The concave aspect of the kidney (hilum) faces towards the midline. This is the site of where the ureters emerge and where the main renal artery and vein supply the kidney. The kidney is divided into an outer cortex and an inner medulla (Figure 1.2) The cortex forms the columns of Bertin which lie underneath the individual units of the medulla. The medulla is conical in shape with the tip or papillae protruding into the urine collecting system (calyceal system). Each kidney bears 10-18 medullary pyramids. The functional unit of the kidney parenchyma is called the nephron which has two components the glomerulus and the tubular system. The glomerulus is in the initial site of blood filtration and the tubules are sites of salt and water homeostasis.

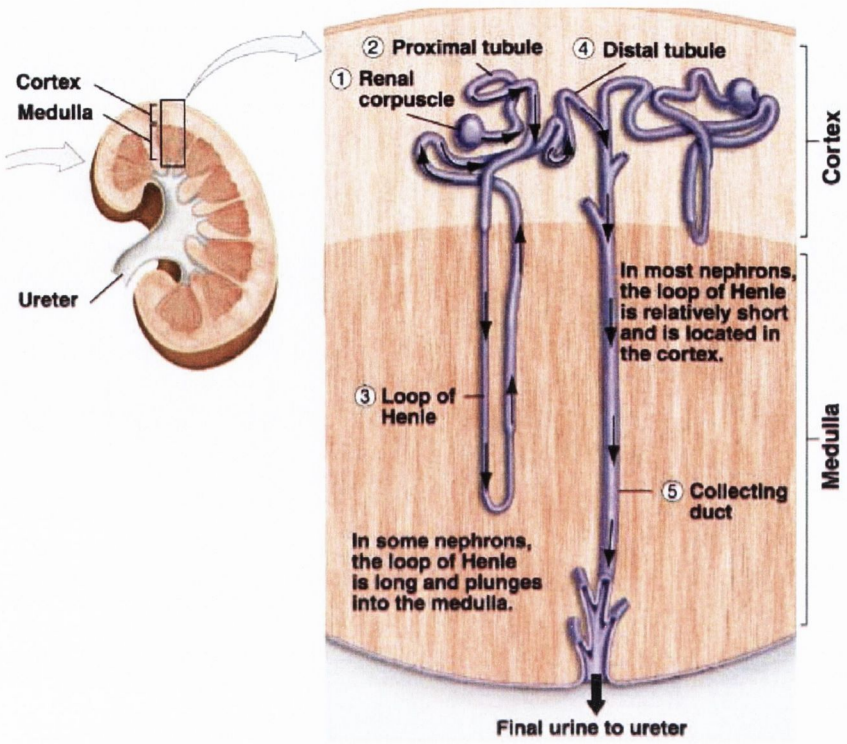

Figure 1.2 Schematic diagram of normal gross and microscopic appearance of the kidney (Adapted from http://www.uic.edu).

The pelvicaclyceal system are hollow muscular tubes lined by a specialized mutilayered epithelium called urothelium. This epithelium is resistant to damage by the osmolarity of urine and by the concentration of toxic substances within it (Figure 1.3) The smooth muscle in the walls of the tubes are capable of pushing fluid towards the bladder by a process known as peristalsis. The bladder acts as a reservoir and a pump and has the same basic structure as the pelvicalyceal system. The kidney is essential for fluid, electrolyte and acid-base balance and also secretes erythropoietin and renin hormones. The lower urinary tract including the bladder serve as a series of conduits and reservoirs for the storage and excretion of urine.

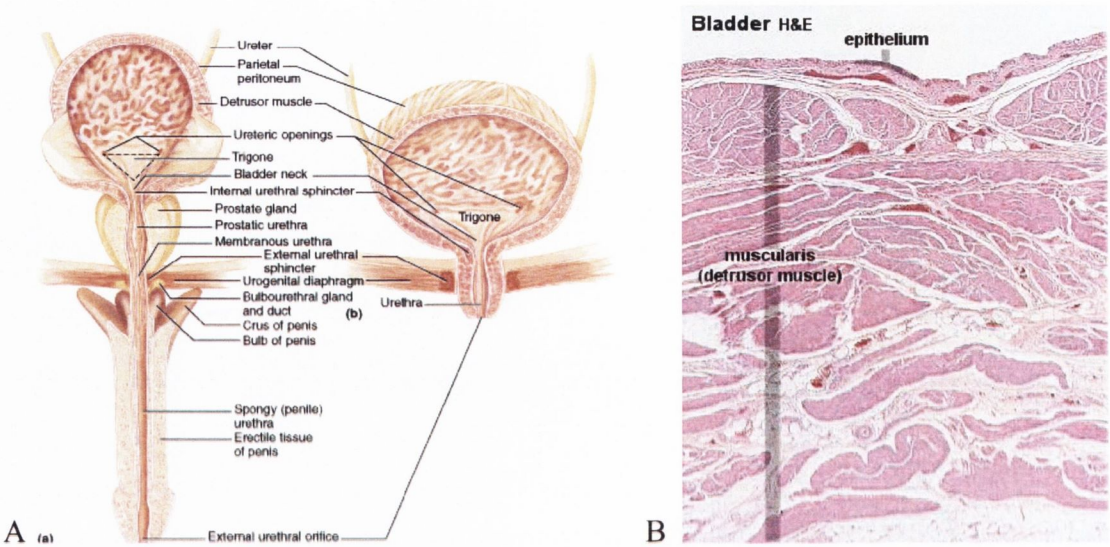

Figure 1.3 Schematic diagram of normal gross lower urinary tract anatomy (A) and histology (B) (Adapted from http://www.**legacy.owensboro.kctcs.edu)**

The ovaries are paired almond-shaped bodies weighing 3-5g each and measuring approximately 3x2x1cm in the adult. They normally become larger in pregnancy and involute after the menopause. After puberty the ovarian surface becomes irregular in contour in the course of maturation and rupture of the ovarian follicles. The ovary usually lies against the lateral wall of the pelvis in a depression called the ovarian fossa. The position of the ovary however is extremely variable and is often hanging down in the recto-uterine pouch (pouch of Douglas). During pregnancy the enlarging uterus pulls the ovary up into the abdominal cavity. After parturition, when the broad ligament is lax, the ovary takes up a variable position in the pelvis.

The hilum of the ovary is attached to the broad ligament by loose fibromuscular mesovarium. The muscular ovarian ligament attaches the medial pole of the ovary to the uterine cornu below and behind the fallopian tube. The lateral pole of the ovary is attached to the pelvic wall by the suspensory ligament, a peritoneal fold containing the principal vascular and lymphatic supply of the ovary. The arterial supply of the ovary is the ovarian artery, which arises from the aorta at the level of the first lumbar vertebra. The ovarian vein drains into the inferior vena cava on the right side and into the left renal vein on the left. The lymph vessels of the ovary follow the ovarian artery and drain into the para-aortic nodes. The nerve supply to the ovary is derived from the aortic plexus and accompanies the ovarian artery.

The ovaries are surrounded by a thin fibrous capsule, the tunica albuginea (Figure 1.4). This capsule is covered externally by a single layer of cuboidal cells called the germinal epithelium, a modified area of peritoneum. The body of the ovary consists of spindle-shaped cells, fine collagen fibres and ground substance which together constitute the ovarian stroma. The stromal cells are mainly fibroblasts but also include bundles of smooth muscle cells. In the peripheral zone of the stroma, known as the cortex, are numerous follicles which contain female gametes at various stages of development (undeveloped follicles are known as primordial follicles). In addition, there may be post-ovulatory follicles of various kinds namely corporea lutea (responsible for oestrogen and progesterone production), degenerate former corpora lutea (corpora albicantes) and degenerate (atretic) follicles. The central zone of the ovarian stroma, the medulla, is highly vascular being supplied by the ovarian artery and ovarian branches of the uterine artery.

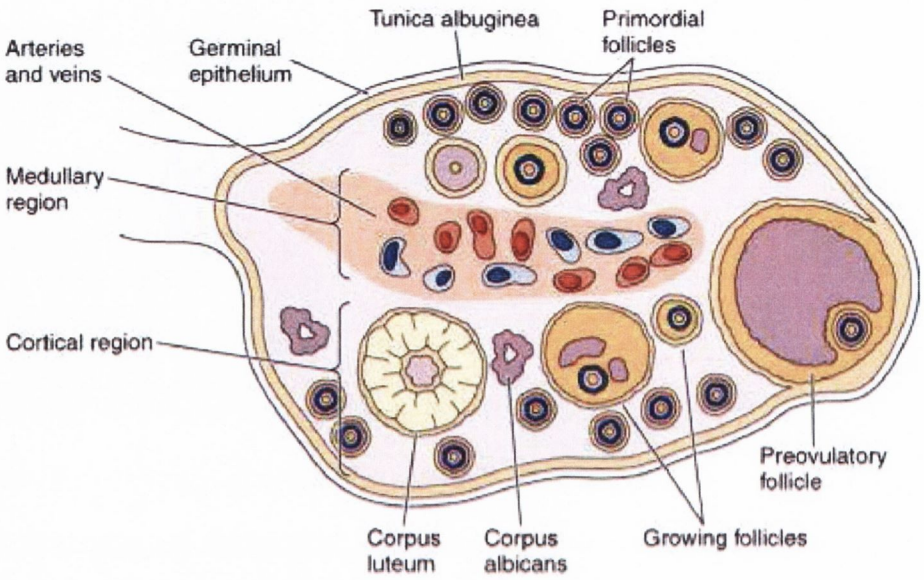

Figure 1.4 Schematic diagram of normal ovarian histology (Carneiro).

The ovary has two major functions: the release of mature ova at the time of ovulation and the secretion of steroid hormones. These are controlled by the cyclical release of pituitary follicle-stimulating hormone (FSH) and luteinizing hormone (LH). These hormones are in turn regulated by gonadotrophin-releasing hormone (GnRH), which the hypothalamus secretes into the pituitary portal circulation (Figure 1.5). The ovarian steroid hormones stimulate growth of the reproductive organs, foster development of the secondary sexual characteristics and help maintain the implanted blastocyst. The production of these hormones depends on the development and ripening of the follicles and the formation of the corpus luteum.

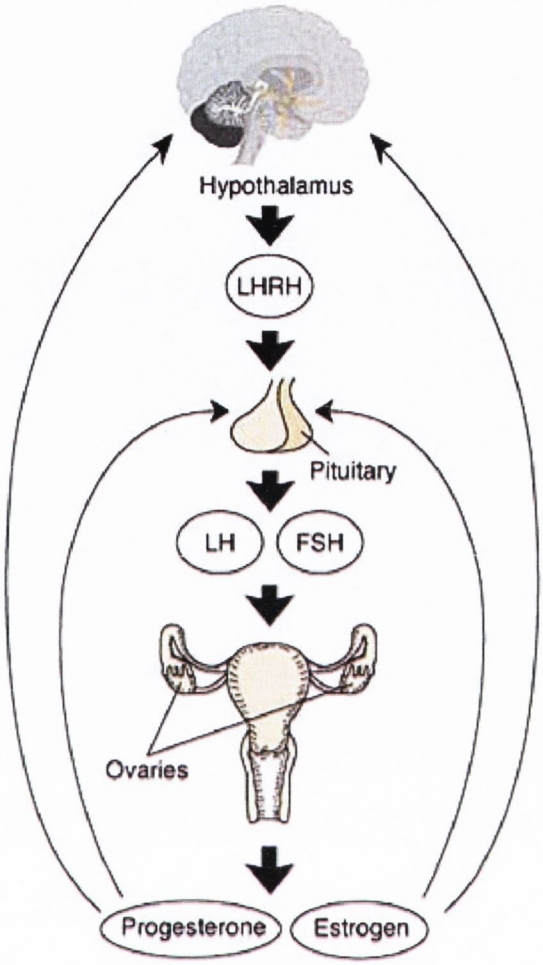

Figure 1.5: Regulation of ovarian hormonal production by cyclical release of GnRH, FSH and LH (http://embryology.med.usw.edu).

1.5 Papillary neoplasms of the urogenital tract

1.5.1 Papillary renal cell carcinoma

These tumours make up approximately 10-15% of all renal cell carcinomas. Males are more commonly affected than females in the ratio of 2:1. The peak age of presentation is between 50 – 55 years of age. The mortality rate is approximately 16% at 10 years from diagnosis. (Lager et al., 1995; Mancilla-Jimenez et al., 1976; Renshaw and Corless, 1995) These tumours are associated with trisomy and tetrasomy of chromosomes 7 and 17, with loss of chromosome Y in males.

Grossly, these tumours tend to be large, tan and friable with a surrounding rim of fibrous tissue. There may be associated areas of haemorrhage, necrosis and calcifications. The architecture is predominately papillary or tubulopapillary. Papillae have delicate fibrovascular cores lined by a single layer of epithelial cells. Some papillae may have central oedma or collections of foamy macrophages (Figure 1.6). Psammoma bodies may be present. Delahunt and Elbe divide them into two categories: type I and II. Type I PRCC is the more common and consists of small cells with inconspicuous cytoplasm, small round nuclei with inconspicuous nucleoli. (Delahunt and Eble, 1997) Type II PRCC consists of cells with more voluminous eosinophilic cytoplasm, pseudostratified nuclei and prominent nucleoli.

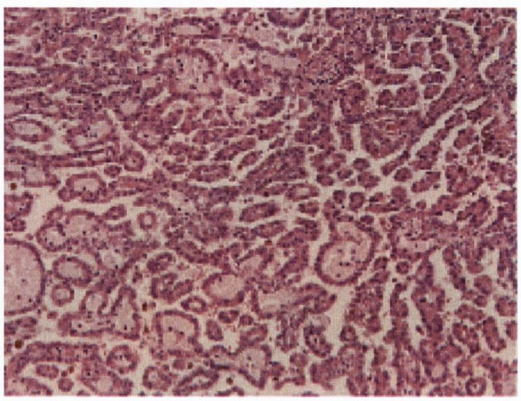

Figure 1.6 Microscopic image of a papillary renal cell carcinoma exhibiting the typical papillary morphology and central oedematous cores (H&E x20).

1.5.2 Papillary urothelial cell carcinoma

This tumour is typically seen in patients over 50 years of age, being three times as more common in males than females. Patients tend to present with haematuria and less frequently dysuria. 50% of patients with upper urinary tract tumours have had a previous history of urothelial cell tumours of the ureters or bladder. Tumours of the pelvicalyceal system are twice as common as tumours of the ureters. Non-invasive papillary urothelial carcinoma accounts for up to 25% of all papillary urothelial tumours of the bladder. Papillary urothelial carcinoma typically appears as small papillary excresences or a larger 'cauliflower-like' mass (Figure 1.7). These tumour are soft and friable, white-tan. Multiple tumours are often present. They typically have tall branching papillae which are covered with more than seven layers of urothelium, the cells of which may appear bland to highly atypical. The cores of the papillae are usually slender and vascular.

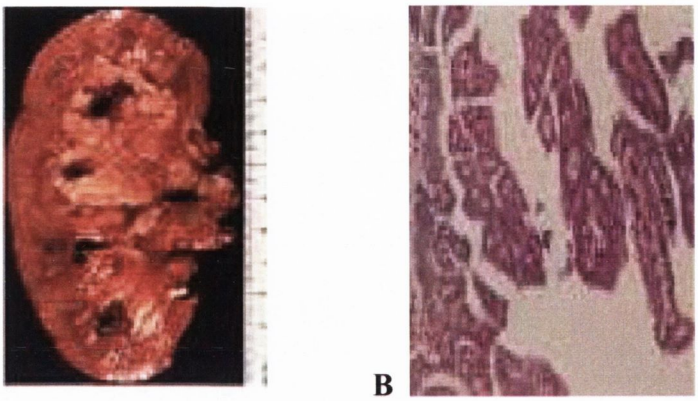

Figure 1.7 A, Gross image of pelvicalyceal urothelial cell carcinoma exhibiting a white friable tumour with papillary excrescences (Rosai). B, Microscopic image exhibiting the typical broad papillae lined by urothelium (H&E x10).

1.5.3 Ovarian serous papillary tumours

This is the most common form of ovarian cancer, accounting for 85% to 95% of all ovarian cancers. Histologically cells resemble the lining of the fallopian tube. They tend to be high grade and are the cancers most often seen in *BRCA* mutation carriers. They can be classified into benign, borderline and malignant subtypes.

Benign serous tumours account for approximately 16% of all ovarian epithelial neoplasms (Figure 1.8). The majority of benign serous tumours arise in adults in the 4^{th} -6^{th} decades although they may occur in patients younger than twenty or older than eighty. These tumours arise preferentially in the cortex of the ovary or on its surface (8%). They are usually bilateral especially in older women.

Often the tumours are metachronous with intervals that range from three to fourteen years. Similar tumours in extraovarian sites occasionally accompany benign serous tumours. Usually the tumour is asymptomatic and discovered incidentally during ultrasound examination. These tumours usually measure 1-10cm in diameter but can occasionally reach 30cm. They are typically unilocular or multilocular cystic lesions, the external surface is smooth and the inner surface may contain small papillary projections. The cyst contents are watery and very rarely opague or bloody. Adenofibromas and cystadenofibromas are composed of an admixture of solid and cystic areas. Surface papillomas appear as warty excrescences on the surface of the ovary. These tumours are typically lined by ciliated and less frequently non-ciliated secretory cells similar to the fallopian tube lining (Figure 1.8)

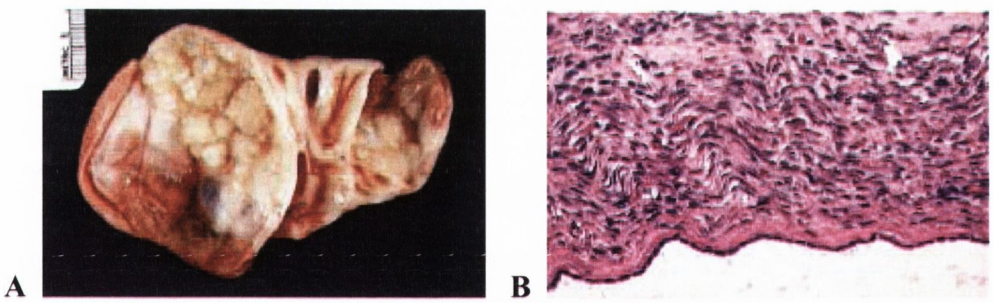

Figure 1.8: Benign serous cystadenoma. A, Gross image of a benign serous tumour with a cystic cut surface exhibiting papillary excrescences. B, Microscopic image exhibiting the typical flattened non-ciliated lining (H&E x10) (Rosai).

Serous borderline tumours (SBT) are ovarian tumours of low malignant potential exhibiting an atypical epithelial proliferation of serous type cells greater than that seen in their benign counterparts but without destructive stromal invasion. Patients with SBT are approximately 10-15 years younger than those with serous carcinoma (i.e. 45 years v 60 years). About 30-50% are bilateral. The tumour is often asymptomatic but may rarely present with abdominal enlargement or pain due to rupture of a cystic tumour or torsion. This tumour is also associated with a high rate of infertility. Macroscopically, the tumour may be cystic with a variable number of excrescences, form a solid purely surface papillary growth or have a combination of these features. In contrast to carcinomas they lack necrosis and haemorrhage. The cysts usually contain serous fluid.

The histopathological hallmarks that distinguish SBT from a benign cystadenoma are the presence of epithelial hyperplasia forming papillae, micropapillae associated with "floating" cell clusters and mild-moderate atypia. It is distinguished from serous carcinoma by lack of destructive stromal invasion (an uncommon SBT with microinvasion occurs in 10-15% of SBT where individual cells or clusters of neoplastic cells exhibit early stromal invasion in one or more foci not exceeding $10mm^2$). The tumour cells vary from small cells with hyperchromatic nuclei to larger cells displaying eosinophilic cytoplasm with variable and generally low mitotic activity. Psammoma bodies may be present. SBT are divided into two types: ***typical and micropapillary*** types. The typical make up the vast majority (90%) of SBT and have a classic branching papillary pattern and epithelial tufts overlying papillae.

The micropapillary type accounts for a small proportion (5-10%) of tumours (Figure 1.9). The micropapillae are elongated thin micropapillae with little or no stromal support and have a non-hierarchical branching pattern creating a "Medusa head-like" pattern. Less common patterns are solid and cribriform proliferations. A continuous 5mm growth of these patterns is required for a diagnosis of micropapillary SBT. Up to 30% of SBTs are associated with tumour on the outer surface of the ovary and two-thirds are associated with peritoneal implants. (Burks et al., 1996; Segal and Hart, 1992) Pelvic and para-aortic lymph nodes are involved by SBT in up to 20% of cases, a finding which appears to be without clinical significance.

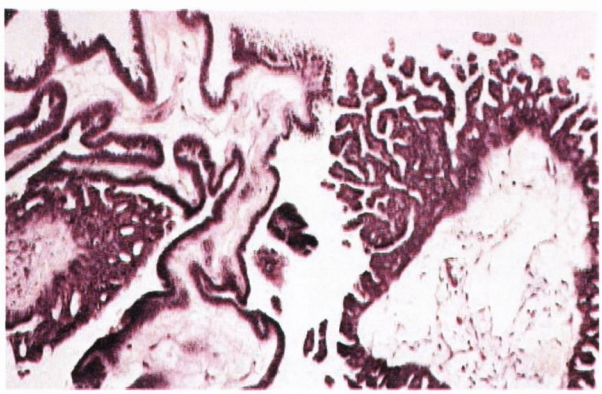

Figure 1.9: Microscopic image of a micropapillary SBT exhibiting the characteristic 'Medusa head-like' branching pattern (H&E x10; Rosai).

Stage I SBTs do not progress and have an indolent clinical course with a 5 year survival rate of up to 99%. (Kurman and Trimble, 1993) In stage III SBTs, i.e. distributed throughout the abdominal cavity with peritoneal implants, the 5-year survival ranges between 55-75%.

Micropapillary SBTs have a higher frequency of bilaterality, increased risk of recurrence among higher stage lesions, more frequent ovarian surface involvement and probable higher frequency of advanced stage at presentation than typical SBT. (Burks et al., 1996; Slomovitz et al., 2002) No difference in survival has been reported between typical and micropapillary SBT, (Eichhorn et al., 1999) even though micropapillary SBT is characterized by its lack of response to platinum-based chemotherapy. (Bell et al., 2001)

Malignant serous tumours are invasive ovarian epithelial neoplasms composed of cells ranging in appearance from those resembling fallopian tube epithelium in well differentiated tumours to anaplastic epithelial cells with severe nuclear atypia in poorly differentiated tumours. These tumours range in size from a few mm to tumors over 20cm in diameter and are bilateral in two-thirds of cases but only bilateral in one-third of stage I cases. Well differentiated tumours are solid and cystic with soft papillae within the cystic spaces or on the surface (Figure 1.10). Rare tumours are confined to the ovarian surface. Poorly differentiated tumours are solid, friable, multinodular masses with necrosis and haemorrhage. The architecture of the tumour varies from glandular to papillary to solid. The glands are typically slit-like or irregular. The papillae are usually irregularly branching and highly cellular. In poorly differentiated tumours solid areas are extensive and composed of poorly differentiated cells in sheets with small papillary clusters separated by myxoid or hyaline stroma. Psammoma bodies (rounded calcifications) may be present. The stroma may e scanty or desmoplastic. Serous carcinomas may contain other cell types as a minor component (<10%) that may cause diagnostic problems but do not influence outcome. Serous psammocarcinoma is a rare variant characterized by massive psammoma body formation and low grade cytology.

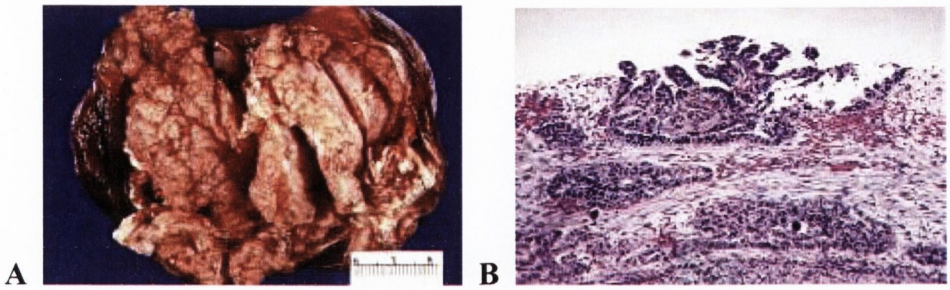

Figure 1.10: Serous carcinoma of the ovary: A, Gross image highlighting the solid nature of the tumour. Soft friable papillae are also seen. B, Microscopic image highlighting serous tumour invading underlying ovarian stroma (H&E x 20; Rosai).

All malignant tumours are graded from 1-3 (well-poorly differentiated) using either the WHO or Silverberg grading systems. These tumours are thought to arise via two pathways. In one pathway, conventional serous carcinoma arises de novo as a high grade neoplasm, displaying p53 mutations but no KRAS mutations. In the other pathway a serous borderline tumour progresses in a step-wise fashion through a non-invasive micropapillary stage before becoming invasive or through microinvasion in a typical serous borderline tumour. These low-grade tumours typically display mutations in KRAS and BRAF. Although, the majority of high-grade and low-grade carcinomas develop independently in rare cases, a high-grade serous carcinoma may arise from an atypical proliferative serous (borderline) tumor. (Dehari et al., 2007)

Women with germline BRCA-1 mutations typically develop serous carcinomas of the ovary, fallopian tube or peritoneum. The overall 5 year survival is 40%; however most of those alive at 5 years are alive with disease. Up to 85% of patients present with widespread metastatic disease, with survival in this group at 10-20%. Patients with disease confined to the ovary or pelvis have a 5 year survival of 80%.

1.5.4 Primary Peritoneal Carcinoma

Primary epithelial tumours that resemble malignant surface-epithelial stromal tumours of ovarian origin are termed primary peritoneal carcinoma. Primary peritoneal carcinoma (PPC) occurs almost exclusively in women with a median age of 62 years. The lifetime risk is estimated to be 1 case per 500 women, since approximately 15% of "typical" epithelial ovarian cancers are actually PPCs. (Schorge et al., 2000b; Schorge et al., 1998)

Histological and immunohistochemical examination of PPC is virtually indistinguishable from epithelial ovarian carcinoma (Figure 1.11). The most common histological variant is serous adenocarcinoma, but clear cell, mucinous, transitional cell and squamous cell carcinoma have all been reported. Rare cases of psammocarcinoma have also been described. (Gilks et al., 1990) The following are the criteria required for a diagnosis of PPC: 1) Both ovaries must be normal in size or enlarged by a benign process, 2) The involvement in the extraovarian sites must be greater than the involvement on the surface of either ovary, 3) The ovarian tumour involvement must be either non-existent, confined to the ovarian surface epithelium without stromal invasion or involving the cortical stroma with tumour size less than 5x5mm. (Schorge et al., 2000b) (GOG).

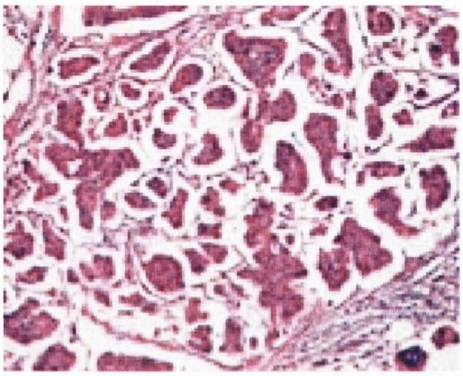

Figure 1.11 Microscopic image highlighting primary peritoneal serous carcinoma (H&E x 20).

PPC is believed to develop de novo from the peritoneal lining of the pelvis and abdomen, (Schorge et al., 2000b) although similar to epithelial ovarian cancer (EOC) the distal fallopian tube has emerged as a potential origin for this malignancy. PPC may develop in women years after having a bilateral oophorectomy. (Piver et al., 1993) PPC exhibits a distinct pattern of allelic loss compared to EOC. (Bandera et al., 1998; Cass et al., 2001; Huang et al., 2000) Overexpression of p53, EGFR, ERBB2, ERBB3, and ERBB4 genes has been reported in addition to loss of normal WT-1 expression. (Schorge et al., 2000a; Schorge et al., 2000b) p53 mutations commonly occur in PPC, but KRAS mutations are infrequent. (Schorge et al., 2000b) Germline BRCA-1 mutations occur in PPC with a frequency comparable to the BRCA-1 mutation rate in ovarian cancer. The staging, treatment and prognosis are similar to those of epithelial ovarian cancer.

1.5.5 Serous adenocarcinoma of the endometrium

This is a primary adenocarcinoma of the endometrium characterized by a complex pattern of papillae with cellular budding and not infrequently containing psammoma bodies. There is no known associated with exogenous or endogenous hyperestrogenism, and it is not associated with endometrial hyperplasia unlike endometrioid adenocarcinoma.

Serous adenocarcinoma is characterized by a papillary architecture with broad fibrovascular cores, secondary or even tertiary papillary processes and prominent sloughing of cells (Figure 1.12) There may be solid nests, foci of necrosis and a complex branching architecture. Nuclei are typically rounded, apically located and have macronucleoli. Mitoses, often atypical , are common. This tumour is considered high grade by definition. Serous endometrial intraepithelial carcinoma is believed to be a precursor lesion to the invasive tumour and typically arise in a background of atrophic endometrium. Deep myometrial and lymphatic invasion is common as is extrauterine spread, and as such recurrence is common and the overall prognosis is poor.

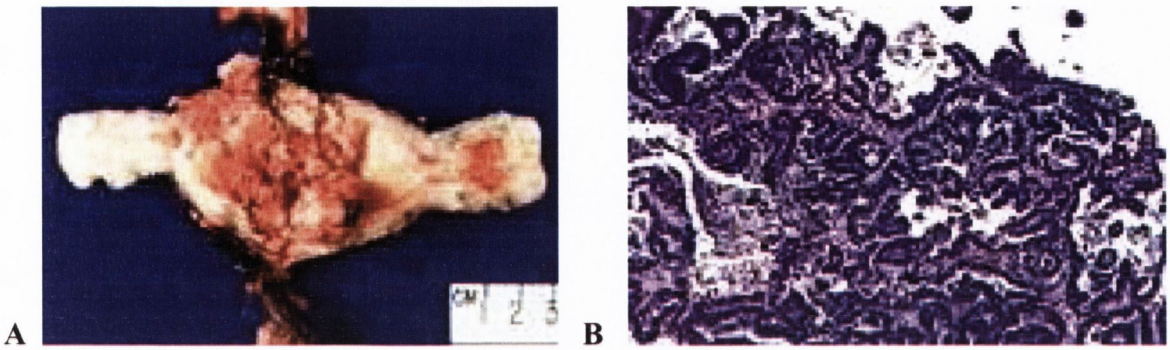

Figure 1.12 Serous carcinoma of the endometrium A, Gross image with white friable tumour exhibiting papillary excrescences. B, Microscopic image exhibiting the typical papillary pattern (H&E x10; Rosai).

1.6 Epidemiology of urogenital tract malignancy

Renal cell carcinoma is almost exclusively a disease of adults. Its incidence increases up until the 6th decade. Approximately 28000 new cases are diagnosed yearly in the US alone. (Motzer et al., 1996) Kidney and renal pelvis cancer accounted for 1.4% of all cancers in Ireland between the years 1995-2004 (Figure 1.13). (www.ncri.ie) 3743 cases were diagnosed during this tine period. The cumulative risk varied from 0.5% for females to 1.0% for males. Up to 25% of patients have metastastes at presentation and as such the overall 5 year survival is about 45%.

Bladder cancer tends to be more commen in men than in women with a ratio of 3:1. About 80% of patients are aged between 50 and 80 years. More than 50 000 cases of bladder cancer are detected annually with the death toll approximately 10 000 annually. (Landis et al., 1998) Bladder cancer accounted for 2.1% of all cancers in Ireland between the years 1995-2004 (Figure 1.13). (www.ncri.ie) 5596 cases were diagnosed during this time period. The cumulative risk varied from 0.5% for females to 1.5% for males. Prognosis is grade and stage dependant with 98% 10-year survival with grade I lesions and 40% 10-year survival with grade III or higher lesions.

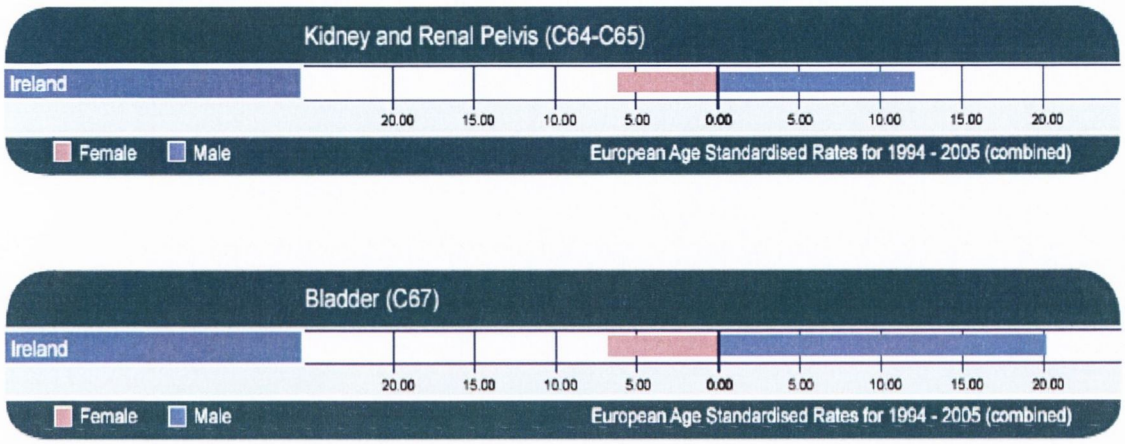

Figure 1.13 European Age-standardised Rate for kidney, renal pelvis and bladder cancer in Ireland (1994-2005). (www.ncri.ie)

Endometrial carcinoma is the most common invasive cancer of the female genital tract and accounts for 7% of all invasive cancers in women. 34 000 cases are diagnosed annually in the US. It tends to be exclusively a disease of post/peri-menopausal women and is uncommon in women under 40 years of age. (Brinton et al., 1992) Corpus uteri cancer accounted for 1.1% of all cancers in Ireland from the years 1994-2005 (Figure 1.14). (www.ncri.ie) 2915 cases were diagnosed during this period. The cumulative risk was 1.2% for females. The overall prognosis is stage dependant with 90% survival with stage I disease with less than 20% survival rates in stage III or more.

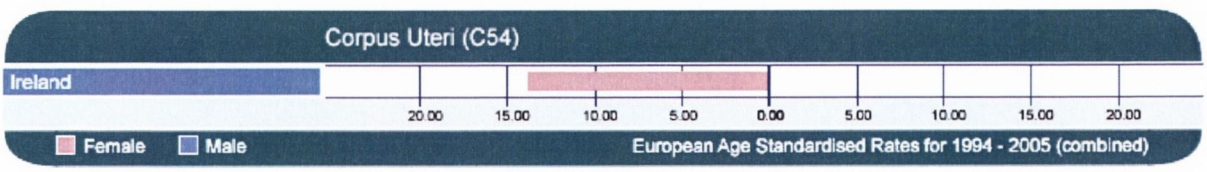

Figure 1.14 European Age-standardised Rate for corpus uteri cancer in Ireland (1994-2005). (www.ncri.ie)

Ovarian cancer is one of the most common cancers in women and the leading cause of death from gynaecological malignancy in the western world. (WJ, 1998) Cancer of the ovary represents about 30% of all cancers of the female genital organs. About 205000 cases of ovarian cancer are diagnosed worldwide each year. (Ferlay J, 2001) It accounts for 3% of female cancers in Ireland with approximately 350 new cases diagnosed each year (Figure 1.15) (www.ncri.ie) Ovarian cancer often presents at an advanced stage and at an advanced age, and despite improvements in drug therapy, overall survival is poor. (Christine and Holscheider, 2000) In the US, more women die from ovarian cancer than from all other gynaecological malignancies combined. (Greenlee RT, 2001)

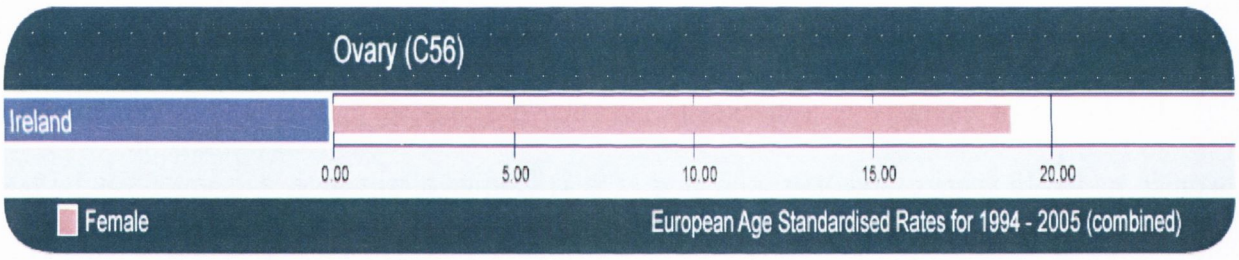

Figure 1.15 European Age-standardised Rate for ovarian cancer in Ireland (1994-2005). (www.ncri.ie)

1.7 Aetiology of urogenital tract malignancy

1.7.1 Urothelial carcinoma

Urothelial cell carcinoma of the urinary tract is associated with cigarette smoking and exposure to aniline dyes. Phenacetin abuse is associated with upper urinary tract lesions, as is Balkan nephropathy and exposure to thorium-containing radiologic contrast material. (Christensen et al., 1983; McLaughlin et al., 1983; Palvio et al., 1987) Industrial exposure to aryl ammines, Schistosoma haematobium infection, long term use of analgesics and cyclophosphamide increase the risk of bladder cancer.

1.7.2 Renal cell carcinoma

Cigarette smoking is the most prominent risk factor. Other risk factors include obesity, hypertension, unopposed oestrogen therapy, exposure to asbestos, petroleum products and heavy metals. (Savage, 1996) There is an increases incidence in patients with chronic renal failure, acquired cystic disease and tuberous sclerosis. Hereditary papillary renal cell carcinoma in its autosomal dominant form is manifested by bilateral tumours and mutations in the Met proto-oncogene on chromosome 7 (receptor for HGF).

1.7.3 Endometrial carcinoma

Carcinoma of the endometrium is seen with a higher frequency in women who are obese, diabetic, hypertensive and are infertile (women tend to be nulliparous with a history of menstrual irregularities). (Brinton et al., 1992) Women with serous carcinoma of the endometrium less commonly exhibit the stigmata of hyperoestrogenism.

1.7.4 Ovarian carcinoma

Nulliparity and a positive family history are two of the major risk factors for ovarian cancer. Mutations in BRCA-1 and BRCA-2 increase the susceptibility to ovarian cancer. Additional variables associated with ovarian cancer with various degrees of correlation include the use of talc, tobacco smoke, radiation exposure, psychotropic medication and high level of physical activity. (Harlow et al., 1998) No statistically significant relations exist for consumption of specific dairy foods, galactose, caffeine or vitamin D. (Koralek et al., 2006) There is emerging evidence that the Western lifestyle in particular obesity is associated with an increased risk. (Calle et al., 2003) Oral contraceptive pill use is associated with reduced risk.

1.8 Molecular Pathology of Carcinogenesis

Carcinogenesis results from the subversion of the processes that control the normal growth, location and mortality of cells. This loss of normal control mechanisms arises from the acquisition of mutations in three broad categories of genes:

1. Proto-oncogenes, the normal products of which are components of signalling pathways that regulate proliferation and which, in their mutated form, become dominant oncogenes.
2. Tumour suppressor genes, which generally exhibit recessive behaviour, the loss of function of which in cancer leads to deregulated control of cell cycle progression, cellular adhesion, etc.
3. DNA repair enzymes, mutations in which promote genetic instability.

Tumours are thought to develop as a result of the sequential (multi-step) accumulation of alterations in the genes involved in the control of cell proliferation, differentiation or death. Therefore, a sequence of somatic mutational events leads to the clonal expansion of genetically modified cells that progressively show a selective growth advantage over normal non-transformed cells and acquire an invasive and metastatic potential, thus resulting in malignant transformation of cells and tumour progression. The incidence of human cancers suggests that typically six to seven events are required over a span of twenty to forty years to induce tumour growth. (Petro, 1997)

1.8.1 RET

The RET oncogene was identified by Takahashi and colleagues in 1985 who reported a novel gene rearrangement with transforming activity in NIH 3T3 cells transfected with human lymphoma DNA. (Takahashi et al., 1985) The name RET stems from "*re*arranged during *t*ransfection". The human RET gene lies on the chromosome band 10q11.2 and comprises 21 exons. RET encodes a transmembrane receptor tyrosine kinase (TK) with a cadherin-related motif and a cysteine-rich domain that binds TGFβ-related neurotrophic factors, including the glial cell line derived neurotrophic factor (GNDF) family. Binding of the ligand causes receptor dimerization, autophosphorylation of tyrosine residues within the intracellular domain, and activation of the signalling cascade.

RET protein is composed of three domains; an extracellular ligand-binding domain with four cadherin-like repeats and a cysteine-rich region, a hydrophobic transmembrane domain, and a cytoplasmic portion with the TK domain split by an insertion of 27 amino acids (Figure 1.16). (Arighi et al., 2005) Three isoforms of RET are generated by alternative 3' splicing. The long, intermediate and short RET isoforms, which differ by 51, 43 and 9 amino acids in the C terminus, are referred to as RET51, RET43 and RET9 respectively. RET is normally expressed in cells of neural crest origin such as neural and ganglion cells. Tumours of neural crest origin such as neuroblastoma, phaeochromocytoma and medullary thyroid carcinoma also express RET. It is clear that RET plays a significant role during embryogenesis, particularly with development of the neural and excretory systems. In 1996, glial cell line-derived neurotrophic factor (GDNF) was identified as a long sought after RET ligand by several groups. (Durbec et al., 1996; Jing et al., 1996; Treanor et al., 1996; Trupp et al., 1996)

Mutations (both germline and somatic) in the RET proto-oncogene are associated with several diseases including multiple endocrine neoplasia, types IIA and IIB (MEN2A and MEN2B), Hirschsprung disease, and medullary thyroid carcinoma. Like most receptor tyrosine kinases, RET has the ability to activate a variety of signalling pathways, including RAS/RAF/MEK/ERK, phosphatidylinositol 3-kinase (PI3K)/AKT, p38 MAPK and c-Jun N-terminal kinase (JNK) pathways.

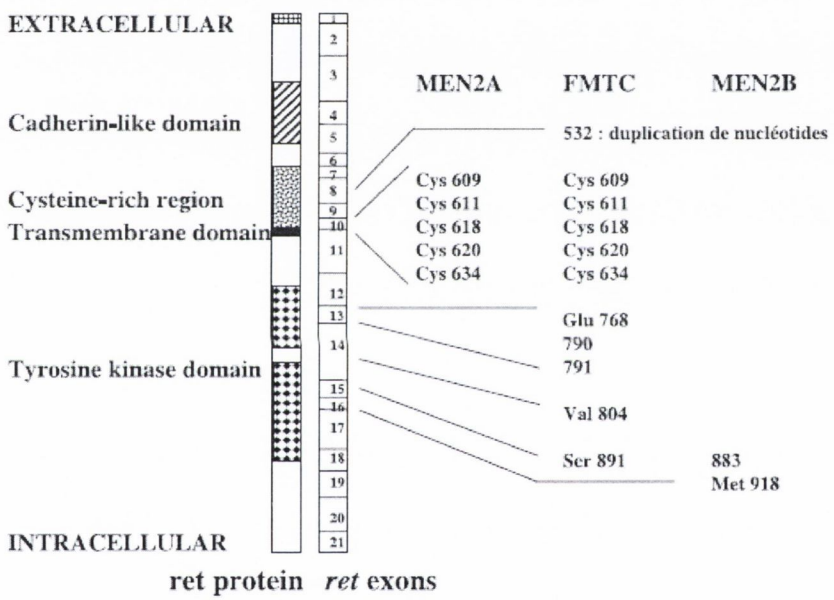

Figure 1.16 The RET gene and protein. (Leboulleux et al., 2004)

1.8.2 ret/PTC oncogenes

In 1987 the demonstration of an activating oncogene specific for papillary thyroid carcinoma was shown using NIH 3T3 transfection assays. (Fusco et al., 1987) This oncogene was shown to be a rearranged form of RET called ret/PTC. To date, at least 16 chimeric mRNAs involving eleven distinct donor genes have been described. ret/PTC 1-9, PCM1-ret, ELKS-ret, and RFP-ret have been isolated from sporadic and radiation associated PTCs (Table 1.1). In each case, the intracellular domain of RET is fused to different activating genes, namely H4 (for ret/PTC-1), RIα (ret/PTC2), RFG/ELE1/ARA70 (ret/PTC3 and ret/PTC4), RFG5 (ret/PTC5), hTIF (ret/PTC-6), RFG7/TF1γ (ret/PTC7), kinectin (ret/PTC8), RFG9 (ret/PTC9), PCM1 (PCM1-ret), ELKS (ELKS-ret), and RFP (RFP-ret). This results in ligand-independent dimerization and constitutive activation of these chimeric proteins. (Arighi et al., 2005)

ret/PTC rearrangements activate the transforming potential of RET by multiple mechanisms. First, by substituting its transcriptional promoter with those of the fusion partners, they allow the expression of RET in the epithelial follicular thyroid cells, where it is normally transcriptionally silent. Secondly, the rearrangements generate constitutively active chimeric oncoproteins which are distributed in the cytosolic compartment of the cell. Finally, activation of the RET kinase is mediated by fusion to domains that are capable of dimerization.

Genes	Translocation	Reference
RET/PTC1 RET - H4/D10S170	Inv (10;10)(q11.2;q21)	(Smanik et al., 1995)
RET/PTC2 RET - PRKAR1A	t(10;17)(q11.2;q23)	(Smanik et al., 1995)
RET/PTC3 RET/PTC4 or 3R2 RET - ELE1/RFG	Inv (10;10)(q11.2q23)	(Santoro et al., 1994) (Fugazzola et al., 1996) (Rabes et al., 2000)
RET/PTC5 in RET - RET-II/RFG5	14q22.1	(Rabes et al., 2000)
RET - ELKS	t(10;12)(q11;p13)	(Yokota et al., 2000)
RET/PTC8 RET - KTN1	RFG8 (18q21-22) t(10;14)(q11.2;q22.1)	(Salassidis et al., 2000)
RET/PTC6 RET - TIF1	7q32-34	(Rabes et al., 2000)
RET/PTC7 RET - RFG7	1p13.1	(Rabes et al., 2000)
RET/PTC9 PTC8 bis RET - RFG9	Rearrangement (18q21-22) RET/RFG9	
PCM1 - RET	t(8;10)(p21-22;q11)	(Corvi et al., 2000)

Table 1.1 The more commen chimeric ret oncogenes.

The prevalence of ret/PTC rearrangements in thyroid cancer varies widely among studies, with rates between 3 and 85% being reported. (Asa, 2001; Kondo et al., 2006; Nikiforov, 2002; Tallini and Asa, 2001) This wide variation probably reflects geographic location and the detection methods used. ***The different types of ret/PTC rearrangements are thought to reflect phenotypic differences in neoplastic thyroid cells.*** ret/PTC-3 rearrangements are more often associated with the solid/follicular variant of PTC, whereas ret/PTC-1 rearrangements are more common in the classic papillary type. (Finn et al., 2003; Thomas et al., 1999)

1.8.3 BRAF

BRAF belongs to the family of RAF proteins (ARAF, BRAF, CRAF), which are intracellular effectors of the MAP kinase (MAPK) signalling cascade. The discovery of activating mutations of the gene for BRAF has expanded the array of the known genetic alterations that activate the MAPK pathway and underscores the importance of this pathway in human cancer. (Davies et al., 2002) Upon activation triggered by RAS binding and protein recruitment to the cell membrane, these serine-threonine kinases phosphorylate and activate MAPK/ERK kinase (MEK), which in turn activates ERK and consequently effectors of the MAPK cascade.

BRAF activating missense point mutations in the kinase domain are clustered in exons 11 and 15 of the gene and the T1799A transversion mutation accounts for more than 80% of all the BRAF mutations. (Davies et al., 2002) The T1799A mutation results in a V600E amino acid substitution in the protein product and subsequent constitutive activation of the BRAF kinase. BRAF mutations have been reported in numerous cancers, being most prevalent in melanomas and nevi. (Davies et al., 2002; Treanor et al., 1996) BRAF mutation is the most common genetic event occurring in sporadic adult papillary carcinomas of the thyroid; it prevails in approximately 45% of all cases. (Ciampi and Nikiforov, 2005; Xing, 2005) Virtually all mutations found in these tumours are V600E. Akin to the different types of ret/PTC rearrangements, BRAF mutations reflect phenotypic differences in thyroid malignancy: BRAF V600E mutations are highly prevalent in classical papillary carcinomas and the tall cell variant of PTC, but are rare in the follicular variant.

1.9 Aims and Objectives

The overall aim of the study was to propose that ret rearrangements may have a role in papillary tumour morphogenesis. Specific objectives were:

i) To assess whether ret/PTC-1 rearrangements are present in papillary tumours of the urogenital tract and to look for an association with the phenotypic expression of papillary morphology.

ii) To assess whether BRAF T1799A mutations are associated with the phenotypic expression of papillary morphology and to assess what role they may have in progression from well to poorly differentiated tumours.

1.10 References

Arighi, E., M. G. Borrello, and H. Sariola. 2005. RET tyrosine kinase signaling in development and cancer. Cytokine Growth Factor Rev 16:441-67.

Asa, S. L. 2001. How familial cancer genes and environmentally induced oncogenes have changed the endocrine landscape. Mod Pathol 14:246-53.

Bandera, C. A., M. G. Muto, W. R. Welch, R. S. Berkowitz, and S. C. Mok. 1998. Genetic imbalance on chromosome 17 in papillary serous carcinoma of the peritoneum. Oncogene 16:3455-9.

Bell, K. A., A. E. Smith Sehdev, and R. J. Kurman. 2001. Refined diagnostic criteria for implants associated with ovarian atypical proliferative serous tumors (borderline) and micropapillary serous carcinomas. Am J Surg Pathol 25:419-32.

Brinton, L. A., M. L. Berman, R. Mortel, L. B. Twiggs, R. J. Barrett, G. D. Wilbanks, L. Lannom, and R. N. Hoover. 1992. Reproductive, menstrual, and medical risk factors for endometrial cancer: results from a case-control study. Am J Obstet Gynecol 167:1317-25.

Brown, R. 1827. A Brief Account of Microscopical Observations. London (not published).

Burks, R. T., M. E. Sherman, and R. J. Kurman. 1996. Micropapillary serous carcinoma of the ovary. A distinctive low-grade carcinoma related to serous borderline tumors. Am J Surg Pathol 20:1319-30.

Calle, E. E., C. Rodriguez, K. Walker-Thurmond, and M. J. Thun. 2003. Overweight, obesity, and mortality from cancer in a prospectively studied cohort of U.S. adults. N Engl J Med 348:1625-38.

Cass, I., R. L. Baldwin, E. Fasylova, A. L. Fields, H. P. Klinger, C. D. Runowicz, and B. Y. Karlan. 2001. Allelotype of papillary serous peritoneal carcinomas. Gynecol Oncol 82:69-76.

Carneiro, J. A. Basic Histology, A text and atlas:450.

Christensen, P., M. R. Madsen, and O. M. Jensen. 1983. Latency of thorotrast-induced renal tumours. Survey of the literature and a case report. Scand J Urol Nephrol 17:127-30.

Christine, H., and J. S. B. Holscheider. 2000. Ovarian cancer: Epidemiology, biology, and prognostic factors. Seminars in Surgical Oncology 19:3-10.

Ciampi, R., and Y. E. Nikiforov. 2005. Alterations of the BRAF gene in thyroid tumors. Endocr Pathol 16:163-72.

Corvi, R., N. Berger, R. Balczon, and G. Romeo. 2000. RET/PCM-1: a novel fusion gene in papillary thyroid carcinoma. Oncogene 19:4236-42.

Davies, H., G. R. Bignell, C. Cox, P. Stephens, S. Edkins, S. Clegg, J. Teague, H. Woffendin, M. J. Garnett, W. Bottomley, N. Davis, E. Dicks, R. Ewing, Y. Floyd, K. Gray, S. Hall, R. Hawes, J. Hughes, V. Kosmidou, A. Menzies, C. Mould, A. Parker, C. Stevens, S. Watt, S. Hooper, R. Wilson, H. Jayatilake, B. A. Gusterson, C. Cooper, J. Shipley, D. Hargrave, K. Pritchard-Jones, N. Maitland, G. Chenevix-Trench, G. J. Riggins, D. D. Bigner, G. Palmieri, A. Cossu, A. Flanagan, A. Nicholson, J. W. Ho, S. Y. Leung, S. T. Yuen, B. L. Weber, H. F. Seigler, T. L. Darrow, H. Paterson, R. Marais, C. J. Marshall, R. Wooster, M. R. Stratton, and P. A. Futreal. 2002. Mutations of the BRAF gene in human cancer. Nature 417:949-54.

Dehari, R., R. J. Kurman, S. Logani, and M. Shih Ie. 2007. The development of high-grade serous carcinoma from atypical proliferative (borderline) serous tumors and low-grade micropapillary serous carcinoma: a morphologic and molecular genetic analysis. Am J Surg Pathol 31:1007-12.

Delahunt, B., and J. N. Eble. 1997. Papillary renal cell carcinoma: a clinicopathologic and immunohistochemical study of 105 tumors. Mod Pathol 10:537-44.

Drife J, M. B. e. 2004. Clinical Obstetrics and Gynaecology. Saunders. Elsevier Ltd.

Durbec, P., C. V. Marcos-Gutierrez, C. Kilkenny, M. Grigoriou, K. Wartiowaara, P. Suvanto, D. Smith, B. Ponder, F. Costantini, M. Saarma, and et al. 1996. GDNF signalling through the Ret receptor tyrosine kinase. Nature 381:789-93.

Eichhorn, J. H., D. A. Bell, R. H. Young, and R. E. Scully. 1999. Ovarian serous borderline tumors with micropapillary and cribriform patterns: a study of 40 cases and comparison with 44 cases without these patterns. Am J Surg Pathol 23:397-409.

Espinasse, M. 1962. Robert Hooke. 2nd ed. University of California Press, Berkeley and Los Angeles.

Ferlay J, B. F., Pisani P, Parkin DM. 2001. Cancer Incidence, Mortality and Prevalence Worldwide. IARC Press:Lyon. Globocan 2000.

Finn, S. P., P. Smyth, J. O'Leary, E. C. Sweeney, and O. Sheils. 2003. Ret/PTC chimeric transcripts in an Irish cohort of sporadic papillary thyroid carcinoma. J Clin Endocrinol Metab 88:938-41.

Ford, B. J. 1991. The Leeuwenhoek Legacy. Biopress, Bristol, and Farrand Press, London. .

Fugazzola, L., M. A. Pierotti, E. Vigano, F. Pacini, T. V. Vorontsova, and I. Bongarzone. 1996. Molecular and biochemical analysis of RET/PTC4, a novel oncogenic rearrangement between RET and ELE1 genes, in a post-Chernobyl papillary thyroid cancer. Oncogene 13:1093-7.

Fusco, A., M. Grieco, M. Santoro, M. T. Berlingieri, S. Pilotti, M. A. Pierotti, G. Della Porta, and G. Vecchio. 1987. A new oncogene in human thyroid papillary carcinomas and their lymph-nodal metastases. Nature 328:170-2.

Gilks, C. B., D. A. Bell, and R. E. Scully. 1990. Serous psammocarcinoma of the ovary and peritoneum. Int J Gynecol Pathol 9:110-21.

Greenlee RT, H.-H. M., Murray T, Thun M. 2001. Cancer Statistics, 2001. CA Cancer J Clin 51:15-36.

Harlow, B. L., D. W. Cramer, J. A. Baron, L. Titus-Ernstoff, and E. R. Greenberg. 1998. Psychotropic medication use and risk of epithelial ovarian cancer. Cancer Epidemiol Biomarkers Prev 7:697-702.

Huang, L. W., A. P. Garrett, J. O. Schorge, M. G. Muto, D. A. Bell, W. R. Welch, R. S. Berkowitz, and S. C. Mok. 2000. Distinct allelic loss patterns in papillary serous carcinoma of the peritoneum. Am J Clin Pathol 114:93-9.

Jing, S., D. Wen, Y. Yu, P. L. Holst, Y. Luo, M. Fang, R. Tamir, L. Antonio, Z. Hu, R. Cupples, J. C. Louis, S. Hu, B. W. Altrock, and G. M. Fox. 1996. GDNF-induced activation of the ret protein tyrosine kinase is mediated by GDNFR-alpha, a novel receptor for GDNF. Cell 85:1113-24.

Kondo, T., S. Ezzat, and S. L. Asa. 2006. Pathogenetic mechanisms in thyroid follicular-cell neoplasia. Nat Rev Cancer 6:292-306.

Koralek, D. O., E. R. Bertone-Johnson, M. F. Leitzmann, S. R. Sturgeon, J. V. Lacey, Jr., C. Schairer, and A. Schatzkin. 2006. Relationship between calcium, lactose, vitamin D, and dairy products and ovarian cancer. Nutr Cancer 56:22-30.

Kurman, R. J., and C. L. Trimble. 1993. The behavior of serous tumors of low malignant potential: are they ever malignant? Int J Gynecol Pathol 12:120-7.

Lager, D. J., B. J. Huston, T. G. Timmerman, and S. M. Bonsib. 1995. Papillary renal tumors. Morphologic, cytochemical, and genotypic features. Cancer 76:669-73.

Landis, S. H., T. Murray, S. Bolden, and P. A. Wingo. 1998. Cancer statistics, 1998. CA Cancer J Clin 48:6-29.

Leboulleux, S., E. Baudin, J. P. Travagli, and M. Schlumberger. 2004. Medullary thyroid carcinoma. Clin Endocrinol (Oxf) 61:299-310.

Mancilla-Jimenez, R., R. J. Stanley, and R. A. Blath. 1976. Papillary renal cell carcinoma: a clinical, radiologic, and pathologic study of 34 cases. Cancer 38:2469-80.

McLaughlin, J. K., W. J. Blot, J. S. Mandel, L. M. Schuman, E. S. Mehl, and J. F. Fraumeni, Jr. 1983. Etiology of cancer of the renal pelvis. J Natl Cancer Inst 71:287-91.

Motzer, R. J., N. H. Bander, and D. M. Nanus. 1996. Renal-cell carcinoma. N Engl J Med 335:865-75.

Nikiforov, Y. E. 2002. RET/PTC rearrangement in thyroid tumors. Endocr Pathol 13:3-16.

Palvio, D. H., J. C. Andersen, and E. Falk. 1987. Transitional cell tumors of the renal pelvis and ureter associated with capillarosclerosis indicating analgesic abuse. Cancer 59:972-6.

Petro, R. 1997. Epidemiology multistage models, short term mutagenesis tests, Origins of Human Cancer. New York, Cold Spring Harbor Laboratoty Press.

Piver, M. S., M. F. Jishi, Y. Tsukada, and G. Nava. 1993. Primary peritoneal carcinoma after prophylactic oophorectomy in women with a family history of ovarian cancer. A report of the Gilda Radner Familial Ovarian Cancer Registry. Cancer 71:2751-5.

Rabes, H. M., E. P. Demidchik, J. D. Sidorow, E. Lengfelder, C. Beimfohr, D. Hoelzel, and S. Klugbauer. 2000. Pattern of radiation-induced RET and NTRK1 rearrangements in 191 post-chernobyl papillary thyroid carcinomas: biological, phenotypic, and clinical implications. Clin Cancer Res 6:1093-103.

Renshaw, A. A., and C. L. Corless. 1995. Papillary renal cell carcinoma. Histology and immunohistochemistry. Am J Surg Pathol 19:842-9.

Rosai, J. Rosai and Ackerman's Surgical Pathology, 9th Ed., Mosby.

Salassidis, K., J. Bruch, H. Zitzelsberger, E. Lengfelder, A. M. Kellerer, and M. Bauchinger. 2000. Translocation t(10;14)(q11.2:q22.1) fusing the kinetin to the RET gene creates a novel rearranged form (PTC8) of the RET proto-oncogene in radiation-induced childhood papillary thyroid carcinoma. Cancer Res 60:2786-9.

Santoro, M., N. A. Dathan, M. T. Berlingieri, I. Bongarzone, C. Paulin, M. Grieco, M. A. Pierotti, G. Vecchio, and A. Fusco. 1994. Molecular characterization of RET/PTC3; a novel rearranged version of the RET proto-oncogene in a human thyroid papillary carcinoma. Oncogene 9:509-16.

Savage, P. D. 1996. Renal cell carcinoma. Curr Opin Oncol 8:247-51.

Schorge, J. O., Y. B. Miller, L. J. Qi, M. G. Muto, W. R. Welch, R. S. Berkowitz, and S. C. Mok. 2000a. Genetic alterations of the WT1 gene in papillary serous carcinoma of the peritoneum. Gynecol Oncol 76:369-72.

Schorge, J. O., M. G. Muto, S. J. Lee, L. W. Huang, W. R. Welch, D. A. Bell, E. Z. Keung, R. S. Berkowitz, and S. C. Mok. 2000b. BRCA1-related papillary serous carcinoma of the peritoneum has a unique molecular pathogenesis. Cancer Res 60:1361-4.

Schorge, J. O., M. G. Muto, W. R. Welch, C. A. Bandera, S. C. Rubin, D. A. Bell, R. S. Berkowitz, and S. C. Mok. 1998. Molecular evidence for multifocal papillary serous carcinoma of the peritoneum in patients with germline BRCA1 mutations. J Natl Cancer Inst 90:841-5.

Segal, G. H., and W. R. Hart. 1992. Ovarian serous tumors of low malignant potential (serous borderline tumors). The relationship of exophytic surface tumor to peritoneal "implants". Am J Surg Pathol 16:577-83.

Slomovitz, B. M., T. A. Caputo, H. F. Gretz, 3rd, K. Economos, D. V. Tortoriello, P. W. Schlosshauer, R. N. Baergen, C. Isacson, and R. A. Soslow. 2002. A comparative analysis of 57 serous borderline tumors with and without a noninvasive micropapillary component. Am J Surg Pathol 26:592-600.

Smanik, P. A., T. L. Furminger, E. L. Mazzaferri, and S. M. Jhiang. 1995. Breakpoint characterization of the ret/PTC oncogene in human papillary thyroid carcinoma. Hum Mol Genet 4:2313-8.

Takahashi, M., J. Ritz, and G. M. Cooper. 1985. Activation of a novel human transforming gene, ret, by DNA rearrangement. Cell 42:581-8.

Tallini, G., and S. L. Asa. 2001. RET oncogene activation in papillary thyroid carcinoma. Adv Anat Pathol 8:345-54.

Thomas, G. A., H. Bunnell, H. A. Cook, E. D. Williams, A. Nerovnya, E. D. Cherstvoy, N. D. Tronko, T. I. Bogdanova, G. Chiappetta, G. Viglietto, F. Pentimalli, G. Salvatore, A. Fusco, M. Santoro, and G. Vecchio. 1999. High prevalence of RET/PTC rearrangements in Ukrainian and Belarussian post-Chernobyl thyroid papillary carcinomas: a strong correlation between RET/PTC3 and the solid-follicular variant. J Clin Endocrinol Metab 84:4232-8.

Treanor, J. J., L. Goodman, F. de Sauvage, D. M. Stone, K. T. Poulsen, C. D. Beck, C. Gray, M. P. Armanini, R. A. Pollock, F. Hefti, H. S. Phillips, A. Goddard, M. W. Moore, A. Buj-Bello, A. M. Davies, N. Asai, M. Takahashi, R. Vandlen, C. E. Henderson, and A. Rosenthal. 1996. Characterization of a multicomponent receptor for GDNF. Nature 382:80-3.

Trupp, M., E. Arenas, M. Fainzilber, A. S. Nilsson, B. A. Sieber, M. Grigoriou, C. Kilkenny, E. Salazar-Grueso, V. Pachnis, and U. Arumae. 1996. Functional receptor for GDNF encoded by the c-ret proto-oncogene. Nature 381:785-9.

WJ, H. 1998. Prospective on ovarian cancer: why prevent? J Cell Biochem Suppl 23:189-199.

www.ncri.ie.

Xing, M. 2005. BRAF mutation in thyroid cancer. Endocr Relat Cancer 12:245-62.

Yokota, T., T. Nakata, S. Minami, J. Inazawa, and M. Emi. 2000. Genomic organization and chromosomal mapping of ELKS, a gene rearranged in a papillary thyroid carcinoma. J Hum Genet 45:6-11.

Chapter 2

Materials and Methods

2.1 Introduction

This chapter is a comprehensive account of all the methodologies employed in this thesis, accompanied by background information on some of the newer techniques. Several of the techniques are used in a number of chapters. Where this occurs, the full description of the technique is restricted to this chapter, with specifics appearing in their relevant chapters only.

2.2 Tissue Collection

2.2.1 Formalin fixed paraffin embedded tissue

Formalin fixed (10% buffered) and paraffin embedded tumour samples were selected from the pathology files of St. James's Hospital, Dublin. Haematoxylin & Eosin (H&E) stained slides of all tumour samples were reviewed by a pathologist and classified according to appropriate criteria. (Eble et al., 2004; Tavassoli & (Eds). 2003)

2.3 Laser capture microdissection

Laser capture microdissection was carried out on formalin fixed paraffin embedded (FFPE) material using the PixCell®II LCM System (Arcturus Engineering, Inc., CA, USA). Briefly, 4-7μm FFPE histological sections were cut and stained with a standard hematoxylin and eosin (H&E) stain. Upon drying they are placed on the PixCell®II microscopic stage and the following protocol is observed (Figure 2.1):

- Enable the laser via the keyswitch located on front of controller.

- Remove the CapSure® cassette module from the PixCell®II platform. It should slide out smoothly over the detents.
- Press down on the flanges of the cassette module. Press the end locking pins in to hold the plate down in the load position.
- Slide a CapSure® cartridge, which holds four film carriers, into the cassette module until it hits a stop. The cassette loads from one end only.
- If more than four caps are required, load a second cartridge in the same manner, making sure there is no space between the two loaded cartridges.
- Press down on the flanges of the loaded cassette. Retract the locking pins and gently raise the cassette to its loaded position.
- The cartridge is now ready to be loaded into the PixCell®II.
- Slide the loaded CapSure® cassette module to any detent position.
- After LCM, when the CapSure® cartridges are empty, press down on the plate and lock into position by pushing the locking pins in. Carefully slide out the spent cartridges and discard.
- Move the joystick to the vertical position. This centres the translation stage, on the optical axis and ensures proper registration of the sample slide relative to the capture area. This also maximises the transfer area available for microdissection.
- Turn off the vacuum chuck via the switch located on the front of the controller.
- Place the slide on the translation stage, covering the vacuum chuckhole. Manually position it to locate the transfer area in the centre of the field of view.
- Choose the appropriate objective for the desired magnification. Turn on the vacuum chuck.

- Adjust illumination control.
- Adjust focus control.
- Rotate the CapSure® placement arm over the tissue sample.
- Insert the visualiser by pressing the silver plunger button located above the joystick.
- Adjust the microscope light source to obtain a good image on the monitor.
- To perform a microdissection, retract the visualiser by pressing the tab located below the plunger button, and re-adjust the microscope light source.
- Slide the CapSure® cassette module to a detent position, making sure there is a CapSure® cap at the load line.
- Rotate the placement arm to the cap pick-up position. The arm will automatically line up with the cap.
- Raise the placement arm vertically to remove the cap from the cassette module.
- Rotate the placement arm to transfer position over the slide. Release the placement arm. The cap will automatically lower onto the slide. Upon contact with the slide, the placement arm will seat the cap properly on the sample.

When the laser is enabled, an aiming beam is visible on the monitor.

- Select the laser spot size with the 'Spot Size Adjust' located on the left of the laser tower.
- Use the joystick or the XY controls to aim the laser beam on the capture region.

Use the front panel digital controls on the controller to adjust laser parameters. Typical values are:

Spot Size	Power	Duration
<7.5 μm	40mW	450μs
~15 μm	25mW	1.5ms
~30 μm	20mW	5ms

- Fire the laser by pressing the remote thumb switch or the 'fire' button on the front of the controller.
- There is an audible beep when the laser fires. The activated portion of the transfer film will be visible as a ring of film fused to the tissue.
- Use the joystick to move to other areas in the tissue and capture other cells of interest.
- To remove the captured tissue, lift the placement arm in a smooth but swift motion.
- With the cap in place, lift and rotate the placement arm to the unload platform.
- Lower the placement arm onto the unload platform – dropping the cap into the extraction slot.
- Rotate the placement arm to the rest position. The cap will be extractred form the arm and suspended in the unload platform.
- Slide the cap insertion tool onto the unload platform. Make sure the open end of the insertion tool faces the suspended cap and the groove fits over the guide rail.

- Slide the insertion tool down the groove until the cap is engaged.
- Remove with cap attached.
- Insert cap into 0.5ml reagent tube.
- Press down firmly to ensure an even seal.

Continue extraction according to appropriate protocol.

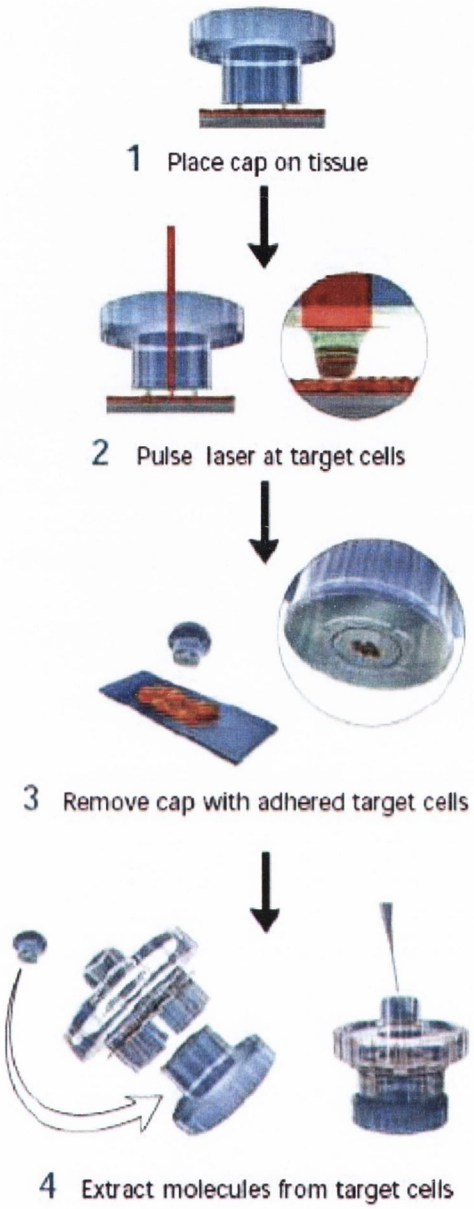

Figure 2.1 The laser capture microdissection process

(Adapted from http://www.arctur.com/products/pixcell_obtain_results.htm)

2.4 Nucleic Acid Extraction

Throughout this thesis various analyses were carried out on nucleic acids from a variety of thyroid tissue types stored in different formats (e.g. fresh frozen, FFPE, etc.). The extraction protocol employed was largely dictated by the quantity and quality of nucleic acid required and by the format of the starting tissue.

The extraction of pure, intact RNA is important in a variety of molecular biological techniques, and is essential for gene expression analysis. Ribonucleases however can cause difficulty with RNA isolation because they are very stable, active enzymes that require no cofactors for enzymatic activity. Cell lysis in an environment that causes denaturation of ribonucleases is therefore essential. So too is adequate decontamination of work surface areas, solutions and plastic disposables. DNA extraction need not be as stringent, as simple resuspension with a chelating agent confers nuclease protection to the molecule; however it is wise to be consistent with precaution.

2.4.1 Extraction of RNA from FFPE

This was generally performed on samples following LCM. The PURESCRIPT® total RNA isolation kit (Gentra Systems Inc., MN, USA) was utilised for this function, with slight modifications.

Cell lysis

- Perform microdissection and place cap in a 0.5ml microfuge tube containing 300µl Cell Lysis Solution and 1.5µl Proteinase K solution (20mg/ml).
- Incubate overnight at 55°C with constant agitation (i.e. a rotary oven).

Protein-DNA precipitation

- Transfer solution to a fresh 1.5ml microcentrifuge tube and add 100µl Protein-DNA Precipitation Solution to the cell lysate.
- Invert tube gently 10 times and place tube into an ice bath for 5 minutes.
- Centrifuge at 13,000-16,000 x g for 3 minutes. The precipitated proteins and DNA will form a tight pellet.
- (optional) Transfer the supernatant to a fresh tube and repeat ice incubation and centrifugation steps.

RNA precipitation

- Pipette the supernatant containing the RNA (leaving behind the precipitated protein-DNA pellet) into a clean 1.5ml microcentrifuge tube containing 300µl 100% isopropanol (2-propanol) and 0.5µl glycogen (20mg/ml).
- Mix the sample by inverting gently 50 times and incubate @ -20°C for 1 hour. Centrifuge at 13,000-16,000 x g (@ 4°C if possible) for 3min; the RNA will be visible as a small, translucent pellet.

- Pour off supernatant and drain tube on clean absorbent paper. Add 300µl 70% ethanol. Invert the tube several times to wash the RNA pellet.
- Centrifuge at 13,000-16,000 x g for 1min. Carefully pour off the ethanol.
- Invert and drain the tube on clean absorbent paper and allow to air dry for 15 min.

RNA hydration

- Add 25µl RNA Hydration Solution.
- Allow RNA to rehydrate at least 30 minutes on ice. Alternatively, store RNA sample at -70°C to -80°C until use.
- Before use, vortex sample vigorously for 5 seconds and pulse spin. Pipette sample up and down several times to ensure adequate mixing.
- Store RNA sample at -70°C to -80°C.

2.4.2 Extraction of DNA from FFPE

This was generally performed on samples following LCM. The PUREGENE® DNA isolation kit (Gentra Systems Inc., MN, USA) was utilised for this function, with slight modifications.

Cell lysis

- Perform microdissection and place cap in a 0.5ml microcentrifuge tube containing 300µl Cell Lysis Solution and 1.5µl Proteinase K solution (20mg/ml).
- Incubate overnight at 55°C with constant agitation (i.e. a rotary oven).

RNase treatment (optional)

- Add 1.5µl RNase A Solution (4 mg/ml) to the cell lysate.
- Mix the sample by inverting the tube 25 times and incubate at 37°C for 15-60 minutes.

Protein precipitation

- Cool sample to room temperature.
- Transfer solution to a fresh 1.5ml microcentrifuge tube and add 100µl Protein Precipitation Solution to the cell lysate and vortex vigorously for 20s.
- Place tube into an ice bath for 5min.
- Centrifuge at 13,000-16,000 x g for 3min. The precipitated proteins will form a tight pellet.
- (optional) Transfer the supernatant to a fresh tube and repeat ice incubation and centrifugation steps.

DNA precipitation

- Pipette the supernatant containing the DNA (leaving behind the precipitated protein pellet) into a clean 1.5ml microcentrifuge tube containing 300µl 100% isopropanol (2-propanol) and 0.5µl glycogen (20mg/ml).
- Mix the sample by inverting gently 50 times and incubate @ -20°C for 1 hr.
- Centrifuge at 13,000-16,000 x g (@ 4°C if possible) for 5 minutes.
- Pour off supernatant and drain tube on clean absorbent paper. Add 300µl 70% ethanol. Invert the tube several times to wash the DNA pellet.
- Centrifuge at 13,000-16,000 x g for 1 min. Carefully pour off the ethanol.
- Invert and drain the tube on clean absorbent paper and allow to air dry 15min.

DNA hydration

- Add 20µl DNA Hydration Solution.
- Allow DNA to rehydrate for 1 hr @ 65°C and/or overnight at room temperature. If possible, tap tube periodically to aid in dispersing the DNA.
- Store DNA at 4°C. For long-term storage, store at -20°C or -80°C.

2.5 Nano-Drop® 1000 spectrophotometer

Nucleic acid samples were checked for concentration and quality using the NanoDrop® ND-1000 spectrophotometer (Figure 2.2). To measure nucleic acid samples select the 'Nucleic Acid' application module. The NanoDrop® ND-1000 is a full-spectrum (220-750nm) spectrophotometer that measures 1 uL samples with high accuracy and reproducibility. It utilizes a patented sample retention technology that employs surface tension alone to hold the sample in place. In addition, the ND-1000 has the capability to measure highly concentrated samples without dilution (50X higher concentration than the samples measured by a standard curvette spectrophotometer).

2.5.1 Loading of samples (nucleic acid and water)

- With the sampling arm open, pipette the sample onto the lower measurement pedestal.
- Close the sampling arm and initiate a spectral measurement using the operating software on the PC. The sample column is automatically drawn between the upper and lower measurement pedestals and the spectral measurement made.

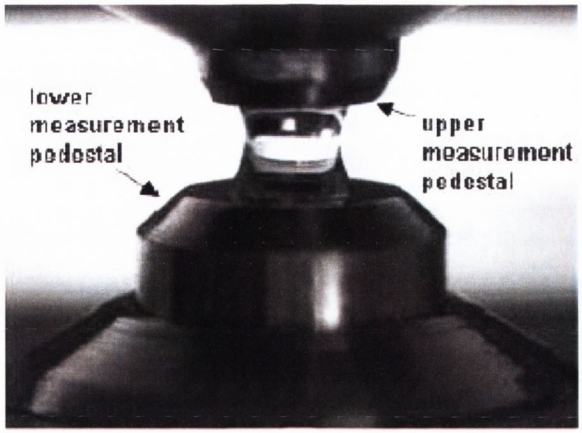

Figure 2.2 NanoDrop® spectrophotometer sample pedestal

- When the measurement is complete, open the sampling arm and wipe the sample from both the upper and lower pedestals using a soft laboratory wipe. Simple wiping prevents sample carryover in successive measurements for samples varying by more than 1000 fold in concentration.

2.5.2 Blank measurement

- Ensure measurement pedestal surfaces are clean. Load 1 μL water sample onto the lower measurement pedestal and then click 'OK'. After clicking OK, the message "*Initializing Spectrometer- please wait*" will appear. When this message disappears, the instrument will be ready for use.

- Before making a sample measurement, a blank must be measured and stored. This will assure the user that the instrument is working well and that any non-specific fluorescence is not a concern.
- Load a blank sample (the buffer, solvent, or carrier liquid used with your samples) onto the lower measurement pedestal and lower the sampling arm into the 'down' position. Click on the 'Blank' button.
- Wipe the blanking buffer from both pedestals using a laboratory wipe.
- Analyze an aliquot of the blanking solution as though it were a sample. This is done using the 'Measure' button. The result should be a spectrum with a relatively flat baseline. Wipe the blank from both measurement pedestal surfaces and repeat the process until the spectrum is flat.

2.5.3 Sample measurement

- 1 uL samples are sufficient to ensure accurate and reproducible results when measuring aqueous nucleic acid samples. After Blank measurement load the sample as outlined above in 2.6.2.

- *Results*

A260: absorbance of the sample at 260 nm represented as if measured with a conventional 10 mm path. *Note*: This is 10X the absorbance actually measured using the 1 mm path length and 50X the absorbance actually measured using the 0.2 mm path length.

A280: sample absorbance at 280 nm represented as if measured with a conventional 10 mm path. *Note*: This is 10X the absorbance actually measured using the 1 mm path length and 50X the absorbance actually measured using the 0.2 mm path length.

260/280: ratio of sample absorbance at 260 and 280 nm. The ratio of absorbance at 260 and 280 nm is used to assess the purity of DNA and RNA. A ratio of ~1.8 is generally accepted as "pure" for DNA; a ratio of ~2.0 is generally accepted as "pure" for RNA. If the ratio is appreciably lower in either case, it may indicate the presence of protein, phenol or other contaminants that absorb strongly at or near 280 nm.

260/230: ratio of sample absorbance at 260 and 230 nm. This is a secondary measure of nucleic acid purity. The 260/230 values for "pure" nucleic acid are often higher than the respective 260/280 values. They are commonly in the range of 1.8-2.2. If the ratio is appreciably lower, this may indicate the presence of co-purified contaminants.

Concentration (ng/uL): sample concentration in ng/uL based on absorbance at 260 nm and the selected analysis constant.

2.6 **Agarose Gel Electrophoresis**

The integrity and size distribution of total purified DNA was checked using denaturing agarose gel electrophoresis and ethidium bromide staining.

Agarose is a polysaccharide derived from seaweed, which forms a solid gel when dissolved in aqueous solution at concentrations between 0.5% and 2% (w/v). When an electric field is applied to an agarose gel in the presence of a buffer solution, DNA fragments move through the gel towards the positive electrode at a rate, which is dependent on their size and shape. The nucleic acid is visualised after electrophoresis by staining with Ethidium bromide and illuminating the gel under UV light.

- Dissolve 1.5g agarose in 100ml of 1x TAE buffer (1.5% gel).Heat in the microwave oven until the agarose has dissolved. (At full power for approx 2 minutes)
- Allow the solution to cool (until the steam has disappeared) and add in 5µl of Ethidium bromide. This solution can be stored at 37°C.
- Place a strip of tape across each end of the glass plate to seal the ends. This forms a mould. The gel can then be poured into the plate until it is level with the top of the plate (3 - 5mm thick).
- Place an 8 well comb in position along one of the red lines. (This allows the wells to be seen clearly when loading the DNA).
- Leave the gel to set for 10 minutes. When set, the comb can be removed and the tape removed from each end.
- Prepare the electrophoresis tank by filling it with 1x TAE buffer, to cover the gel.

  Place the gel, still on the plate, into the tank with the wells to the left.

- To load the DNA, it must first be stained with a loading buffer (supplied with the DNA ladder) at a ratio of 1µl loading buffer to 6µl of DNA. Load 5µl of the DNA ladder into one well to allow size comparisons of the bands. For best results, mix 10µl of DNA with 2µl of loading buffer and pipette directly into the well.
- Close the lid on the tank and attach the leads to the terminals and to the EC 105 power pack, (negative to negative (black), positive to positive (red)). Turn the voltage to 100v and leave to run for approx 15 minutes. (Check there are bubbles rising from the electrodes to indicate there is current flowing). By this time, the dye front should be half way down the gel. Turn off the current and remove the leads from the tank.
- The gel can now be removed from the tank and taken to the dark room for U.V. illumination and photographing.

2.7 TaqMan® PCR

A TaqMan® PCR-based system was selected for mRNA detection in this study. The TaqMan® system was chosen for a number of reasons. Firstly TaqMan® PCR and Reverse-Transcriptase (RT) PCR requires only a few nanograms of target DNA/RNA. This is highly significant since the amount of DNA/RNA extractable from archival FFPE material is low. Secondly, TaqMan PCR and RT-PCR products are small (generally less than 200 base pairs) and thus can be used to amplify partially degraded or fragmented DNA/RNA such as that obtained from FFPE material.

TaqMan® PCR exploits the 5′ nuclease activity of AmpliTaq Gold® DNA Polymerase to cleave a TaqMan probe during PCR. The TaqMan probe contains a reporter dye at the 5′ end of the probe and a quencher dye at the 3′ end of the probe. During the reaction, cleavage of the probe separates the reporter dye and the quencher dye, resulting in increased fluorescence of the reporter. Accumulation of PCR products is detected directly by monitoring the increase in fluorescence of the reporter dye, as shown in Figure 2.3.

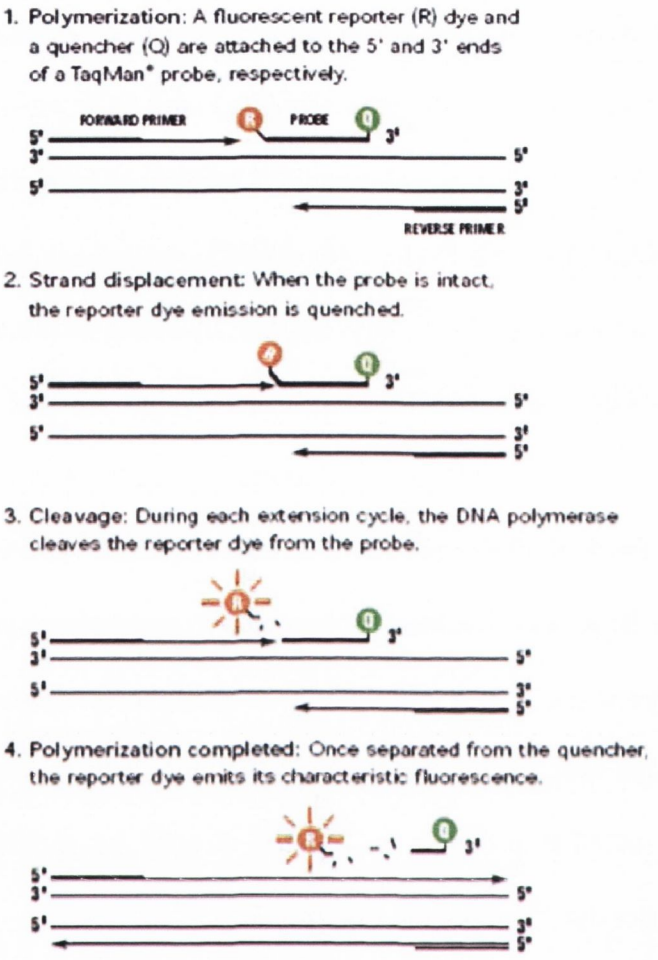

Figure 2.3 The forklike-structure-dependent, polymerisation-associated, 5′–3′ nuclease activity of AmpliTaq® Gold DNA Polymerase during PCR (Wang et al., 2006)

When the probe is intact, the proximity of the reporter dye to the quencher dye results in suppression of the reporter fluorescence primarily by Förster-type energy transfer (Forster, 1948; Lakowicz, 1983). During PCR, if the target of interest is present, the probe specifically anneals between the forward and reverse primer sites.

The 5′-3′ nucleolytic activity of the AmpliTaq® Gold DNA Polymerase cleaves the probe between the reporter and the quencher only if the probe hybridises to the target. The probe fragments are then displaced from the target, and polymerisation of the strand continues. The 3′ end of the probe is blocked to prevent extension of the probe during PCR. This process occurs in every cycle and does not interfere with the exponential accumulation of product.

The probe consists of an oligonucleotide with a 5′-reporter dye and a 3′-quencher dye. A fluorescent reporter dye, such as FAM (6-carboxyfluorescein), is covalently linked to the 5′ end of the oligonucleotide. TET (6-carboxy-4,7,2′,7′-tetrachlorofluorescein), JOE (6-carboxy-4,5-dichloro-2,7-dimethoxyfluorescein), and VIC are also used as reporter dyes. In older TaqMan® probes each of the reporters is quenched by TAMRA (6-carboxy-N,N,N′,N′-tetramethylrhodamine) at the 3′ end.

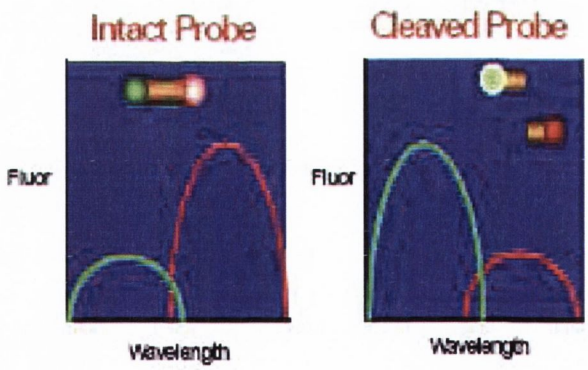

Figure 2.4 Increased fluorescence activities due to cleaved probe

2.7.1 Plus/Minus RT-PCR Assay

The ABI Prism® 7000 Sequence detection System supports plus/minus assays. Plus/minus scoring is the process by which the 7000 system detects the presence of a specific nucleic acid in a prepared sample. Plus/minus assays can be accomplished with or without the use of an internal positive control (IPC); however an IPC ensures that a failed PCR is not mistaken for a negative result. As all the samples were checked for housekeeping endogenous GAPDH expression an IPC was not included in our experimental design. The plus/minus assay is not real-time; it is an end point application. The plus/minus plate reports normalised reporter signal (Rn), post-read only results for unknown samples.

Plus/minus scoring on the 7000 system is made possible by using the fluorogenic 5' nuclease assay. Plus/minus assays use the same chemistry as described in 2.7. The fluorescence generated from the PCR amplification is measured by the software and can determine the presence or absence of the target nucleic acid in each sample on the plate. The calls for the unknown samples are based on a threshold determined by the no template control (NTC).This threshold determines the minimum fluorescent signal that must be achieved to assign a positive call to the sample. The confidence value assigned to this call can be determined by selecting a value between 95.0 - 99.9%.

2.7.2 Reverse transcription and TaqMan® PCR analysis

One-Step RT-PCR was carried out according to the manufacturers instructions under the following conditions: 1X One-Step Master Mix, 1X MultiScribe and RNase Inhibitor Mix (0.25U/µl MultiScribe and 0.4U/µl RNase Inhibitor), 300nM forward and reverse primers, 100nM probe, RNA template (10pg-100ng) and nuclease-free water to 25µl. One-Step RT-PCR was performed using an Applied Biosystems 7000 Sequence Detection System (Applied Biosystems, CA, USA) with the following thermocycling parameters: 48°C 30min, 95°C 10mins and 40 cycles of [95°C 15s, 60°C 1min].

2.7.3 Taqman® SNP genotyping/allelic discrimination assay

Detection of nucleotide mutations and polymorphisms is central to the modern science of molecular genetics. For example, allelic discrimination detects different forms of the same gene that differ by nucleotide substitution, insertion or deletion. Methods for mutation detection can be divided into two groups: scanning methods that can discover previously unknown nucleotide differences and diagnostic methods designed to detect specific, known mutations and polymorphisms. Large-scale scoring of known SNPs requires techniques with few steps and the ability to automate each of these steps. In this regard, the 5' nuclease assay is ideal because it combines PCR amplification and detection into a single step.

Figure 2.5 demonstrates how fluorogenic probes and the 5' nuclease assay can be used for allelic discrimination. For a bi-allelic system, probes specific for each allele are included in the PCR assay. The probes can be distinguished because they are labelled with different fluorescent reporter dyes (typically FAM and VIC). A fully hybridised probe remains bound during strand

displacement, resulting in efficient probe cleavage and release of the reporter dye. A mismatch between probe and target greatly reduces the efficiency of probe hybridisation and cleavage. Therefore, substantial increases in either FAM or VIC fluorescence indicates homozygosity for the FAM- or VIC-specific allele. an increase in both signals indicates heterozygosity. The feasibility of this approach was first demonstrated by Lee et al. when the used the technology to distinguish between the ΔF508 and normal alleles of the human cystic fibrosis gene. (Lee et al., 1993)

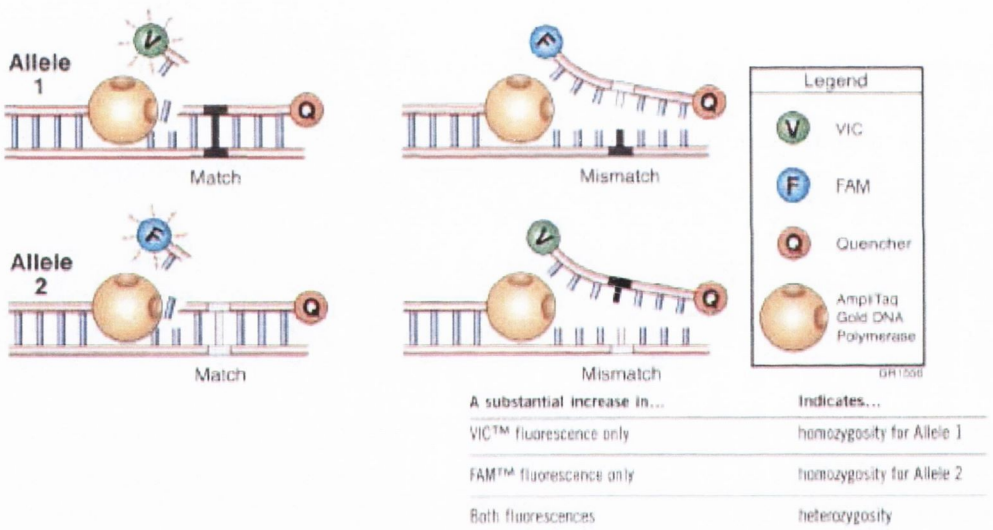

Figure 2.5 Allelic discrimination using the 5' nuclease assay

Three factors contribute to the discrimination based on a single mismatch. First, the mismatch has a disruptive effect on hybridisation. A mismatched probe will have a lower T_m than a perfectly matched probe. Proper choice of annealing/extension temperature during PCR will favour hybridisation of an exact-match probe over a mismatched probe. Second, the assay is performed under competitive conditions with both probes present in the same reaction tube. Therefore, mismatched probes are prevented from binding due to stable binding of exact match probes. Third, the 5' end of the probe must start to be displaced before cleavage occurs. The 5' nuclease activity of Taq polymerase recognises a forked structure with a displaced 5' strand of at least 1 to 3 nucleotides. (Lyamichev et al., 1993) Once a probe starts to be displaced, complete dissociation occurs faster with a mismatch than an exact match. This means there is less time for cleavage to occur with a mismatch probe. Thus, the presence of a mismatch promotes dissociation rather than cleavage of the probe.

Unknown samples are typically performed in duplicate. 6 no template controls (NTC) and known samples for all 3 possible outcomes (heterozygote, homozygote allele 1 and 2) are included with each run for allele calling purposes. A generic graphical output from an AD run is shown in Figure 2.6.

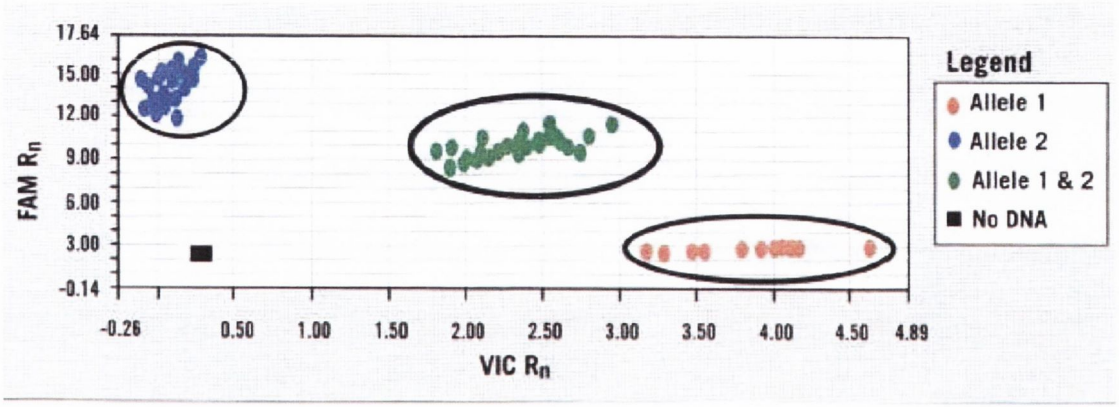

Figure 2.6 Typical allelic discrimination output

2.8 Immunohistochemisty

2.8.1 Background

Immunohistochemistry is a technique for identifying cellular or tissue constituents (antigens) by means of antigen-antibody interactions, the site of antibody binding being identified either by direct labeling of the antibody, or by use of a secondary labeling method. After an antigen retrieval step to unmask antigen sites, the ABC method was used. The first step of the procedure is to incubate the section with primary antibody raised against the antigen of interest, such as mouse antibody to a tumour-associated antigen. Next, a biotin-labeled secondary antibody is added, for example biotinylated anti-mouse IgG. This introduces many biotins into the section at the location of the primary antibody. The avidin:biotinylated enzyme complex (ABC) is then added and binds to the biotinylated secondary antibody.

In the last step of the procedure, the tissue antigen is localized by incubation with a substrate for the enzyme, in this case diaminobenzidene (DAB) which yields a crisp, insoluble, dark brown reaction end product (Fig 2.7).

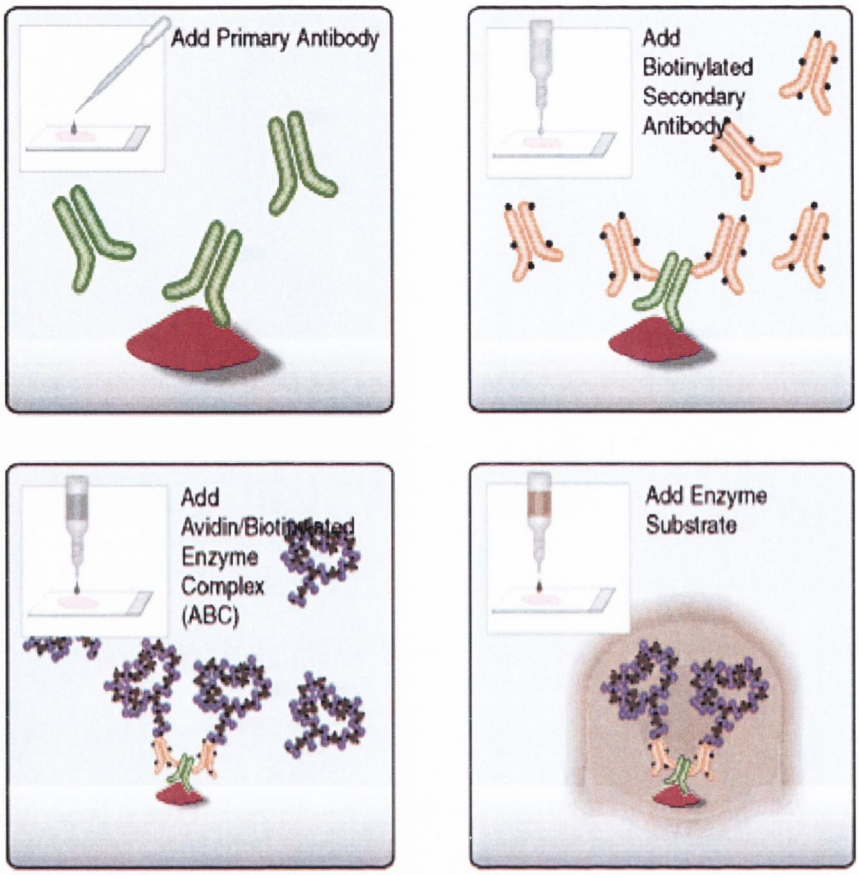

Figure 2.7 The ABC method (Adapted from Vectastain® ABC kits)

Table 2.1 details the species, clonality, dilution (diluted in TBS) and the positive control that was used for all primary antibodies.

Primary Antibody	Species/Clonality	Dilution	Positive control
RET	Mouse/Monoclonal	1:15	Appendix
TTF-1	Mouse/Monoclonal	1:1400	Lung
Thyroglobulin	Rabbit/Polyclonal	1:40	Thyroid

Table 2.1 Primary antibodies

2.8.2 ABC (*elite*) peroxidase method

- 4 μm sections of TMA blocks are cut using a microtome and placed on charged slides.
- Sections are dried overnight at 37°C or for 1 hour at 60°C.
- Sections are deparaffinised in xylene (Sigma-Aldrich, St. Louis, MO) for 5 minutes, 4 minutes and 4 minutes.
- Sections are dehydrated in ethanol (Sigma-Aldrich, St. Louis, MO) for 3, 2 and 1 minutes.
- Sections are brought to running water (6 minutes).

- Sections are incubated in 0.3% methanol (Sigma-Aldrich, St. Louis, MO) for 30 minutes to block endogenous peroxidases.
- Rinse sections in running water.

Antigen retrieval

- 15 mL of antigen unmasking solution (Vector Laboratories Inc. CA, USA) is added to 1600 mL of deionised water and placed in a pressure cooker (Medical Supply Company Ltd. Dublin, Ireland).
- Sections are added and antigen retrieval takes place on high pressure for approximately 10 minutes (length of antigen retrieval can vary depending on antibody).
- Rinse sections in running water.

Note: sections are now transferred to the Lab Vision Autostainer (Lab Vision Corporation, CA, USA) which automates the following steps:

- Sections are rinsed in Tris buffered saline (10X) (TBS) (Sigma-Aldrich, St. Louis, MO) and left covered in TBS for 5 minutes.
- Sections are covered in 0.1% bovine serum albumin (BSA) (Vector Laboratories Inc. CA, USA) for 10 minutes.

- Sections are decanted and covered with diluted primary antibody for approximately 30-60 minutes (primary antibody concentration and incubation time is optimised for RET antibody; primary antibody was omitted for the negative control).
- Sections are washed with TBS and left covered in TBS for 5 minutes.
- Sections are decanted, and incubated in secondary antibody for 30 minutes.
- Sections are washed with TBS and left covered in TBS for 5 minutes.
- Sections are decanted and incubated in ABC reagent (Vectastain ABC kit, Vector Laboratories Inc. CA, USA), for 30 minutes. ABC reagent must be made up 30 minutes before use by adding 2 drops of reagent A to 5 mL of TBS and then adding 2 mL of reagent B, mixing well and allowing to stand.
- Wash slides in TBS and leave covered for 5 minutes.
- Incubate sections in diaminobenzidine chromogen (DAB) (DakoCytomation, West Sussex, UK) solution for 7-10 minutes. DAB is made by adding 20 µL of liquid DAB to 1 mL of substrate buffer.
- Wash sections with TBS.

Note: sections are removed from the Autostainer and the following steps are carried out manually.

- Wash sections in running water for 2 minutes.
- Counterstain sections in haematoxylin (Vector Laboratories Inc. CA, USA) for 10 seconds.
- Differentiate sections in 1% acid alcohol (Sigma-Aldrich, St. Louis, MO) for 10 seconds.

- Blue in lukewarm running water for 3-5 minutes, dehydrate and clear sections by going backwards through the ethanol and xylene baths.
- Apply pertex (Medite, Burgdorf, Germany) and coverslip.

2.9 Fluorescent *in situ* hybridisation

Fluorescent *in situ* hybridisation (FISH) is a rapid method for detecting genetic aberrations that can be utilized on formalin fixed paraffin embedded tissues. FISH probes consist of DNA probe sequences homologous to specific gene sequences or DNA regions. Probes are labelled with fluorophores that are visible under fluorescent light. After tissue digestion and denaturation of probe and tissue DNA, probe is applied to the tissue. Tissue and probe are hybridized overnight and unbound probe is washed away. When visualized, probes then show amplifications, deletions or translocations of specific genes or chromosomal regions.

2.9.1 Interphase FISH analysis for RET/PTC rearrangement detection

Yeast artificial probes (YAC) probes were used in this study. YAC clones 313F4 and 214H10 map proximal to and include the RET locus, whereas clone 344H4 contains DNA sequences distal to RET. These three YACs were always used in combination to investigate the RET locus. Total yeast DNA was extracted and labelled either with digoxigenin-11-dUTP (344H4) or with biotin-16-dUTP (214H10, 313F4) using nick translation. Interphase FISH was performed on 10-μm paraffin-embedded sections. All sections had been microdissected to ensure that only tumour tissue was present on the slide for subsequent laser scanning microscopy scoring.

2.9.1.1 Slide Preparation

1) Place paraffin blocks for cutting on a cooling block for approximately 5 minutes.
2) Cut sections from each block at 10 μm intervals using a microtome.
3) Place sections in a heated water bath and mount on charged slides.
4) Dry slides in an incubator at 56 °C overnight.

2.9.1.2 Tissue Pretreatment

1) Sections are deparaffinised in xylene for 5 minutes x3.
2) Sections are dehydrated in ethanol for 1 minute x2.
3) Sections are brought to running water (6 minutes).
4) Pretreat slides in citrate buffer at 100°C for 15 minutes in a microwave.
5) Digest with pronase E (0.5μg/ml) in PBS solution at 37°C for variable time.
6) Incubate slides in glycine solution (2mg/ml) in PBS for 5 minutes.
7) Incubate slides in 4% formalin for 5 minutes.

2.9.1.3 DNA Denaturation and Probe Hybridisation

1) Pipette 200 μl of 70% formamide 2X saline sodium citrate solution onto a coverslip and invert slide onto this. Incubate at 72°C for 5 minutes on a thermal cycler to denature target DNA.
2) Drain off coverslips and place slides sequentially into 70%, 90% and 100% ice-cold alcohol for 1 minute each. Air dry slides.
3) Denature the RET-specific probes by heating at 72°C for 5 minutes.
4) Pipette 10 μl probe onto a coverslip and invert slide onto this. Seal with rubber cement.

5) Incubate on a thermal cycler for approximately 48-72 hours at 37°C.

2.9.1.4 Post-Hybridisation Washes

1) Wash slides in 50% formamide-2X saline sodium citrate for 15 minutes at 42°C X3.
2) Wash slides in 2X saline sodium citrate for 15 minutes at 42°C.
3) Wash slides in phosphate buffer with 0.1% nonidet P40 (PN) buffer for 15 minutes at 42°C.
4) Wash slides in PN buffer for 15 minutes at room temperature.

Note: Bound labeled DNA probes are detected with streptavidin-fluorescein isothiocyanate (FITC) (Dianova, Hamburg, Germany) and antidigoxigenin-Cy3 (Dianova). Signals were amplified by sequential incubation in biotinylated antistreptavidin (Dianova) and rat-antimouse-Cy3/mouse-anti-rat-Cy3 (Dianova) antibodies.

5) Incubate slides with PN buffer with 5% nonfat dry milk and 0.02% sodium azide before each antibody incubation.
6) Incubate each antibody for 20 minutes at 37°C.
7) Wash in PN buffer for 2 minutes at room temperature after each incubation step X2.
8) Counterstain tissue sections with TOPRO-3 (Molecular Probes, Leiden, The Netherlands); 0.1μM in PBS diluted at 1:5 with purified water.
9) Apply pertex (Medite, Burgdorf, Germany) and coverslip.

2.9.1.5 Microscopic analysis

Microscopic analyses were carried out using a confocal laser scanning microscope (Zeiss LSM 510, Zeiss, Jena, Germany). Up to 20 viewing areas per case were scanned in 0.5µm steps for three different channels (FITC, Cy3 and TOPRO-3) throughout the thickness of the respective section. Images were then superimposed by laser scanning microscopy software (AxioVision LE, Zeiss, Germany). Aberrant cell nuclei were identified by scoring of captured images.

The analysis software allowed a step-wise scoring every 0.5µm to ensure that signals in different layers of the sections were evaluated accurately.

Cell nuclei exhibiting rearranged *RET* gene show a split FISH signal in red (distal to *RET*) and green (proximal to *RET*) in addition to an overlapping signal. Normal cells show 2 overlapping nuclei. 100 nuclei with strong and well delineated signals were scored. Only cells with two overlapping signals or one split and one overlapping signal were counted to ensure only complete cell nuclei had been scored. The TPC-1 cell line carrying a *RET/PTC*1 rearrangement was used as control, with rearrangement positive cells present in each cell scored. Epithelium from normal thyroid, ovary, kidney and endometrium were also scored as control.

2.9.2 Interphase FISH for ploidy analysis

Interphase FISH was performed using centromeric probes for chromosomes 10 (green) and 17 (red) on RET/PTC rearranged cases for determination of ploidy status. Microscopic analyses and image capture was performed as described above. 100 nuclei with strong and well delineated signals were scored. Only cells with two or more signals were counted to ensure only complete cell nuclei had been scored.

2.10 References

Eble JN, Sauter G, Epstein JL and Sesterhenn IAE. (2004). *IARC Press, Lyon*

Forster V. (1948). *Annal of Physics*, **2,** 55-75.

Lakowicz J. (1983). *Principles of Fluoresence Spectroscopy.* Plenum Press: New York.

Lee LG, Connell CR and Bloch W. (1993). *Nucleic Acids Res*, **21,** 3761-6.

Lyamichev V, Brow MA and Dahlberg JE. (1993). *Science*, **260,** 778-83.

Tavassoli FA and (Eds). DP. (2003). *IARC Press: Lyon 2003.*

Wang Y, Barbacioru C, Hyland F, Xiao W, Hunkapiller KL, Blake J, Chan F, Gonzalez C, Zhang L and Samaha RR. (2006). BMC Genomics, 7, 59.

Chapter 3

RET/PTC rearrangement occurring in primary peritoneal carcinoma

3.1 Summary

RET/PTC rearrangements are initiating events in the development of a significant proportion of papillary thyroid carcinomas. Activated *RET/PTC* mutations are thought to be restricted to thyroid disease, but in this study we propose that these events maybe features of papillary morphology. 57 non-thyroid papillary tumours were examined for *RET/PTC* rearrangements using interphase FISH, Taqman™ RT-PCR and immunohistochemistry. 20% (3/15) of primary peritoneal carcinoma had detectable *RET/PTC*1 rearrangements by all three methodologies. A further case of similar histotype had an alternate *RET/PTC* rearrangement. No *RET/PTC*1 rearrangements were detected in the remaining tumour cohort. Our results indicate that *RET/PTC* rearrangements occur in a small subset of non-thyroid papillary tumours. These rearrangements may not be directly implicated in tumour growth; rather representing 'passenger' mutations reflecting *RET* instability in secondary tumour subclones.

3.2 Introduction:

This chapter encompasses the main body of work of the thesis. RET/PTC rearrangements are initiating events in the development of a significant proportion of papillary thyroid carcinomas (PTC). Activated ret/PTC mutations were once thought to be restricted to thyroid disease, but in this study we propose that these events are features of papillary morphology.

3.2.1 RET oncogene.

RET (rearranged during transfection) proto-oncogene is a tyrosine kinase receptor, coded for on chromosome 10q11.2. Ret oncogene was first identified in 1985 following the transfection of NIH3T3 cells with DNA from a human T-cell lymphoma. (Takahashi et al., 1985) The transforming gene resulted from a recombination event between two unlinked DNA sequences which occurred from the transfection process; hence the name *ret* for "REarranged during Transfection". The chimeric gene encoded a fusion protein comprising an amino terminal region that displayed a putative zinc finger motif fused to a tyrosine kinase domain. Glial cell line-derived neurotrophic factor (GDNF) family ligands (a subclass of the transforming-growth factor-β (*TGF-β*) superfamily) signal through a multicomponent complex consisting of glycosyl-phoshatidylinositol and *RET* tyrosine kinase. (Takahashi, 2001) The GDNF/*RET* signalling pathway has an important role in regulating the development of the peripheral nervous system and kidney together with germ cell differentiation. (Manie et al., 2001; Takahashi, 2001) Germline mutations in c-*RET* have been implicated in multiple endocrine neoplasia types 2A and B, familial medullary thyroid carcinoma (Asa, 2001; Jhiang, 2000) and Hirschsprung's disease. (Romeo et al., 1994) Sporadic mutations in *RET* are associated with the development of PTC. (Grieco et al., 1990; Santoro et al., 1992)

3.2.2 ret/PTC rearrangements

Chimeric ret oncogenes, designated ret/PTC, display a ligand-independent constitutive tyrosine kinase activity. They are formed from the juxtaposition of the genomic region coding for the tyrosine kinase domain of RET with the 5'-promoter regions of a variety of unrelated genes. At least 16 chimeric mRNAs involving eleven distinct donor genes have been described. (Jhiang, 2000; Klugbauer et al., 2000; Salassidis et al., 2000) Of these, the most commonly occurring in papillary thyroid carcinoma (PTC) are ret/PTC-1 [H4-(CCDC6)-RET] and ret/PTC-3 [ELE1-RET] (Figure 3.1). (Smanik et al., 1995)

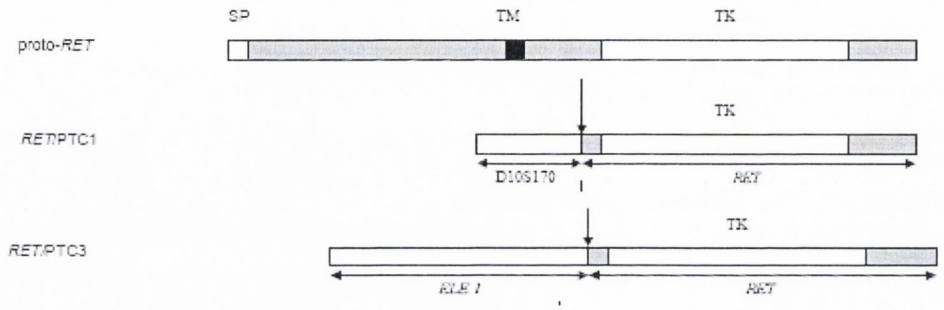

Figure 3.1 Schematic illustration of the RET proto-oncogene product and its oncogenic variants RET/PTC1 and 3. SP- signal peptide; TM-transmembrane domain; TK-tyrosine kinase domain; D10S170-locus of gene labelled with H4; Arrows indicate fusion points, following the RET/PTC rearrangements. (Suarez, 1998)

PTC-1 consists of the fusion of the *RET* TK domain with the 5' end of the H4 gene. (Grieco et al., 1994; Pasini et al., 1995) The chimeric protein localizes to the cytosol where it is constitutively phosphorylated. *H4* is a 55KD nuclear and cytosolic protein, whose loss of function might have a role in thyroid carcinogenesis by impairing apoptosis. (Celetti et al., 2004)

Studies have shown sporadic ret/PTC detection rates in PTC vary from 2.5% to as high as 85% depending on geographical location and the detection methods used. (Chua et al., 2000; Farid et al., 1994; Santoro et al., 1992; Sheils et al., 2000; Smyth et al., 2005; Sugg et al., 1996) The typical detection rate for most western countries is a more moderate 10-35%. *ret* rearrangements are highly prevalent in paediatric PTCs from children exposed to radiation; (Elisei et al., 2001; Kitamura et al., 1999; Russell et al., 2003) however *ret* rearrangements are known to occur sporadically in PTC without a history of radiation exposure. To date ret/PTC rearrangements have not been described in non-thyroid malignancies.

High prevalence of ret/PTC rearrangements (especially ret/PTC-3) has been demonstrated in early PTC cases that developed in Belarus within the first decade after the Chernobyl accident. In 1994, Ito et al, reported the presence of RET rearrangements in 57% of post Chernobyl PTCs. (Ito et al., 1994) Similar results were obtained by two separate groups on a series of Belarussian samples. (Fugazzola et al., 1995; Rabes et al., 2000) Nikiforova et al analysed post Chernobyl Belarussian papillary carcinomas and found that 58% of the cases were positive for ret/PTC-3, and 16% for ret/PTC-1. (Nikiforov et al., 1997) Intriguingly, 79% of solid variant tumours had ret/PTC-3 whereas only 7% had ret/PTC-1. Thomas *et al* also indicated that a high frequency of ret/PTC activation is a feature of both Belarusian and Ukrainian cases; indeed a strong correlation between the solid-follicular variant of papillary carcinoma and activation of the ret/PTC-3 oncogene was observed.(Thomas et al., 1999)

Follicular-variant of PTC is characterised by solid nests of tumour cells, often with small follicular lumina; it may also show a minor papillary component. This tumour phenotype is consistently found in post-Chernobyl cases. These tumours tends to follow an aggressive clinical course showing intra-glandular dissemination and extension to the peri-thyroid tissue

with distant metastasis at clinical presentation. Targeted expression of the ret/PTC-3 oncogene in transgenic mice generates aggressive carcinomas with a prevalent solid component which are highly prone to metastasis to regional lymph nodes. (Jhiang et al., 1998) Similarly, transgenic studies have shown that targeted expression of the ret/PTC-1 oncogene in the thyroid gland generated papillary carcinomas of the classic type. These results indicate that ret/PTC-1 is favoured in thyroid tumours displaying classic papillary morphology with distinctive nuclear features in contrast to the ret/PTC-3 isoform which tends to be observed in follicular-variant of PTC. ***More importantly, these reports suggest that the different types of ret rearrangement confer neoplastic thyroid cells with distinct phenotypic properties.***

It is still unknown what differentiates the two RET oncoproteins to explain their different effects in vivo. The RET component of the two chimeric proteins is identical, and recent findings show there is no significant difference in the extent of activation of the intrinsic RET kinase function in ret/PTC-1 and ret/PTC-3. Thus although the function of H4 and RFG genes is still ambiguous it is tempting to speculate that the functional difference or difference in oncogenicity between the two ret fusion partners many contribute to the different neoplastic phenotypes. Celetti *et el* reported that over-expression of the H4 gene was able to induce apoptosis of thyroid follicular epithelial cells. (Celetti et al., 2004) No known function has been described for RFG. Basolo et al have reported that ret/PTC-3 has higher mitogenic and signalling activity than ret/PTC-1 and that activation of the MAPK cascade by ret/PTC-3 is greater than ret/PTC-1 in epithelial thyroid cells in vitro. Furthermore, ret/PTC-3 expressing thyroid cells have also been shown to have a significantly higher proliferation rate. (Basolo et al., 2002) Moreover, ret/PTC-3 rearrangement is particularly prevalent in radiation induced tumours in children but whether the aggressive solid variant is linked

primarily to the nature of the carcinogenic agent or to the age of the child remains to be determined. (Elisei et al., 2001)

3.2.3 Ret rearrangements in alternate thyroid tumour histotypes

Previous work has identified *ret/PTC* activation in other thyroid tumour histotypes such as oncocytic adenomas and carcinomas, (Cheung et al., 2000) and non-neoplastic entities such as hyperplastic nodules (Elisei et al., 2001; Ishizaka et al., 1991) and Hashimoto's thyroiditis (Rhoden et al., 2006; Sheils et al., 2000; Wirtschafter et al., 1997). These reports challenge the validity of *RET/PTC* as a tumour marker and its specificity for papillary thyroid carcinoma.

3.2.4 Role of ret in tumourigenesis

Several publications have reported *ret* oncogene involvement in the regulation of various cancer-related processes such as cell proliferation and differentiation, apoptosis, and cell structure and motility. (Borrello et al., 2005; Fischer et al., 1998; Fusco et al., 2002; Jhiang, 2000) The signalling and modulating pathways that have been shown in previous reports to be associated with *ret* oncogene activation are illustrated in Figure 3.2. (Musholt et al., 2006)

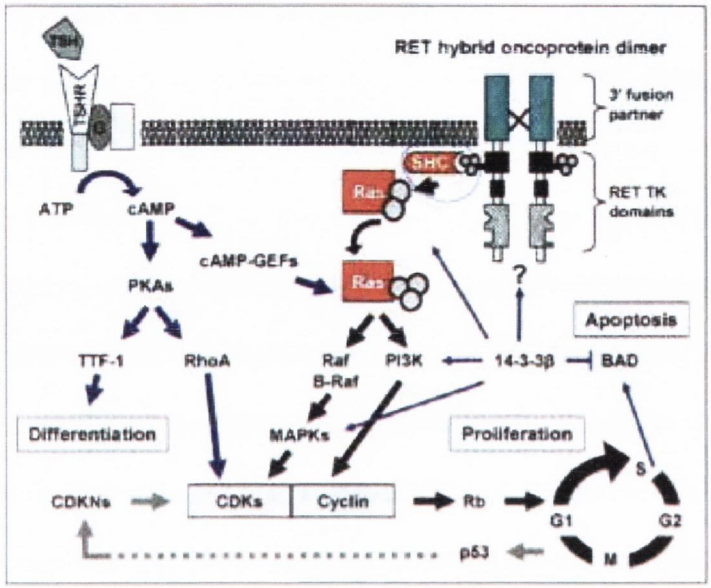

Figure 3.2 RET associated signalling and modulating pathways in the oncogenesis of PTC. (Musholt et al., 2006)

Activation of the RET hybrid receptor following chromosomal rearrangement with the promoter of a fusion partner gene, leads to tyrosine kinase (TK) activity, which initiates cell proliferation through RAS pathway involving Raf, B-Raf and phosphatidylinositol-3-kinase (PI3K). Processes affected include differentiation, cell cycle control, apoptosis and proliferation. 14-3-3β interacts with proteins of several levels of the Ras signal cascade. Upregulation of 14-3-3 β will result in increased mitosis and will halt apoptosis through signalling in the cascade and inhibiting the pro-apoptotic protein BAD. (Musholt et al., 2006)

3.3 Aim

The primary objective of this study was to investigate the possibility that *RET/PTC* rearrangements may be expressed in non-thyroid papillary tumours using three independent techniques.

3.4 Materials and Methods

Ethical approval for the study in accordance with the Helsinki Declaration was obtained from the St. James's and Federation of Dublin Voluntary Hospitals Ethics committee.

3.4.1 Case Selection

Papillary tumours were selected from archival formalin-fixed, paraffin-embedded tissue (N=57), between the years 1991-2007 from St. James's Hospital and The Adelaide and Meath National Children's Hospital (Dublin, Ireland). The study cohort included 15 primary peritoneal carcinoma, 10 serous tumours of the ovary (including 2 borderline tumours), 10 papillary renal cell carcinoma, 10 urothelial cell carcinoma, 5 serous carcinoma of the endometrium, 2 endometrioid carcinoma of the endometrium, 1 adenoacanthoma of the endometrium and 4 carcinomas with mixed phenotypes (Figure 3.3). Slides were reviewed by a histopathologist (RF), original diagnoses confirmed and classified according to World Health Organisation guidelines. Primary peritoneal carcinoma was identified according to Gynaecological Oncology Group criteria. Patient data is summarised in Table 3.1.

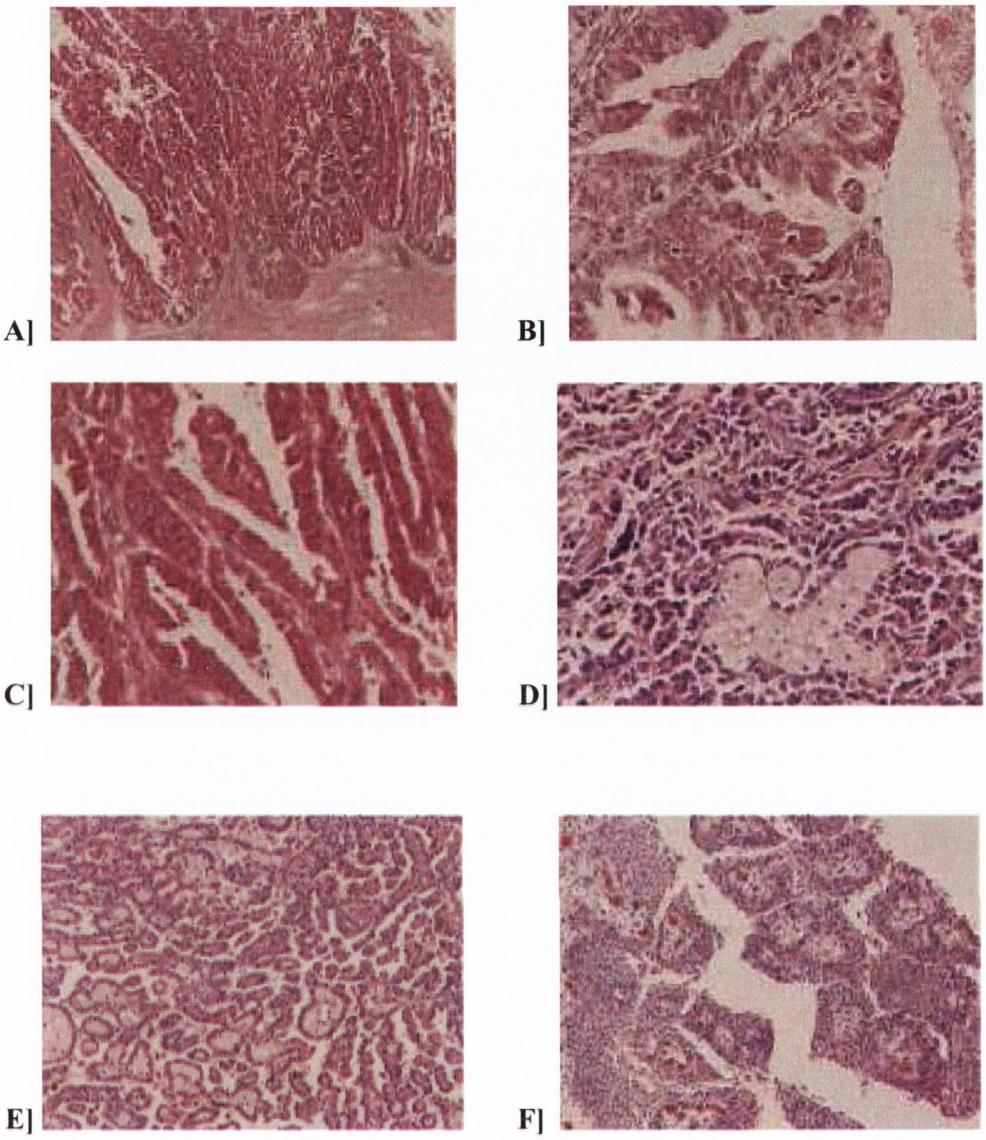

Figure 3.3 H&E photomicrographs of sample papillary tumours included in study cohort.

A) serous carcinoma of the endometrium (x10), (B) primary peritoneal carcinoma (x40), (C) serous carcinoma of the ovary (x10), (D) papillary renal cell carcinoma type 2 (x10), (E) papillary renal cell carcinoma type 1 (x10), (F) urothelial cell carcinoma (x10).

Sample	Tissue Source	Histopathology	Age	Sex	Grade[β]	pTNM Stage[γ]	% split RET signals[δ]	Ret/PTC1 rearrangement[ε]	RET protein[μ]
1	Bladder	Urothelial ca	73	M	High	T1 at least	3	0	0
2	Bladder	Urothelial ca	70	F	Low	TA	3.3	0	0
3	Bladder	Urothelial ca	71	M	Low	TA	10.1	0	0
4	Bladder	Urothelial ca	55	F	High	T1	5.6	0	0
5	Bladder	Urothelial ca	66	F	High	TA	3	0	2
6	Bladder	Urothelial ca	79	F	High	TA	1	0	0
7	Endometrium	Adenoacanthoma	56	F	2	T3A	8.6	0	0
8	Endometrium	Serous ca (squamous differentiation)	91	F	2	T3A	2	0	3
9	Endometrium	Serous ca	57	F	3	T1B	0	0	0
10	Endometrium	Serous ca	52	F	3	T1A at least	3	0	0
11	Endometrium	Endometrioid ca	77	F	1	T1C	3.6	0	0
12	Endometrium	Serous ca	57	F	3	T2A	6.1	0	0
13	Endometrium	Serous ca	49	F	3	T3B	1.8	0	0
14	Endometrium	Serous ca	63	F	3	T4	0	0	0
15	Endometrium	Endometrioid ca	57	F	3	T1B	0	0	0
16	Kidney	Urothelial ca	57	M	High	T3	0	0	0
17	Kidney	Urothelial ca	57	M	High	T3	ND	0	0
18	Kidney	Papillary renal cell ca. type 2	66	F	3	T2	0	0	0
19	Kidney	Papillary renal cell ca. type 2	52	F	3	T1A	7	0	0
20	Kidney	Papillary renal cell ca. type 2	52	M	2	T2	1	0	0
21	Kidney	Papillary renal cell ca. type 1	52	M	2	T1	2.6	0	0
22	Kidney	Papillary renal cell ca. type 1	56	M	2	T2	7	0	0
23	Kidney	Papillary renal cell ca. type 2	56	M	4	T2	6.3	0	0
24	Kidney	Papillary renal cell ca. type 1	48	M	2	T1B	7.9	0	1
25	Kidney	Papillary renal cell ca. type 1	62	M	2	T1	12.8	0	0
26	Kidney	Papillary renal cell ca. type 1	49	M	3	T1B	6.6	0	0
27	Kidney	Papillary renal cell ca. type 2	49	M	3	T2	4.7	0	0
28	Kidney	Urothelial ca	63	M	High	T3	3	0	3
29	Kidney	Urothelial ca	67	F	High	TA	6	0	0
30	Ovary	Serous ca	54	F	1	T1A	3	0	1
31	Ovary	Serous ca	86	F	1	T1A	3	0	0
32	Ovary	Serous ca	49	F	2	T3C	10	0	0
33	Ovary	Mixed serous & endometrioid ca	59	F	2	T1A	6.9	0	0
34	Ovary	Serous ca	66	F	3	T3C	1.3	0	0
35	Ovary	Serous ca	76	F	3	T3C	1.2	0	0
36	Ovary	Borderline serous tumour	47	F	N/A	N/A	7.4	0	0
37	Ovary	Borderline serous tumour	58	F	N/A	N/A	3	0	0
38	Ovary	Primary peritoneal ca	68	F	3	T3C	5	0	0
39	Ovary	Primary peritoneal ca (<15% clear cell ca.)	76	F	2	T3C	1.2	0	0
40	Ovary	Primary peritoneal ca	50	F	3	T3C	21.1	1	1
41	Ovary	Serous ca	59	F	2	T3C	ND	0	0
42	Ovary	Primary peritoneal ca	84	F	2	T3C	1.1	0	0
43	Ovary	Primary peritoneal ca	64	F	3	T3C	5	0	1
44	Ovary	Primary peritoneal ca	54	F	3	T3C	18.3	1	3
45	Ovary	Primary peritoneal ca	50	F	3	T3C	3	0	0
46	Ovary	Primary peritoneal ca	72	F	3	T3C	0	0	0
47	Ovary	Primary peritoneal ca	71	F	2	T3C	2	0	0
48	Ovary	Seromucinous ca	77	F	2	T3	4.9	0	1

49	Ovary	Primary peritoneal ca	81	F	2	T3B	14.1	1	1
50	Ovary	Serous ca	64	F	3	T2C	3.6	0	0
51	Ovary	Primary peritoneal ca	69	F	3	T3C	1.9	0	0
52	Ovary	Primary peritoneal ca	64	F	3	T3C	7	0	3
53	Ovary	Primary peritoneal ca	71	F	3	yT3a	10.6	0	1
54	Ovary	Serous ca	65	F	3	T3C	1.9	0	0
55	Ovary	Primary peritoneal ca	63	F	3	T3C	4	0	0
56	Ovary	Primary peritoneal ca	73	F	3	T3	5	0	0
57	Ovary	Primary peritoneal ca	38	F	2	T3A	3.1	0	0

Table 3.1: Summary of patient clinicopathological data.

β By definition, endometrial serous carcinomas are high grade. Urothelial carcinomas were graded according to the WHO 2004 classification system.

γ Tumours were staged using the UICC 2002 Staging system. δ By FISH. ε By RT-PCR; 0= negative, 1=positive

μ *RET* protein was scored from 0-3 according to the intensity of the immunohistochemical stain: 0= negative, 1=weak, 2=moderate, 3=strong.

Abbreviations: N/A = not applicable; ND = not detected; ca = carcinoma

3.4.2 Interphase FISH analysis for ret/PTC rearrangement detection

Interphase FISH was performed on 10-µm paraffin-embedded sections (62 samples, including 57 tumours and 5 reference cases) following previous validated protocols. (Unger et al., 2004) All sections had been microdissected to ensure that only tumour tissue was present on the slide for subsequent laser scanning microscopy scoring. DNA probe generation from three yeast artificial chromosome clones (313F4, 214H10, 344H4) covering the *RET* locus and probe hybridisation were performed as previously described (see Figure 3.4). (Unger et al., 2004) A detailed protocol is described in chapter 2.9. Microscopic analyses were carried out using a confocal laser scanning microscope (Zeiss LSM 510, Zeiss, Jena, Germany).

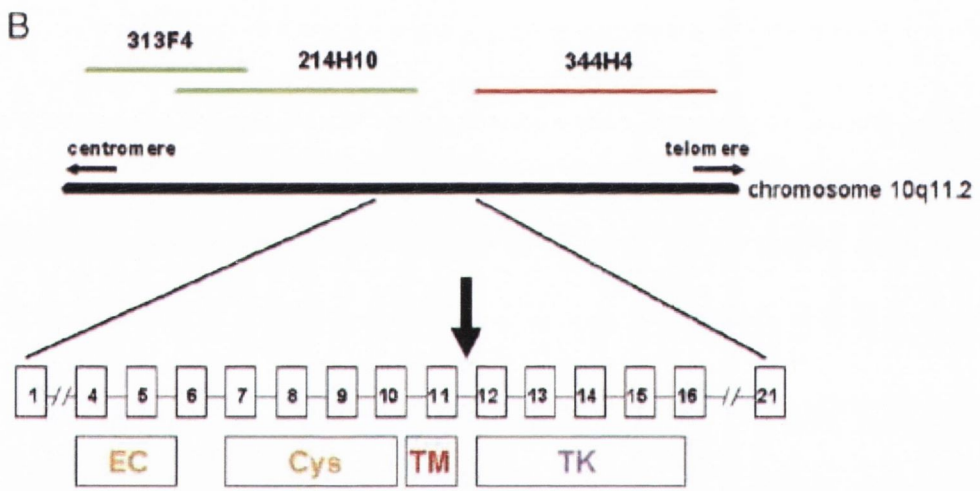

Figure 3.4 Mapping of YAC probes 313F4, 214H10, 344H4 on chromosome 10q11.2.

YAC clones 313F4 and 214H10 (FITC, labelled green) map proximal to and include the ret locus, 344H4 (Cy3-labelled, red) maps distal to ret. Exons and different parts of the ret gene are indicated in the lower diagram (EC, extracellular domain; Cys, cysteine-rich domain; TM, transmembrane domain; TK, tyrosine kinase domain). (Unger et al., 2004)

Cell nuclei exhibiting rearranged *RET* gene show a split FISH signal in red (distal to *RET*) and green (proximal to *RET*) in addition to an overlapping signal. Normal cells show 2 overlapping nuclei. 100 nuclei with strong and well delineated signals were scored. Only cells with two overlapping signals or one split and one overlapping signal were counted to ensure only complete cell nuclei had been scored. Images of tumour cell nuclei were captured as previously described. (Unger et al., 2004) The TPC-1 cell line carrying a *RET/PTC*1 rearrangement was used as control, with rearrangement positive cells present in each cell scored (Figure 3.5).

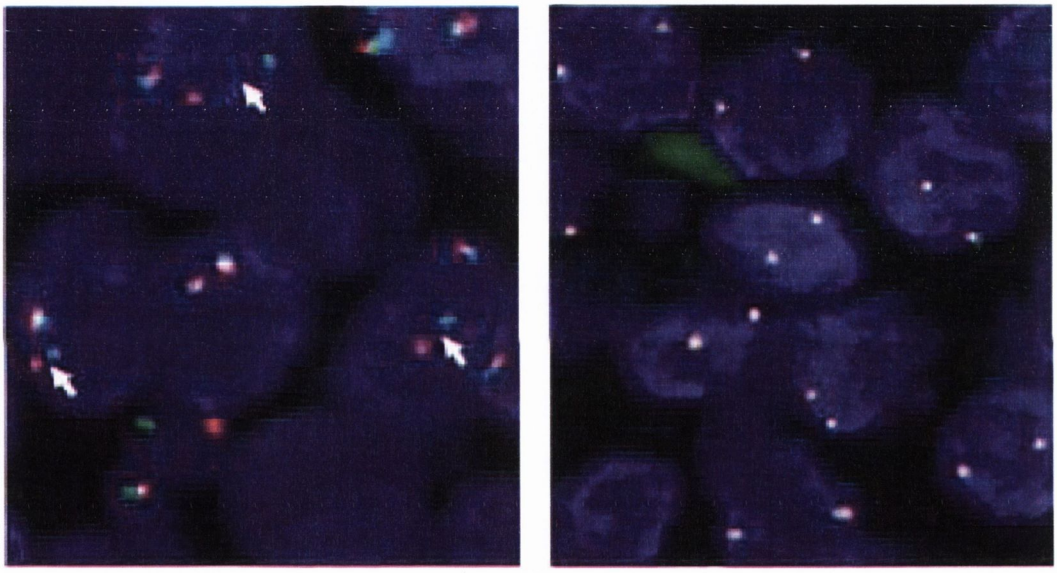

Figure 3.5 FISH analysis with ret-specific YAC probes using confocal laser scanning microscopy (x40).

Left-hand panel exhibits aberrant cells in the TPC-1 cell line exhibiting split ret signals in non-overlapped nuclei (arrows). Right hand panel is of a normal area from a reference case of kidney exhibiting overlapping (yellow) signals.

To determine a meaningful cut-off level indicating a significantly increased proportion of cells with split FISH signals compared with baseline frequency, epithelial cells from five normal samples including normal kidney, ovary and endometrium were scored after careful review of the histology sections to exclude samples with any significant alteration (Table 3.2). The mean value(x) and SE of cells with split signals was determined (Figure 3.6). The mean value (x) ± SE value was 0.8 ± 0.8. Data from a previously analysed cohort of normal thyroids (n=4) selected for interphase FISH was used to validate the FISH scores from the above cohort. (Rhoden et al., 2006; Unger et al., 2004) The resulting x ± SE was 1.5 ± 0.7. No statistically significant difference in FISH score difference between normal thyroids and reference cases was observed (p=0.41). For calculation of a cut-off level, a stringent value of 12.75 times x, equivalent to approximately 10.2% of aberrant cells was adopted to eliminate false-positive cases.

Case	Non-thyroid	Thyroid
1	0	0.9
2	0	2
3	0	0
4	0	3
5	4	-

Table 3.2 Summary of the number of split FISH signals in epithelial cells from non-thyroid (kidney, ovary and endometrium) samples and epithelial cells from thyroid samples.

Non-thyroid cases: case 1= endometrium, case 2&3= ovary, case 4&5=kidney.

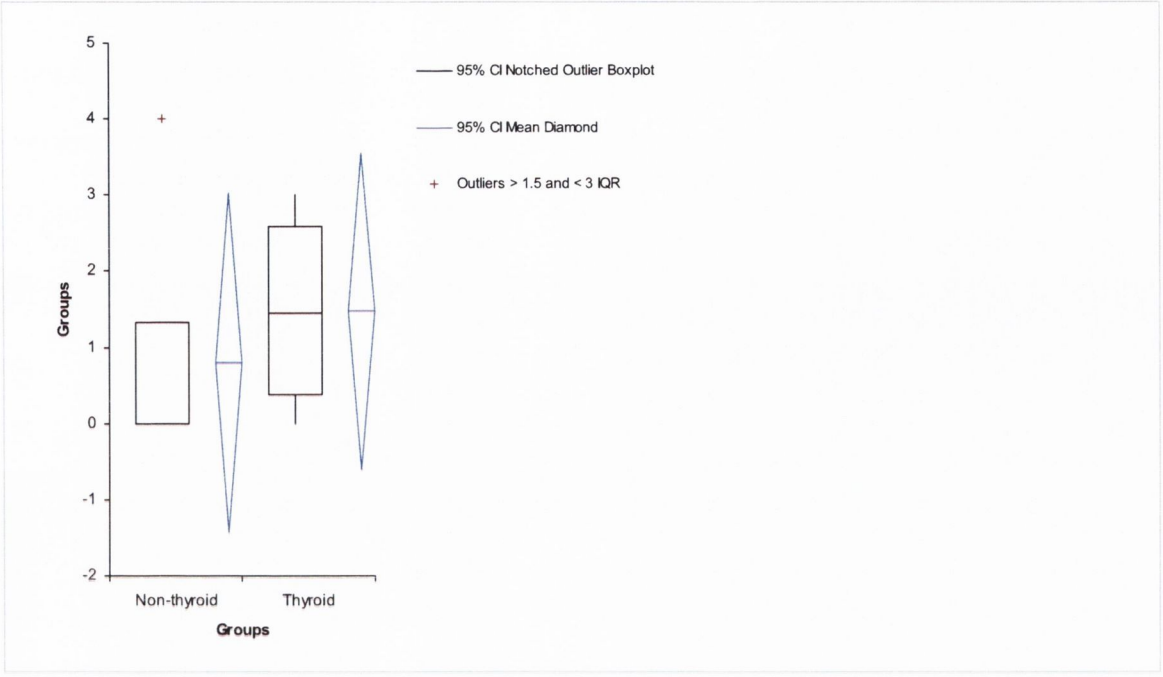

Figure 3.6 Box-plot summarizing the number of split FISH signals in epithelial cells from non-thyroid (kidney, ovary and endometrium) samples and epithelial cells from thyroid samples.

The mean value ± SE was 0.8 ± 0.8 for non-thyroid samples and 1.5 ± 0.7 for thyroid samples. No statistically significant difference in FISH score between normal thyroids and non-thyroid samples was observed (p=0.41).

3.4.3 Interphase FISH for ploidy analysis

Interphase FISH was performed using centromeric probes for chromosomes 10 (green) and 17 (red) on *RET/PTC* rearranged cases for determination of ploidy status (Figure 3.7). Microscopic analyses and image capture was performed as described above. 100 nuclei with strong and well delineated signals were scored. Only cells with two or more signals were counted to ensure only complete cell nuclei had been scored.

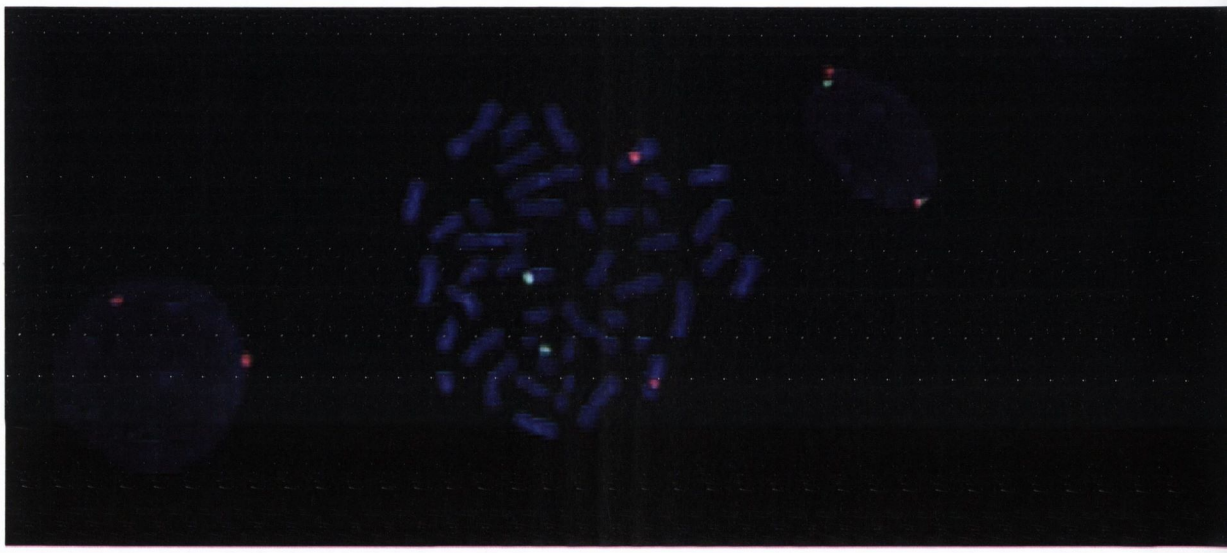

Figure 3.7 FISH image of metaphase spreads with centromeric probes for chromosome 10 (green) and chromosome 17 (red) using confocal laser scanning microscopy.

3.4.4 Total RNA and DNA extraction

5μm sections were cut from each paraffin block, dewaxed and stained with haemotoxylin and eosin (H&E). All tumours (n=57) were laser-capture microdissected using the PixCell 11™ System (Arcturus Engineering Inc., CA, USA) to yield homogenous populations of malignant epithelial cells for subsequent expression analysis. Following microdissection the Capsures™ were placed in sterile Eppendorf tubes and RNA extraction performed using the PURESCIPT® RNA Isolation Kit (Gentra Systems Inc., MN, USA) with modification of the protocol as previously described. (Sheils and Sweeney, 1999) DNA extraction was preformed using PUREGENE® DNA Isolation kit (Gentra Systems Inc., MN, USA).

3.4.5 RT-PCR for ret/PTC-1 expression

Extracted RNA was processed using TaqMan™ One-Step RT-PCR, which offers the convenience of a single tube preparation for RT and PCR amplification and reduces the risks of contamination. The principles of the TaqMan™/5'nuclease assay system have already been described and are detailed in full in chapter 2.7.2. (Pasini et al., 1995) To compensate for potential degradation of target RNA, Taqman™ One-Step RT-PCR was performed in parallel on RNA from each sample using glyceraldehyde phosphate dehydrogense (GAPDH) as an endogenous control. This ensured the integrity of the RNA extracted from paraffin tissue. End-point detection was used to confirm the presence or absence of *GAPDH* and the *RET/PTC*1 chimeric transcript.

One-Step RT-PCR was carried out according to the manufacturer's instructions using an Applied Biosystems 7000 Sequence Detection system (Applied Biosystems, CA, USA). All primers/probes were designed using ABI Prism Primer Express 1.5 software (Applied Biosystems, Chesire, UK) with the probes spanning exonic junctions. Sequences have been

previously published. (Smyth et al., 2001) All probes used in the TaqMan™ reactions were designed to have non-flouresecent quenchers and minor groove binding modifications. At least six negatives were included in each RT-PCR reaction. For *RET/PTC*1 and *GAPDH* detection, cDNA from the cell line TPC-1 was included as a positive control. All samples were run in triplicate.

3.4.6 Immunohistochemistry

Mouse monoclonal IgG antibody directed against the C-terminal (containing the TK domain) of the human *RET* oncoprotein (Labvision/Neomarkers Corp., CA, USA) was used to detect wild-type and rearranged *RET*. Antibody was standardized to a 1:15 dilution. 4μm tissue sections were cut, dewaxed and incubated in absolute methanol solution with 0.3ml of hydrogen peroxide for 30 minutes. Antigen retrieval was carried out by boiling the slides in 0.01mM citrate buffer, pH 6.0, for 90 sec. Slides were then treated with blocking serum for 10 minutes after which they were incubated with primary antibody at 25°C for 60 minutes, followed by biotinylated anti-rabbit IgG (Vectostain ABC kits, Vector Laboratories, Inc) and premixed ABC reagent (Vector Laboratories, Inc).

Negative controls replaced primary antiserum with nonimmune bovine serum. Chromogen detection was performed with diaminobenzdine (DAKO Corp., Carpiteria, CA) solution (0.5ml of stock DAB in 4.5ml of Tris buffer with 20μl of hydrogen peroxide). Slides were counterstained with haemotoxylin. Two pathologists (RF and SF, blinded to the original diagnosis) scored the sections independently. A score of 0-3 (0= absent; 1=weak; 2 = moderate; 3= strong) was assigned to the intensity of staining (Figure 3.8). Only slides with >10% quantity of tumour staining were deemed positive.

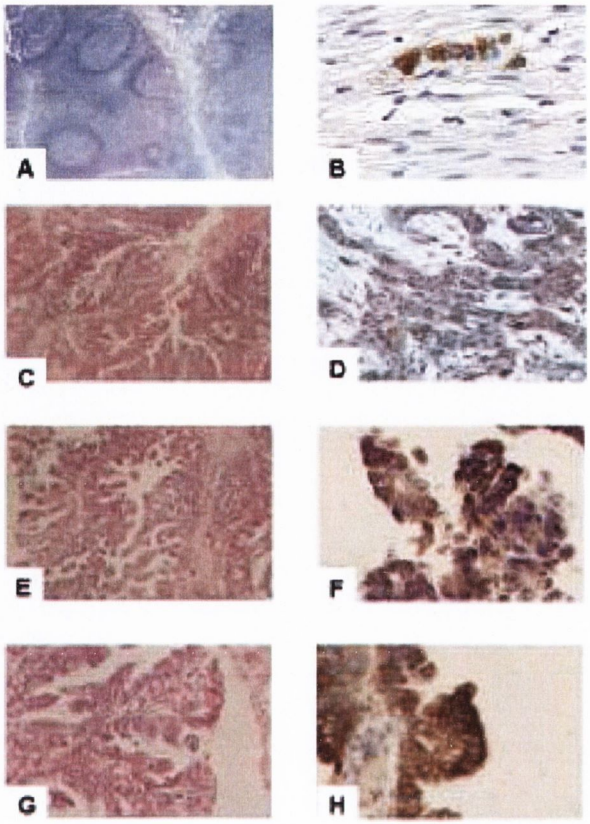

Figure 3.8 Immunohistochemical staining for ret oncoprotein. A, Negative control (tonsil, x 20); B, Positive control (enteric ganglion cells of appendix, x20); C(x20), E(x20), G(x40) primary peritoneal carcinoma (cases 49, 52 and 44) demonstrating D, 1+ (x20), F, 3+ (x40) and H, 3+ (x40) cytoplasmic staining for ret oncoprotein.

Tumours positive for *RET/PTC*1 by RT-PCR were also stained for TTF-1 and thyroglobulin (both DAKO Corp., Carpiteria, CA), at dilutions of 1:1400 and 1:40 using the standard ABC technique, to rule out the possibility of thyroid metastasis.

3.4.7 Statistical analysis

The associations between *RET/PTC* rearrangement and clinicopathological characteristics were examined by means of Fisher's exact test (Analyse-It™ Software Ltd). Comparison of FISH scores was examined by means of a Mann-Whitney test. All tests were two-tailed, and the significance level was set at $p<0.05$.

3.5 Results

Table 3.1 is a summary of the results. 13 patients were male of whom 8 had papillary renal cell carcinoma and 5 had urothelial cell carcinoma. The remaining 44 patients were female. The median age of all the patients was 63 years (male 56 years, female 64 years).

3.5.1 Interphase FISH analysis

FISH has the potential to detect *RET* rearrangements regardless of the specific fusion partner involved and allows examination of the rearrangement at a single-cell level (see Figure 3.9). Five of 57(9%) papillary tumours, corresponding to 4 of 15 (27%) primary peritoneal carcinoma and 1 of 10 papillary renal cell carcinoma (10%) had a proportion of cells with split *RET* signals above the cut-off level. (A further 2 of 57 (3.5%) papillary tumours, corresponding to 1 of 10 (10%) urothelial carcinoma and 1of 10 (10%) serous tumours of the ovary had a proportion of cells with split signals that were borderline with respect to significant split *RET* signals). The highest frequency of rearranged cells after FISH interphase analysis was 21.1 (case 40). No extra chromosome 10 copies were detected in these five positive cases (Figure 3.10).

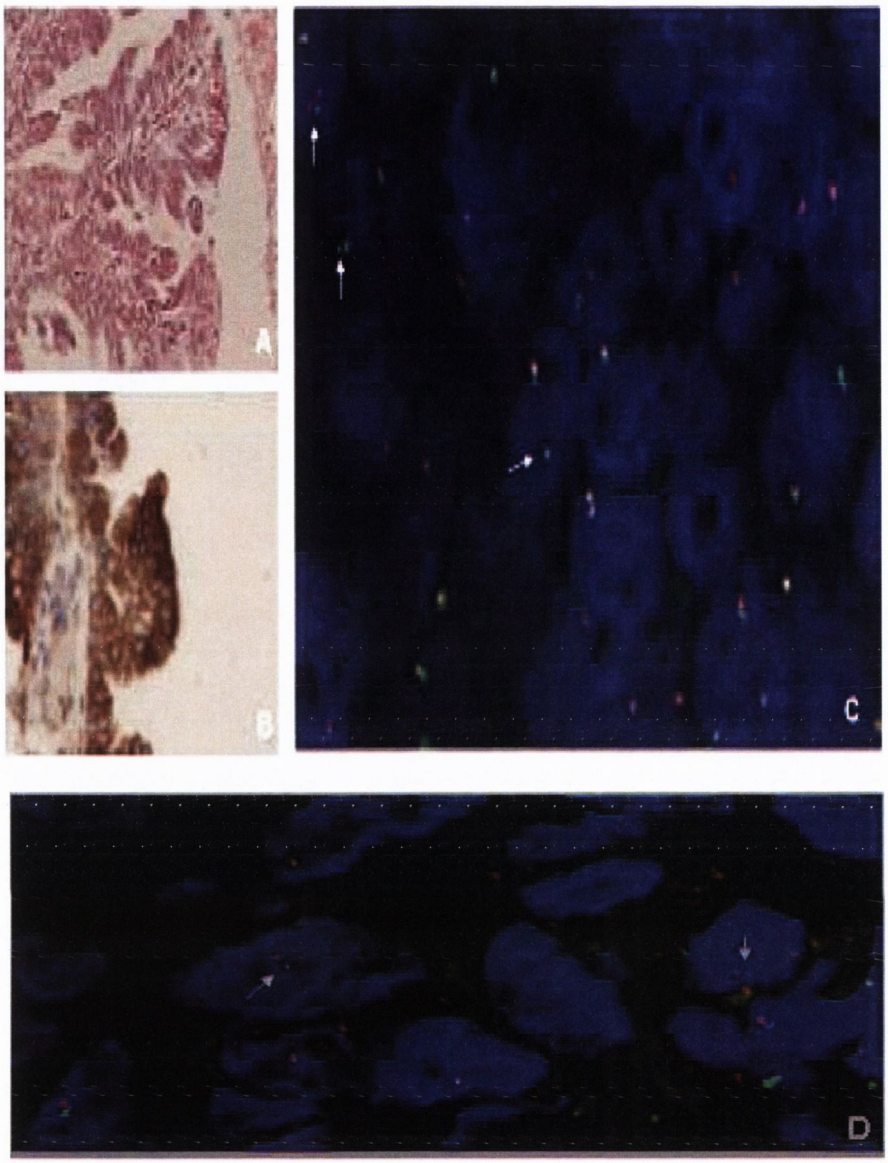

Figure 3.9: Histological appearance of primary peritoneal carcinoma with corresponding FISH images.

Split FISH signals are highlighted with an arrow. Overlapped signals are yellow. A, H&E section of primary peritoneal carcinoma (case 44, x 20). B, *RET* immunohistochemical section of corresponding primary peritoneal carcinoma (x 20). C, FISH image of corresponding primary peritoneal carcinoma (x40). D, FISH image of alternate area in corresponding case highlighting split FISH signals (x60).

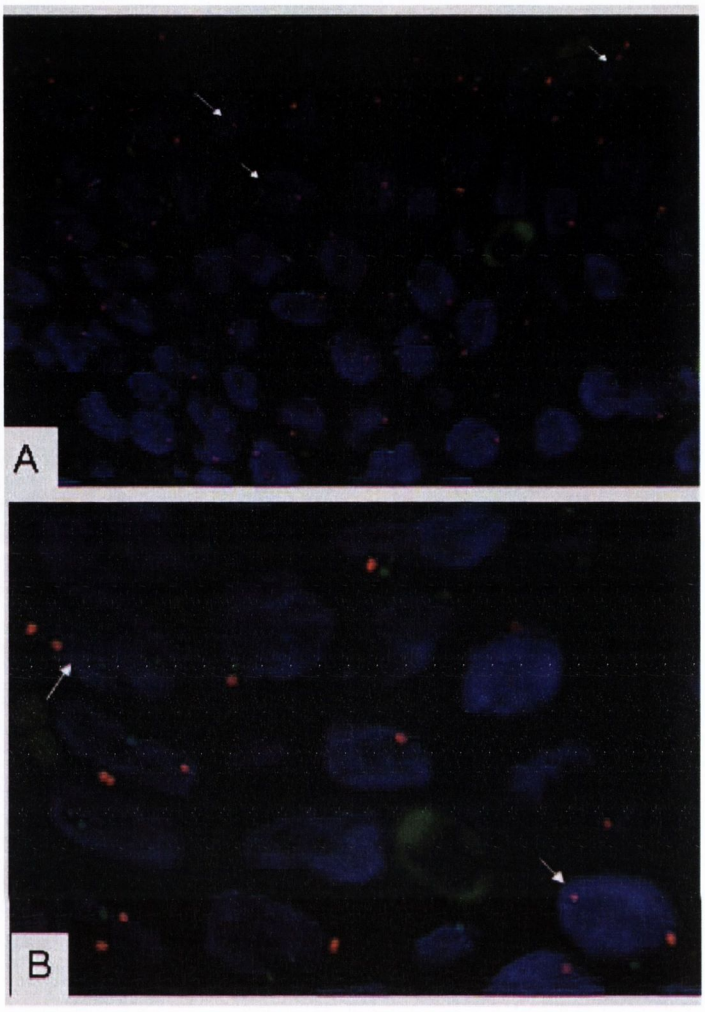

Figure 3.10 FISH analysis of ret/PTC positive case (no. 44) for ploidy status using centromeric probes for chromosome 10 (green) and chromosome 17 (red).

Diploid nuclei are highlighted with an arrow (i.e. 2 green and 2 red signals). Ax10. Bx40.

3.5.2 RT-PCR for ret/PTC-1 expression

All samples had detectable GAPDH (Figure 3.11) Three of 57 (5%) papillary tumours had detectable *RET/PTC*1 mRNA, corresponding to 3 of 15 (20%) primary peritoneal carcinoma. The remaining 54 of 57 (95%) papillary tumours had no detectable *RET/PTC*1 chimeric transcript (Table 3.3).

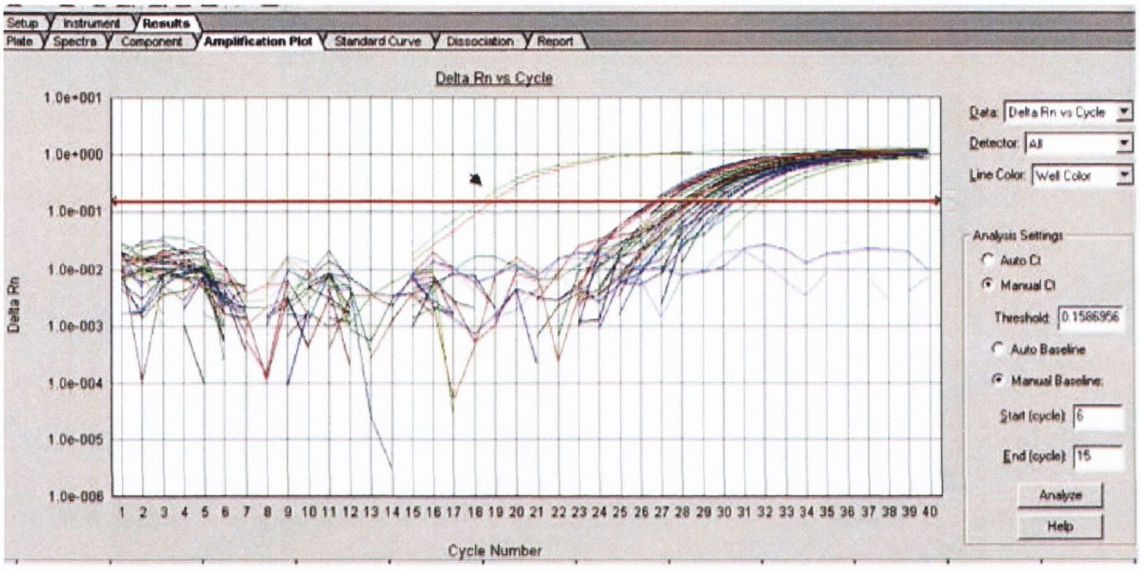

Figure 3.11 Sample real-time output from GAPDH amplification plot.

The GAPDH status of each sample was determined to insure the integrity of extracted RNA. Note end-point detection was used to confirm the presence or absence of GAPDH. Arrow = Amplification plot demonstrating the presence of GAPDH transcripts in the positive control (TPC-1 cell line) at 19 cycles of PCR. The remaining amplification plots demonstrate the presence of GAPDH transcripts in samples at 26 – 31 cycles of PCR.

Sample	Mean Run
1	1.4522
2	1.4961
3	0.913
4	0.9205
5	0.828
6	0.7355
7	1.4932
8	1.4595
9	1.548
10	1.5338
11	1.5378
12	1.4476
13	0.8035
14	0.837
15	0.686
16	1.4677
17	1.023
18	1.486
19	1.359
20	1.05
21	1.1325
22	1.4905
23	1.077
24	1.0375
25	0.96
26	1.091
27	1.135
28	0.8915
29	0.6955
30	1.3949
31	1.3576
32	1.4647
33	1.4087
34	1.4403
35	1.4867
36	1.4142
37	1.4608
38	1.4855
39	1.5147
40	***1.7263***
41	1.2193
42	1.3496
43	1.2752
44	***2.989***
45	0.722
46	1.3477
47	1.3903
48	1.3585
49	***1.77***
50	1.158
51	0.884
52	0.8105
53	0.786
54	0.9515
55	0.805
56	1.031
57	0.685
NTC	*0.936*
TPC-1	***3.29***

Table 3.3 Results of Plus/Minus TaqMan RT-PCR for ret/PTC1 chimeric transcript. Normalised reporter signal (Rn) values for samples 1-55, NTC (No Template Control) and positive control (TPC-1 cell line). Positive results are highlighted in bold.

3.5.3 Immunohistochemistry for ret protein

Twelve of 57 (21%) papillary tumours had detectable wild type or *RET/PTC* chimeric protein. This corresponds to 6 of 15 (40%) primary peritoneal carcinoma, 2 of 10 (20%) urothelial carcinoma, 3 of 17 (18%) serous tumours (endometrial and ovary) and 1 of 10 (10%) papillary renal cell carcinoma (see Figure 3.10). No ret/PTC-1 positive tumour demonstrated thyroglobulin or TTF-1 positive immunohistochemical staining (Figure 3.12).

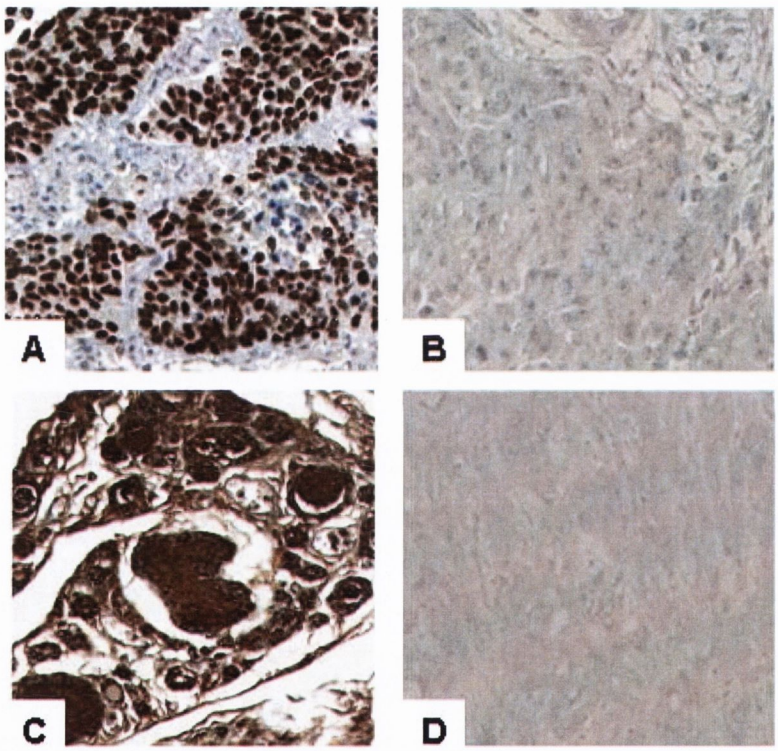

Figure 3.12 Immunohistochemical staining for TTF-1 and thyroglobulin.

A, nuclear staining for TTF-1 in lung small cell carcinoma (positive control, x 20); B, absence of nuclear staining for TTF-1 in a ret/PTC-1+ case of primary peritoneal carcinoma (x20); C, cytoplasmic staining for thyroglobulin in follicular cells of thyroid gland and staining for colloid (positive control, x 20); D, absence of cytoplasmic staining for thyroglobulin in a ret/PTC-1+ case of primary peritoneal carcinoma (x20).

3.5.4 Comparison between FISH, RT-PCR and immunohistochemistry

A comparison between the different approaches used in this study is shown in Figure 3.13. All 3 cases (cases 40, 44 and 49) of primary peritoneal carcinoma with detectable *RET/PTC*1 mRNA by RT-PCR exhibited rearranged cells in FISH analysis above the cut-off level and demonstrated *RET* protein expression.

A single case of primary peritoneal carcinoma (case 53) had split FISH signals in more than 10.2% of cells analysed and demonstrated *RET* protein expression. However no *RET/PTC*-1 mRNA was detected by RT-PCR Therefore, it is likely that this case harbours a *RET* rearrangement other than H4/*RET* (*RET/PTC*-1). A single case of papillary renal cell carcinoma (case 25) showed neither *RET* protein expression or demonstrable *RET/PTC*1 mRNA by RT-PCR. However this case exhibited split FISH signals in more than 10.2% of cells analysed. It is likely, that this case harbours a *RET* rearrangement other than *H4/RET* (*RET/PTC*1) which is not expressed at the protein level, possibly as a result of post-transcriptional regulation. Alternatively, the sensitivity of both the RT-PCR and immunohistochemistry was not high enough to detect a few *RET/PTC*1 rearranged cells which may also be a reflection of tumour heterogeneity. (Unger et al., 2004)

The last subgroup consists of 2 cases of primary peritoneal carcinoma (cases 43 and 52), 2 cases of urothelial cell carcinoma (cases 5 and 28), 3 serous tumours cases (endometrial and ovary: cases 8, 30 and 48) and 1 case of papillary renal cell carcinoma (case 24). None of these cases had demonstrable *RET/PTC*1 mRNA by RT-PCR or split FISH signals greater than the cut-off

level. However they all demonstrated *RET* protein expression which must logically be the wild-type protein. The remaining 44 cases did not demonstrate *RET* rearrangements by any of the three methodologies.

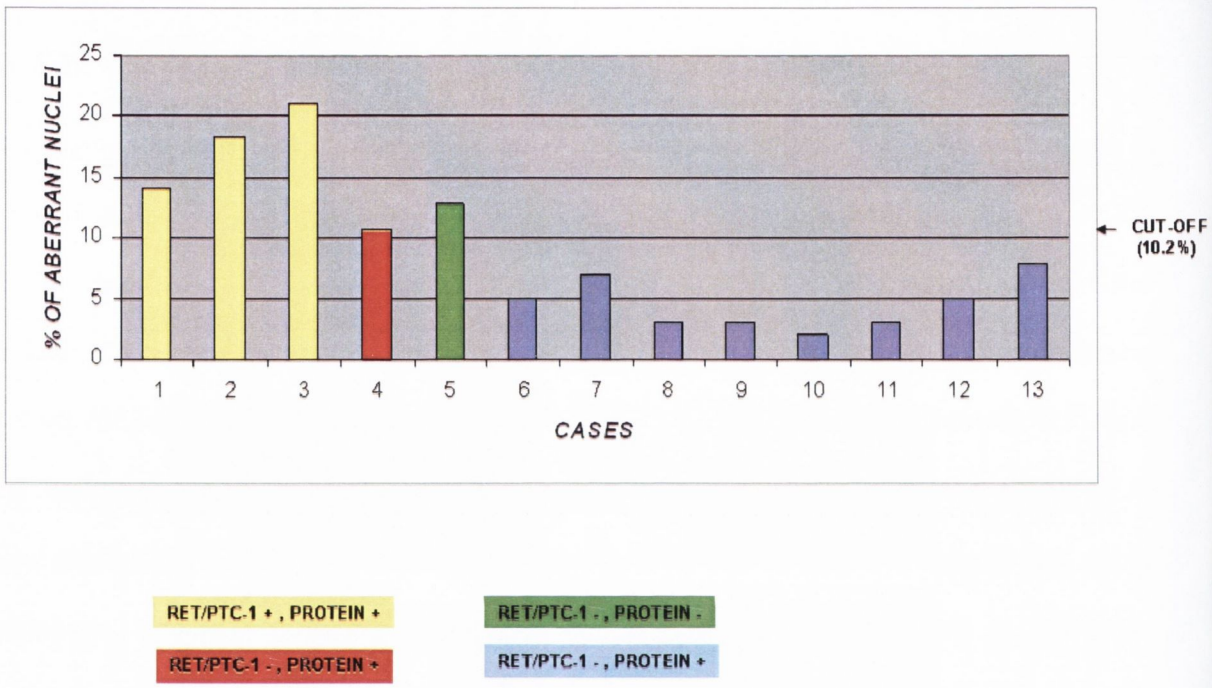

Figure 3.13 Comparison between FISH, RT-PCR and immunohistochemistry.

The columns represent the frequency of aberrant cells per cases detected by interphase FISH. For interpretation of FISH results, a cut-off threshold of 10.2% (arrow) was adopted. Different column colours indicate corresponding RET/PTC-1 and RET protein expression.

3.5.5 Correlation of ret/PTC rearrangement with clinicopathological features

Our next investigation was to consider whether the presence of *RET/PTC* rearrangement had any relationship with the clinicopathological characteristics of the study cohort. We found that there was a statistically significant relationship between the presence of *RET/PTC* rearrangement and tumour histotype (see Table 3.4). Cases with a positive *RET/PTC* rearrangement showed a significant association with primary peritoneal carcinoma histotype (p=0.03).

Characteristics	Cases	ret/PTC		P-value[α]
		Pos	Neg	
Histotype				
Primary Peritoneal ca.	15	4	11	0.03
Other	42	1	41	
Gender				
Male	13	1	12	1
Female	44	4	40	
Age				
<50	7	0	7	1
≥50	50	5	45	
Grade				
I	5	0	5	1
II-III	52	5	47	
Stage				
I-II	28	1	27	0.37
III-IV	29	4	25	

Table 3.4: Relationship between *RET/PTC* rearrangement and clinicopathological characteristics of the study cohort.

Abbreviations: Pos = positive; Neg = negative. **α** Fisher's exact test (P<0.05 for significance).

3.6 Discussion

Specific mutations in the *ret* oncogene have been associated with defined morphological variants of thyroid cancer. Our data demonstrates for the first time *RET* rearrangements in vivo outside of the thyroid gland. Santoro's (Santoro et al., 1993) initial study of 528 non-thyroid tumours which did not identify *RET* activation used Southern blot analysis of genomic DNA. Even though Southern blot analysis is a reliable method for the detection of chromosomal rearrangements it has limited sensitivity and requires at least approximately 10% of tumour cells within the sample for detection. The small number of nuclei with split signals above the threshold level in our tumour cohort indicates that the *RET/PTC* rearrangement is a low-level event in primary peritoneal carcinoma and may have been missed by Southern blot analysis. Furthermore, some of their results were not validated by RT-PCR, a highly sensitive technique which is capable of detection of a small proportion of cells carrying a particular genetic event. Moreover, Santoro's study included only a small sample of ovarian (n=12) and renal cell carcinoma (n=10), from which the authors acknowledge that no inference could be drawn on particular subsets of tumours not included in their study.

A single case in this study (case 25) showed neither *RET* protein expression nor demonstrable *RET/PTC*1 mRNA by RT-PCR. However this case exhibited split FISH signals in more than 10.2% of cells analysed. It is likely, that this case harbours a *RET* rearrangement other than *H4/RET* (*RET/PTC*1) which is not expressed at the protein level, possibly as a result of post-transcriptional regulation. Similarly, alternate chimeric ret oncogenes have been demonstrated in papillary thyroid cancer and the prevalence of ret/PTC rearrangements in thyroid cancer varies widely among studies, with rates between 3 and 85% being reported. (Asa, 2001; Kondo et al., 2006; Nikiforov, 2002; Tallini and Asa, 2001) Furthermore, let-7 microRNA (which is a noncoding ~22 nucleotide RNA that negatively regulates gene expression at the

posttranscriptional level by repressing translation) has recently been demonstrated to critically affect cell growth and differentiation in PTC harbouring RET/PTC rearrangements and highlights a potential mechanism for post-transcriptional regulation of ret protein expression. (Croce, 2008; Ricarte-Filho 2009) Alternatively in this case, the sensitivity of both the RT-PCR and immunohistochemistry was not high enough to detect a few *RET/PTC*1 rearranged cells which may also be a reflection of tumour heterogeneity. (Unger et al., 2004)

The last subgroup in this study (8 cases in total) had neither demonstrable *RET/PTC*1 mRNA by RT-PCR nor split FISH signals greater than the cut-off level. However they all demonstrated *ret* protein expression which must logically be the wild-type protein. Ret protein expression in non neuroendocrine tumours has not has not been widely studied. However, recent evidence has demonstrated wild type ret protein expression in renal, breast, pancreatic and lung tumours which supports the observations in this current study. (Flavin et al, *in press;* Boulay et al, 2008; Ceyhan et al, 2006; Thomas et al, 2007)

The occurrence of *RET/PTC* in primary peritoneal and papillary renal cell carcinoma has interesting implications. Somatic mutations in cancer have been called driver when they are positively selected and causally related to tumour development and passenger when not directly implicated with tumour growth. (Davies et al., 2005) *RET/PTC* rearrangements in our study can hardly be considered as driver mutations in tumours with minimal levels of detectable fusion gene. These rearrangements may reflect *RET* instability in epithelial cells and point to the existence of secondary cell subclones, which are unlikely to be of any pathological consequence in determining biological behaviour.

It is interesting to hypothesize on the association between *RET/PTC* rearrangements and primary peritoneal carcinoma. One hypothesis is that inflammation favours the occurrence of the rearrangement as a secondary phenomenon. The propensity of thyrocytes to undergo *RET* recombination has been explained by the peculiar arrangement of chromatin that juxtaposes *RET* and its fusion partners in interphase nuclei. It is possible that free radical production, cytokine secretion, cellular proliferation and other events related to inflammation trigger the occurrence of the rearrangement predisposed to it by an unstable chromatin confirmation. (Gandhi et al., 2006) Of note, a proinflammatory tumour microenvironment has been described in ovarian cancer which contributes to immune cell recruitment and differentiation ('tumour-immune cell education model'). (Chen et al., 2008) Conversely, the occurrence of *RET/PTC* may directly influence the inflammation within these tumours. Of note, *RET/PTC* protein expression produces a strong inflammatory response in experimental animal models (Powell et al., 2003) and activates numerous inflammatory mediators and molecules within thyroid epithelial cells. (Melillo et al., 2005; Puxeddu et al., 2005; Russell et al., 2004; Shinohara and Rothstein, 2004) *RET/PTC* transformed cells can modify their microenvironment to promote autonomous cell proliferation in neighbouring nonneoplastic thyrocytes. (Melillo et al., 2005) Similarly, ovarian cancer cells can 'educate' immune infiltrates to produce the type of cytokines that will facilitate tumour growth and metastases as well as acquiring immune tolerance. (Chen et al., 2008)

Another hypothesis is that a putative link may exist between X-ray radiation and *RET/PTC*1 activation analogous to the known association in PTC. Increased risk of epithelial ovarian carcinoma has been described following diagnostic X-rays (Harlap et al., 2002) and high frequency of *RET* rearrangements following radiation have been observed in PTC. (Klugbauer et al., 1995; Rabes et al., 2000)

More specifically preferential *RET/PTC*1 induction has been associated with X-rays, (Mizuno et al., 2000) allowed by spatial juxtaposition of the *RET* and H4 proto-oncogenes, (Nikiforova et al., 2000) whereas *RET/PTC*3 rearrangements were more prevalently associated with PTCs arising in children of Belaraus and the Ukraine post-Chernobyl. Interestingly, one of the patients with a demonstrable *RET/PTC* rearrangement in this study (case 53) had pre-operative chemotherapy, however no association between *RET/PTC* induction and this form of therapy has been previously described.

It is interesting to speculate that *RET/PTC*1 activation maybe contributing in part to the adaptation of a papillary growth pattern. Yap et al (Yap et al., 1997) demonstrated that tyrosine phosphorylation alters thyroid epithelial organisation by interfering with actin-associated adhesive junctions. Under the influence of tyrosine phosphorylation, thyroid cells lose their capacity to form follicles, spread and migrate into confluent monolayers and hence the capacity to form follicles in-vivo. Fischer et al (Fischer et al., 1998) cultured thyroid cells infected with a *ret*roviral vector expressing activated *RET/PTC*1 and demonstrated alterations in the nuclear envelope and chromatin structure, found in later work to be induced by *RET/PTC* during interphase. (Fischer et al., 2003) It is plausible therefore that activated *RET/PTC*1 may influence the growth pattern in papillary tumours. Interestingly, the tumours with activated *RET*, whilst having papillary morphology did not have the classical nuclear clearing ('Orphan Annie') of PTC. However, *RET/PTC* rearrangements have been found in tumours (i.e. a subset of Hurthle cell tumours) (Belchetz et al., 2002) that may lack both papillary architecture and/or classic nuclear features. As an adjunct all *RET* rearranged cases were negative for mutated *BRAF*, suggesting distinct alternative pathways in the epipathogenesis of these tumours akin to PTC. (Soares et al., 2003)

This study had some technical limitations. Degraded RNA isolated from formalin-fixed paraffin embedded tissue was used. Highly sensitive RT-PCR carries a higher risk of false-positive amplification compared with other techniques. To minimise the effects of these limitations, 3 methodologies were employed to identify *RET* rearrangements. Specifically, interphase FISH and RT-PCR analysis were employed on laser-microdissected cells (reducing the propensity for contamination by *RET* expressing macrophages) after careful review of the samples before molecular analysis. The number of tumour nuclei with split FISH signals above background was also limited; a stringent cut-off level of 10.2% positive cells was employed to detect the chromosomal rearrangement. This cut-off level parallels previous studies which used a cut-off level of between 5-10% to separate cases from false-positives. (Barr et al., 2002; Unger et al., 2004) Immunohistochemical detection of *RET* protein expression was used to further corroborate our findings. The chimeric *RET/PTC* gene encodes a protein product that contains the cytoplasmic portion of *ret*. (Fusco et al., 1987) Therefore, immunohistochemical detection of the carboxy terminus of the *RET* protein should serve as a reliable marker to detect rearranged *RET*. (Cheung et al., 2001; Sugg et al., 1998)

However, one cannot entirely exclude the possibility of the *RET* antibody detecting only wild-type *RET* as it is feasible that a steric change of the epitope may occur after *RET* rearrangement. Indeed, according to Rebelo et al, (Rebelo et al., 2003) positive staining may correspond to the expression of the wild-type *RET*, *RET* rearrangement or both. Moreover, problems with interpreting the specificity of weak focal immunostaining for *RET* have been reported. (Cerilli et al., 2002; Guyetant et al., 2003) To overcome this problem we only deemed cases with diffuse *RET* immunostaining as being positive as recommended by previous authors. (Cerilli et al., 2002)

Any possibility that the tumours that expressed rearranged *RET* in our series, represented metastases from the thyroid is diminished given the fact no protein expression of TTF-1 or thyroglobulin was detected in any of these tumours.

Importantly, our results have broad implications for molecular diagnostics. When trying to diagnose metastatic PTC, the existence of minor cell subclones with *RET* rearrangements in non-thyroid papillary tumours highlights the importance of using quantitative methods to detect *RET/PTC* rearrangements. In conclusion, this study demonstrates that *RET/PTC* rearrangement is present in a small number of non-thyroid papillary tumours, specifically primary peritoneal and papillary renal cell carcinoma, therefore *RET/PTC* detection should not be equated per se with PTC. It indicates that in some primary peritoneal and papillary renal cell carcinoma, *RET/PTC* represents a passenger mutation occurring in a small number of tumour cells.

3.7 References

Asa, S. L. 2001. How familial cancer genes and environmentally induced oncogenes have changed the endocrine landscape. Mod Pathol 14:246-53.

Barr, F. G., S. J. Qualman, M. H. Macris, N. Melnyk, E. R. Lawlor, D. M. Strzelecki, T. J. Triche, J. A. Bridge, and P. H. Sorensen. 2002. Genetic heterogeneity in the alveolar rhabdomyosarcoma subset without typical gene fusions. Cancer Res 62:4704-10.

Basolo, F., R. Giannini, C. Monaco, R. M. Melillo, F. Carlomagno, M. Pancrazi, G. Salvatore, G. Chiappetta, F. Pacini, R. Elisei, P. Miccoli, A. Pinchera, A. Fusco, and M. Santoro. 2002. Potent mitogenicity of the RET/PTC3 oncogene correlates with its prevalence in tall-cell variant of papillary thyroid carcinoma. Am J Pathol 160:247-54.

Belchetz, G., C. C. Cheung, J. Freeman, I. B. Rosen, I. J. Witterick, and S. L. Asa. 2002. Hurthle cell tumors: using molecular techniques to define a novel classification system. Arch Otolaryngol Head Neck Surg 128:237-40.

Borrello, M. G., L. Alberti, A. Fischer, D. Degl'innocenti, C. Ferrario, M. Gariboldi, F. Marchesi, P. Allavena, A. Greco, P. Collini, S. Pilotti, G. Cassinelli, P. Bressan, L. Fugazzola, A. Mantovani, and M. A. Pierotti. 2005. Induction of a proinflammatory program in normal human thyrocytes by the RET/PTC1 oncogene. Proc Natl Acad Sci USA 102:14825-30.

Boulay, A., M. Breuleux, C. Stephan, C. Fux, C. Brisken, M. Fiche, M. Wartmann, M. Stumm, H.A. Lane, and N.E. Hynes. 2008. The Ret receptor tyrosine kinase pathway functionally interacts with ERα pathway in breast cancer. Cancer Research 68: 3743-51.

Celetti, A., A. Cerrato, F. Merolla, D. Vitagliano, G. Vecchio, and M. Grieco. 2004. H4(D10S170), a gene frequently rearranged with RET in papillary thyroid carcinomas: functional characterization. Oncogene 23:109-21.

Cerilli, L. A., S. E. Mills, C. A. Rumpel, T. H. Dudley, and C. A. Moskaluk. 2002. Interpretation of RET immunostaining in follicular lesions of the thyroid. Am J Clin Pathol 118:186-93.

Ceyhan, G.O., N.A. Giese, M. Erkan, A. G. Kerscher, M. N. Wente, T. Giese, M. W. Buchler, and H. Friess. 2006. The neurotropic factor artemin promotes pancreatic cancer invasion. Ann Surg 244:274-81.

Chen, R., A. B. Alvero, D. A. Silasi, K. D. Steffensen, and G. Mor. 2008. Cancers take their Toll--the function and regulation of Toll-like receptors in cancer cells. Oncogene 27:225-33.

Cheung, C. C., S. Ezzat, J. L. Freeman, I. B. Rosen, and S. L. Asa. 2001. Immunohistochemical diagnosis of papillary thyroid carcinoma. Mod Pathol 14:338-42.

Cheung, C. C., S. Ezzat, L. Ramyar, J. L. Freeman, and S. L. Asa. 2000. Molecular basis of Hurthle cell papillary thyroid carcinoma. J Clin Endocrinol Metab 85:878-82.

Chua, E. L., W. M. Wu, K. T. Tran, S. W. McCarthy, C. S. Lauer, D. Dubourdieu, N. Packham, C. J. O'Brien, J. R. Turtle, and Q. Dong. 2000. Prevalence and distribution of ret/PTC 1, 2, and 3 in papillary thyroid carcinoma in New Caledonia and Australia. J Clin Endocrinol Metab 85:2733-9.

Croce, CM. 2008. Oncogenes and cancer. N Engl J Med 358:502-511.

Davies, H., C. Hunter, R. Smith, P. Stephens, C. Greenman, G. Bignell, J. Teague, A. Butler, S. Edkins, C. Stevens, A. Parker, S. O'Meara, T. Avis, S. Barthorpe, L. Brackenbury, G. Buck, J. Clements, J. Cole, E. Dicks, K. Edwards, S. Forbes, M. Gorton, K. Gray, K. Halliday, R. Harrison, K. Hills, J. Hinton, D. Jones, V. Kosmidou, R. Laman, R. Lugg, A. Menzies, J. Perry, R. Petty, K. Raine, R. Shepherd, A. Small, H. Solomon, Y. Stephens, C. Tofts, J. Varian, A. Webb, S. West, S. Widaa, A. Yates, F. Brasseur, C. S. Cooper, A. M. Flanagan, A. Green, M. Knowles, S. Y. Leung, L. H. Looijenga, B. Malkowicz, M. A. Pierotti, B. T. Teh, S. T. Yuen, S. R. Lakhani, D. F. Easton, B. L. Weber, P. Goldstraw, A. G. Nicholson, R. Wooster, M. R. Stratton, and P. A. Futreal. 2005. Somatic mutations of the protein kinase gene family in human lung cancer. Cancer Res 65:7591-5.

Elisei, R., C. Romei, T. Vorontsova, B. Cosci, V. Veremeychik, E. Kuchinskaya, F. Basolo, E. P. Demidchik, P. Miccoli, A. Pinchera, and F. Pacini. 2001. RET/PTC rearrangements in thyroid nodules: studies in irradiated and not irradiated, malignant and benign thyroid lesions in children and adults. J Clin Endocrinol Metab 86:3211-6.

Farid, N. R., Y. Shi, and M. Zou. 1994. Molecular basis of thyroid cancer. Endocr Rev 15:202-32.

Fischer, A. H., J. A. Bond, P. Taysavang, O. E. Battles, and D. Wynford-Thomas. 1998. Papillary thyroid carcinoma oncogene (RET/PTC) alters the nuclear envelope and chromatin structure. Am J Pathol 153:1443-50.

Fischer, A. H., P. Taysavang, and S. M. Jhiang. 2003. Nuclear envelope irregularity is induced by RET/PTC during interphase. Am J Pathol 163:1091-100.

Flavin, R., S.P. Finn, T.K. Choueiri, H. Ingoldsby, M. Ring, C. Barrett, M. Rogers, P. Smyth, E. O'Regan, E. Gaffney, J.J. O'Leary, M. Loda, S. Signoretti, and O. Sheils. In press. Ret protein expression in papillary renal cell carcinoma. Urol Oncol.

Fugazzola, L., S. Pilotti, A. Pinchera, T. V. Vorontsova, P. Mondellini, I. Bongarzone, A. Greco, L. Astakhova, M. G. Butti, E. P. Demidchik, and et al. 1995. Oncogenic rearrangements of the RET proto-oncogene in papillary thyroid carcinomas from children exposed to the Chernobyl nuclear accident. Cancer Res 55:5617-20.

Fusco, A., G. Chiappetta, P. Hui, G. Garcia-Rostan, L. Golden, B. K. Kinder, D. A. Dillon, A. Giuliano, A. M. Cirafici, M. Santoro, J. Rosai, and G. Tallini. 2002. Assessment of RET/PTC oncogene activation and clonality in thyroid nodules with incomplete morphological evidence of papillary carcinoma: a search for the early precursors of papillary cancer. Am J Pathol 160:2157-67.

Fusco, A., M. Grieco, M. Santoro, M. T. Berlingieri, S. Pilotti, M. A. Pierotti, G. Della Porta, and G. Vecchio. 1987. A new oncogene in human thyroid papillary carcinomas and their lymph-nodal metastases. Nature 328:170-2.

Gandhi, M., M. Medvedovic, J. R. Stringer, and Y. E. Nikiforov. 2006. Interphase chromosome folding determines spatial proximity of genes participating in carcinogenic RET/PTC rearrangements. Oncogene 25:2360-6.

Grieco, M., A. Cerrato, M. Santoro, A. Fusco, R. M. Melillo, and G. Vecchio. 1994. Cloning and characterization of H4 (D10S170), a gene involved in RET rearrangements in vivo. Oncogene 9:2531-5.

Grieco, M., M. Santoro, M. T. Berlingieri, R. M. Melillo, R. Donghi, I. Bongarzone, M. A. Pierotti, G. Della Porta, A. Fusco, and G. Vecchio. 1990. PTC is a novel rearranged form of the ret proto-oncogene and is frequently detected in vivo in human thyroid papillary carcinomas. Cell 60:557-63.

Guyetant, S., S. Michalak, I. Valo, and J. P. Saint-Andre. 2003. [Diagnosis of the follicular variant of papillary thyroid carcinoma. Significance of immunohistochemistry]. Ann Pathol 23:11-20.

Harlap, S., S. H. Olson, R. R. Barakat, T. A. Caputo, S. Forment, A. J. Jacobs, C. Nakraseive, and X. Xue. 2002. Diagnostic x-rays and risk of epithelial ovarian carcinoma in Jews. Ann Epidemiol 12:426-34.

Ishizaka, Y., S. Kobayashi, T. Ushijima, S. Hirohashi, T. Sugimura, and M. Nagao. 1991. Detection of ret/PTC transcripts in thyroid adenomas and adenomatous goiter by an RT-PCR method. Oncogene 6:1667-72.

Ito, T., T. Seyama, K. S. Iwamoto, T. Mizuno, N. D. Tronko, I. V. Komissarenko, E. D. Cherstovoy, Y. Satow, N. Takeichi, K. Dohi, and et al. 1994. Activated RET oncogene in thyroid cancers of children from areas contaminated by Chernobyl accident. Lancet 344:259.

Jhiang, S. M. 2000. The RET proto-oncogene in human cancers. Oncogene 19:5590-7.

Jhiang, S. M., J. Y. Cho, T. L. Furminger, J. E. Sagartz, Q. Tong, C. C. Capen, and E. L. Mazzaferri. 1998. Thyroid carcinomas in RET/PTC transgenic mice. Recent Results Cancer Res 154:265-70.

Kondo, T., S. Ezzat, and S. L. Asa. 2006. Pathogenetic mechanisms in thyroid follicular-cell neoplasia. Nat Rev Cancer 6:292-306.

Kitamura, Y., K. Minobe, T. Nakata, K. Shimizu, S. Tanaka, M. Fujimori, S. Yokoyama, K. Ito, M. Onda, and M. Emi. 1999. Ret/PTC3 is the most frequent form of gene rearrangement in papillary thyroid carcinomas in Japan. J Hum Genet 44:96-102.

Klugbauer, S., A. Jauch, E. Lengfelder, E. Demidchik, and H. M. Rabes. 2000. A novel type of RET rearrangement (PTC8) in childhood papillary thyroid carcinomas and characterization of the involved gene (RFG8). Cancer Res 60:7028-32.

Klugbauer, S., E. Lengfelder, E. P. Demidchik, and H. M. Rabes. 1995. High prevalence of RET rearrangement in thyroid tumors of children from Belarus after the Chernobyl reactor accident. Oncogene 11:2459-67.

Manie, S., M. Santoro, A. Fusco, and M. Billaud. 2001. The RET receptor: function in development and dysfunction in congenital malformation. Trends Genet 17:580-9.

Melillo, R. M., M. D. Castellone, V. Guarino, V. De Falco, A. M. Cirafici, G. Salvatore, F. Caiazzo, F. Basolo, R. Giannini, M. Kruhoffer, T. Orntoft, A. Fusco, and M. Santoro. 2005. The RET/PTC-RAS-BRAF linear signaling cascade mediates the motile and mitogenic phenotype of thyroid cancer cells. J Clin Invest 115:1068-81.

Mizuno, T., K. S. Iwamoto, S. Kyoizumi, H. Nagamura, T. Shinohara, K. Koyama, T. Seyama, and K. Hamatani. 2000. Preferential induction of RET/PTC1 rearrangement by X-ray irradiation. Oncogene 19:438-43.

Musholt, T. J., C. Brehm, J. Hanack, R. von Wasielewski, and P. B. Musholt. 2006. Identification of differentially expressed genes in papillary thyroid carcinomas with and without rearrangements of the tyrosine kinase receptors RET and/or NTRK1. J Surg Res 131:15-25.

Nikiforov, Y. E., J. M. Rowland, K. E. Bove, H. Monforte-Munoz, and J. A. Fagin. 1997. Distinct pattern of ret oncogene rearrangements in morphological variants of radiation-induced and sporadic thyroid papillary carcinomas in children. Cancer Res 57:1690-4.

Nikiforov, Y. E. 2002. RET/PTC rearrangement in thyroid tumors. Endocr Pathol 13:3-16.

Nikiforova, M. N., J. R. Stringer, R. Blough, M. Medvedovic, J. A. Fagin, and Y. E. Nikiforov. 2000. Proximity of chromosomal loci that participate in radiation-induced rearrangements in human cells. Science 290:138-41.

Pasini, B., R. M. Hofstra, L. Yin, R. Bocciardi, G. Santamaria, P. M. Grootscholten, I. Ceccherini, G. Patrone, M. Priolo, and C. H. Buys. 1995. The physical map of the human RET proto-oncogene. Oncogene 11:1737-43.

Powell, D. J., Jr., L. C. Eisenlohr, and J. L. Rothstein. 2003. A thyroid tumor-specific antigen formed by the fusion of two self proteins. J Immunol 170:861-9.

Puxeddu, E., J. A. Knauf, M. A. Sartor, N. Mitsutake, E. P. Smith, M. Medvedovic, C. R. Tomlinson, S. Moretti, and J. A. Fagin. 2005. RET/PTC-induced gene expression in thyroid PCCL3 cells reveals early activation of genes involved in regulation of the immune response. Endocr Relat Cancer 12:319-34.

Rabes, H. M., E. P. Demidchik, J. D. Sidorow, E. Lengfelder, C. Beimfohr, D. Hoelzel, and S. Klugbauer. 2000. Pattern of radiation-induced RET and NTRK1 rearrangements in 191 post-chernobyl papillary thyroid carcinomas: biological, phenotypic, and clinical implications. Clin Cancer Res 6:1093-103.

Rebelo, S., R. Domingues, A. L. Catarino, E. Mendonca, J. R. Santos, L. Sobrinho, and M. J. Bugalho. 2003. Immunostaining and RT-PCR: different approaches to search for RET rearrangements in patients with papillary thyroid carcinoma. Int J Oncol 23:1025-32.

Rhoden, K. J., K. Unger, G. Salvatore, Y. Yilmaz, V. Vovk, G. Chiappetta, M. B. Qumsiyeh, J. L. Rothstein, A. Fusco, M. Santoro, H. Zitzelsberger, and G. Tallini. 2006. RET/papillary thyroid cancer rearrangement in nonneoplastic thyrocytes: follicular cells of Hashimoto's thyroiditis share low-level recombination events with a subset of papillary carcinoma. J Clin Endocrinol Metab 91:2414-23.

Ricarte-Filho, J.C.M., C.S. Fuziwara, A.S. Yamashita, E. Rezende, M.J. da Silva, and E.T. Kimura. 2009. Effects of let-7 microRNA on Cell Growth and Differentiation of Papillary Thyroid Cancer. Trans Oncol 2(4):236-241.

Romeo, G., P. Ronchetto, Y. Luo, V. Barone, M. Seri, I. Ceccherini, B. Pasini, R. Bocciardi, M. Lerone, H. Kaariainen, and G. Martucciello. 1994. Point mutations affecting the tyrosine kinase domain of the RET proto-oncogene in Hirschsprung's disease. Nature 367:377-8.

Russell, J. P., J. B. Engiles, and J. L. Rothstein. 2004. Proinflammatory mediators and genetic background in oncogene mediated tumor progression. J Immunol 172:4059-67.

Russell, J. P., S. Shinohara, R. M. Melillo, M. D. Castellone, M. Santoro, and J. L. Rothstein. 2003. Tyrosine kinase oncoprotein, RET/PTC3, induces the secretion of myeloid growth and chemotactic factors. Oncogene 22:4569-77.

Salassidis, K., J. Bruch, H. Zitzelsberger, E. Lengfelder, A. M. Kellerer, and M. Bauchinger. 2000. Translocation t(10;14)(q11.2:q22.1) fusing the kinetin to the RET gene creates a novel rearranged form (PTC8) of the RET proto-oncogene in radiation-induced childhood papillary thyroid carcinoma. Cancer Res 60:2786-9.

Santoro, M., F. Carlomagno, I. D. Hay, M. A. Herrmann, M. Grieco, R. Melillo, M. A. Pierotti, I. Bongarzone, G. Della Porta, N. Berger, J. L. Peix, C. Paulin, and e. al. 1992. Ret oncogene activation in human thyroid neoplasms is restricted to the papillary cancer subtype. J Clin Invest 89:1517-22.

Santoro, M., N. Sabino, Y. Ishizaka, T. Ushijima, F. Carlomagno, A. Cerrato, M. Grieco, C. Battaglia, M. L. Martelli, C. Paulin, N. Fabin, T. Sugimura, and e. al. 1993. Involvement of RET oncogene in human tumours: specificity of RET activation to thyroid tumours. Br J Cancer 68:460-4.

Sheils, O. M., J. J. O'Leary, V. Uhlmann, K. Lattich, and E. C. Sweeney. 2000. ret/PTC-1 Activation in Hashimoto Thyroiditis. Int J Surg Pathol 8:185-189.

Sheils, O. M., and E. C. Sweeney. 1999. TSH receptor status of thyroid neoplasms--TaqMan RT-PCR analysis of archival material. J Pathol 188:87-92.

Shinohara, S., and J. L. Rothstein. 2004. Interleukin 24 is induced by the RET/PTC3 oncoprotein and is an autocrine growth factor for epithelial cells. Oncogene 23:7571-9.

Smanik, P. A., T. L. Furminger, E. L. Mazzaferri, and S. M. Jhiang. 1995. Breakpoint characterization of the ret/PTC oncogene in human papillary thyroid carcinoma. Hum Mol Genet 4:2313-8.

Smyth, P., S. Finn, S. Cahill, E. O'Regan, R. Flavin, J. J. O'Leary, and O. Sheils. 2005. ret/PTC and BRAF act as distinct molecular, time-dependant triggers in a sporadic Irish cohort of papillary thyroid carcinoma. Int J Surg Pathol 13:1-8.

Smyth, P., O. Sheils, S. Finn, C. Martin, J. O'Leary, and E. C. Sweeney. 2001. Real-time quantitative analysis of E-cadherin expression in ret/PTC-1-activated thyroid neoplasms. Int J Surg Pathol 9:265-72.

Soares, P., V. Trovisco, A. S. Rocha, J. Lima, P. Castro, A. Preto, V. Maximo, T. Botelho, R. Seruca, and M. Sobrinho-Simoes. 2003. BRAF mutations and RET/PTC rearrangements are alternative events in the etiopathogenesis of PTC. Oncogene 22:4578-80.

Suarez, H. G. 1998. Genetic alterations in human epithelial thyroid tumours. Clin Endocrinol (Oxf) 48:531-46.

Sugg, S. L., S. Ezzat, I. B. Rosen, J. L. Freeman, and S. L. Asa. 1998. Distinct multiple RET/PTC gene rearrangements in multifocal papillary thyroid neoplasia. J Clin Endocrinol Metab 83:4116-22.

Sugg, S. L., L. Zheng, I. B. Rosen, J. L. Freeman, S. Ezzat, and S. L. Asa. 1996. ret/PTC-1, -2, and -3 oncogene rearrangements in human thyroid carcinomas: implications for metastatic potential? J Clin Endocrinol Metab 81:3360-5.

Tallini, G., and S. L. Asa. 2001. RET oncogene activation in papillary thyroid carcinoma. Adv Anat Pathol 8:345-54.

Takahashi, M. 2001. The GDNF/RET signaling pathway and human diseases. Cytokine Growth Factor Rev 12:361-73.

Takahashi, M., J. Ritz, and G. M. Cooper. 1985. Activation of a novel human transforming gene, ret, by DNA rearrangement. Cell 42:581-8.

Thomas, G. A., H. Bunnell, H. A. Cook, E. D. Williams, A. Nerovnya, E. D. Cherstvoy, N. D. Tronko, T. I. Bogdanova, G. Chiappetta, G. Viglietto, F. Pentimalli, G. Salvatore, A. Fusco, M. Santoro, and G. Vecchio. 1999. High prevalence of RET/PTC rearrangements in Ukrainian and Belarussian post-Chernobyl thyroid papillary carcinomas: a strong correlation between RET/PTC3 and the solid-follicular variant. J Clin Endocrinol Metab 84:4232-8.

Thomas, R. K., A. C. Baker, R. M. Debiasi, W. Winckler, T. Laframboise, W. M. Lin, M. Wang, W. Feng, T. Zander, L. MacConaill, J. C. Lee, R. Nicoletti, C. Hatton, M. Goyette, L. Girard, K. Majmudar, L. Ziaugra, K. K. Wong, S. Gabriel, R. Beroukhim, M. Peyton, J. Barretina, A. Dutt, C. Emery, H. Greulich, K. Shah, H. Sasaki, A. Gazdar, J. Minna, S. A. Armstrong, I. K. Mellinghoff, F. S. Hodi, G. Dranoff, P.S. Mischel, T. F. Cloughesy, S. F. Nelson, L. M. Liau, K. Mertz, M. A. Rubin, H. Moch, M. Loda, W. Catalona, J. Flecther, S. Signoretti, F. Kaye, K. C. Anderson, G. D. Demetri, R. Dummer, S. Wagner, M. Herlyn, W. R. Sellers, M. Meyerson, and L. A. Garraway. 2007. High throughput oncogene mutation profiling in human cancer. Nature Genetics 39: 347-51.

Unger, K., H. Zitzelsberger, G. Salvatore, M. Santoro, T. Bogdanova, H. Braselmann, P. Kastner, L. Zurnadzhy, N. Tronko, P. Hutzler, and G. Thomas. 2004. Heterogeneity in the distribution of RET/PTC rearrangements within individual post-Chernobyl papillary thyroid carcinomas. J Clin Endocrinol Metab 89:4272-9.

Wirtschafter, A., R. Schmidt, D. Rosen, N. Kundu, M. Santoro, A. Fusco, H. Multhaupt, J. P. Atkins, M. R. Rosen, W. M. Keane, and J. L. Rothstein. 1997. Expression of the RET/PTC fusion gene as a marker for papillary carcinoma in Hashimoto's thyroiditis. Laryngoscope 107:95-100.

Yap, A. S., B. R. Stevenson, V. Cooper, and S. W. Manley. 1997. Protein tyrosine phosphorylation influences adhesive junction assembly and follicular organization of cultured thyroid epithelial cells. Endocrinology 138:2315-24.

Chapter Four

BRAF (T1799A) mutations are not a genotypic link in the papillary phenotype

4.1 Summary

The Ras/Raf/MEK/ERK signalling pathway has been implicated in a variety of human neoplasms, with BRAF mutations having been detected in tumours such as melanoma, low grade serous papillary carcinomas of the ovary and papillary carcinoma of the thyroid (PTC). A missense mutation of thymine to adenine at nucleotide position 1799, results in a valine to glutamic acid change at codon 600 (V600E), which can be found in approximately 80% of BRAF mutations. This BRAF mutation is highly prevalent in PTC's with a papillary or mixed papillary-follicular growth pattern. We investigated the hypothesis that BRAFV600E mutations might be expressed in non-thyroid papillary tumours. 57 non-thyroid papillary tumours (15 primary peritoneal carcinoma, 10 serous carcinoma of the ovary (including 2 borderline tumours), 10 papillary renal cell carcinoma, 10 urothelial cell carcinoma, 5 serous carcinoma of the endometrium, and 7 carcinomas with mixed phenotypes) were analyzed for expression of mutated BRAF T1799A by Taqman™ SNP detection. All 57 tumours were homozygous for wild type BRAF. BRAF V600E mutations are restricted to certain subgroups of papillary tumours (PTC, low grade serous carcinoma of the ovary) and do not serve as a molecular link between tumours with a papillary phenotype.

4.2 Introduction

4.2.1 RAF Kinases

BRAF belongs to the Raf family of serine/threonine kinases that have an important role in cell proliferation, differentiation and cell death. *Raf* genes were first identified as oncogenes in retroviruses, which are the causative agents of tumours in mice and chickens. The very first *raf* gene to be identified was v-raf; the transforming gene of the mouse sarcoma virus MSV 3611 which induces fibrosarcomas and erythroleukaemias in newborn mice. (Rapp and Todaro, 1980) The proto-oncogene homologue of v-raf in humans is Raf-1. Three RAF isoforms exist in humans, namely A-RAF, B-RAF and C-RAF (RAF-1). A-RAF is expressed at highest levels in tissues that comprise the urogenital system. C-RAF is expressed ubiquitously whereas B-RAF is expressed at higher levels in haemopoietic cells, neurons and testis. Although RAF-1 has been the most extensively studied, it is B-RAF which has been found to be the most oncogenic. (Marais et al., 1997) These three proteins act as downstream effectors of Ras and differ in their affinities for RAS and MEK activation.

4.2.2 Expression

The three Raf isoforms differ in their tissue-specific expression and subcellular location. RAF-1 is ubiquitously expressed in human tissues whereas BRAF expression is generally restricted to neuronal tissue, testis and spleen. (Barnier et al., 1995) Although BRAF and RAF-1 are co-expressed in neurons, BRAF is localised to cell bodies and neurite processes whereas RAF-1 is perinuclear. (Morice et al., 1999) Both A-RAF and RAF-1 have been shown to be localised to the mitochondria. (Wang et al., 1996; Yuryev et al., 2000) A-RAF is predominantly expressed in urogenital tissue.

4.2.3 RAF Kinase Structure

All three RAF isoforms, A-RAF, B-RAF and C-RAF, share three highly conserved regions (CR1, CR2, CR3) embedded in variable sequences. The kinase domains are separated into N-terminal and C-terminal lobes and the ATP binding site is located at the interface of the two lobes. The N-terminal lobe contains the glycine loop that is important for localising the phosphates of ATP. The C-terminal lobe contains the substrate recognition sequence. A key element in this region is the activation segment. Phosphorylation of threonine 598 and serine 601 within this segment has been shown to play a key role in B-RAF activation. (Mercer and Pritchard, 2003; Wan et al., 2004)

B-RAF has a number of structural differences from the other two RAF proteins. In the conserved domain, B-RAF has several amino acid differences. The structure of B-RAF is illustrated in Figure 4.1. The variable region is also subjected to alternative splicing of exons 8b and 10a. This differential splicing has been shown to affect the ability of B-RAF to activate MEK. The presence of exon 10a increases its affinity and basal kinase activity toward MEK, whereas the presence of exon 8b has the opposite effect. The two exons are located at the linker region between the amino terminal regulatory region and the catalytic domain and may serve as a hinge in the transition between active and inactive conformations of the kinase.

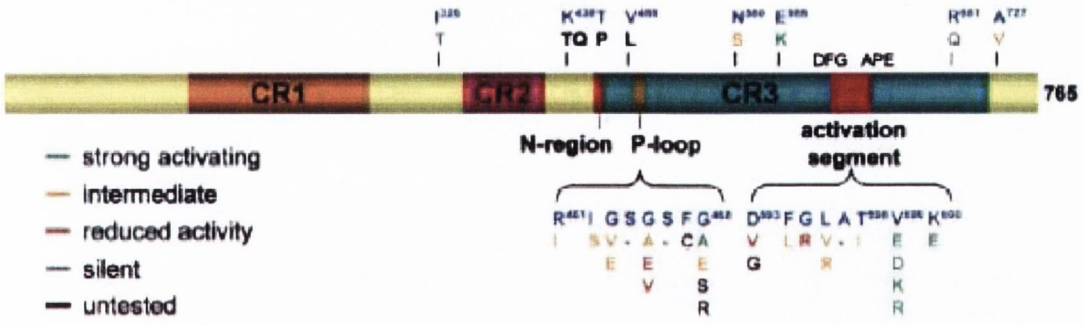

Figure 4.1 B-RAF Primary Structure.

Showing functional domains and position of the 32 observed cancer-associated mutants of B-RAF. The amino acid substitutions are colour coded according to their activity class. (Wan et al., 2004)

CR1 has two domains that bind to Ras-GTP; the Ras binding domain and the cysteine rich domain (CRD). It also has a putative zinc-binding domain. CR2 is rich is serine and threonine residues some of which are regulatory phosphorylation sites. CR3 contains the kinase domain that is the most homologous between the Raf kinases.

4.2.4 Function and Activation of RAF Kinases

RAF proteins play an important role in the conserved RAS/RAF/MEK/ERK pathway (Figure 4.2). This is a classical signal pathway known to mediate cellular proliferation in various cell types. (Melillo et al., 2005; Mitsutake et al., 2005) This pathway is thought to be implicated in up to 30% of all human neoplasms and RAF kinases play a central part in this pathway. RAF proteins are key effectors of RAS proteins in the RAS/RAF/MEK/ERK signalling cascade. They act by relaying signals from activated Ras proteins via MAPK/ERK kinase 1/2 (MEK1/2) to the p42/p44 MAP kinases or ERK 1/2, the key effectors of the pathway. ERKs have many substrates located in different places in the cell. These include transcription

factors, ribosomal proteins, enzymes, genes involved in metastasis and angiogenesis, apoptosis and cytoskeletal proteins that can influence cell fate. Through phosphorylation of these various substrates, active ERKs are able to influence many of the hallmarks of cancer. (Park et al., 2002) Activation of the RAF kinases is initiated by extracellular signals such as epithelial growth factor. These signals bind to their respective receptors on the cell membrane. This action causes receptor dimerisation and autophosphorylation on tyrosine residues. Son of sevenless (SOS), which is a G-protein exchange factor, is then towed to the cell membrane by the growth factor receptor binding protein 2 (Grb2).

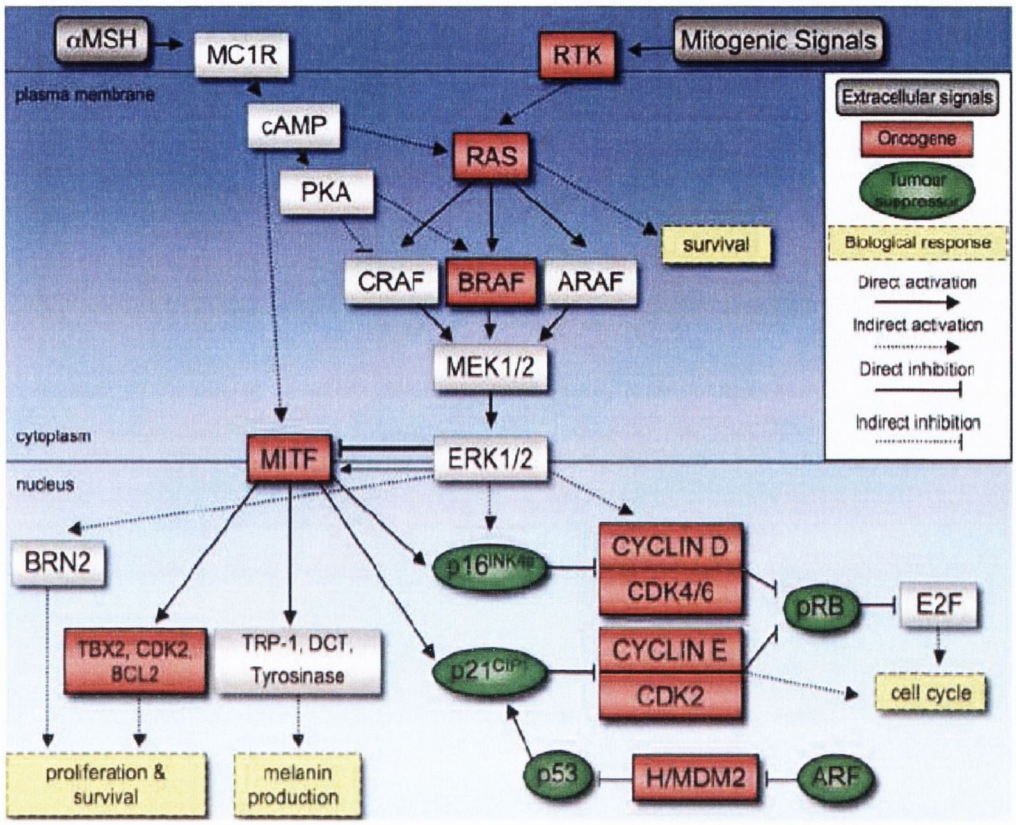

Figure 4.2 MAPK signalling pathway.

This pathway feeds into various effector processes, including those governing cell proliferation and survival. In melanocytes the MITF transcription factor is under control of BRAF-dependent signals to regulate melanin production in response to alpha-MSH. In non-malignant cells BRAF activity is modulated as a function of extracellular signals through RTKs, the cancer-derived $BRAF^{E600}$ mutant functions autonomously. A central cell cycle pathway downstream of BRAF corresponds to the $p16^{ink4a}$/CDK4/pRB/E2F route, which in melanocytes is also under the control of MITF. The CDK inhibitor $p21^{cip1}$ acts as a nodal point connecting the pRB pathway to the p53 tumour suppressor and MITF. (Michaloglou et al., 2008)

This recognises the phosphotyrosines on the cell membrane receptors as docking sites. These in turn activate Ras at the cell membrane which is accompanied by the exchange of GDP with GTP. This step elicits a conformational change in RAS to its active form. Following activation, Ras acts as an adaptor molecule that can bind RAF kinases with high affinity and recruit them to the cell membrane where RAF activation occurs. The binding of activated Ras to B-RAF is sufficient to activate it directly. This has been attributed to a change of amino acid in one of the four phosphorylation activation sites in the wild type BRAF that can mimic phosphorylation, leading to a "pre-activated" raf kinase. Other RAF kinase activation is a more complex process that includes dephosphorylation of inhibitory sites by protein phosphatase 2A (PP2A) and phosphorylation of activating sites by $p21^{rac/cdc42}$-activated kinases (PAKs), Src family and other kinases. Activated RAF kinases are then free to phosphorylate and activate MEKs, which in turn, can do likewise to ERKs. The entire kinase complex is supported by a scaffolding protein known as KSR (kinase suppressor of Ras) which is also important in the regulation of the pathway. A model for B-RAF activation is displayed in Figure 4.3.

B-RAF was identified as the most important mediator of Ras effects and for activating the MEK/ERK pathway. B-RAF has a higher affinity for MEK1 and MEK2 and is more efficient in phosphorylating MEKs than other RAF isoforms. In addition, studies on mice with targeted genetic mutations of the raf genes have shown that RAF-1 is dispensable for MEK/ERK activation but BRAF appears to be the key MEK/ERK activator in most tissues and cell types. (Knauf et al., 2005)

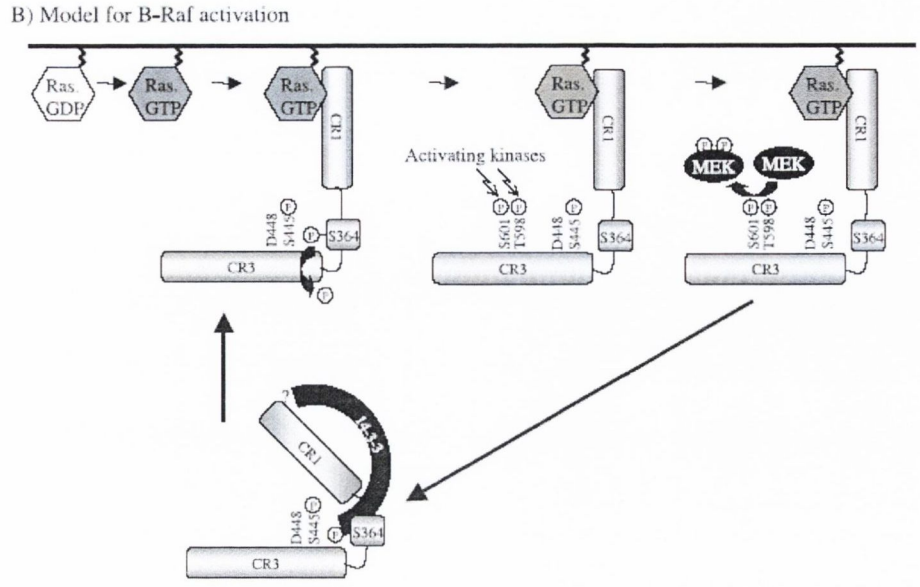

Figure 4.3 Model for how B-RAF may become activated.

In unstimulated cells B-RAF is maintained in the cytoplasm in complex with 14-3-3 and it has an open conformation. Upon ligand binding B-Raf binds to Ras which results in its translocation to the plasma membrane. Activated kinases phosphorylate S601 and T598 resulting in full B-RAF activation.

4.2.5 BRAF Mutations in Cancer

BRAF is the only RAF protein to be frequently mutated in cancer, probably because its constitutive activation requires fewer mutational events. No ARAF mutations have been identified so far. (Emuss et al., 2005; Lee et al., 2005) CRAF mutations are rarely found in some ovarian and pulmonary carcinomas, raising the possibility that CRAF may act as an oncogene in man. (Emuss et al., 2005; McPhillips et al., 2006; Zebisch et al., 2006) The first intensive study of BRAF mutation in human cancers by Davis et al using a sequencing screen of approximately 1000 cancer samples identified missense mutations of the BRAF gene in approximately 70% of human malignant melanomas and 15% of colorectal cancers. (Davies et al., 2002) Mutations were also detected at a low frequency in gliomas, lung cancers, thyroid carcinomas, ovarian carcinomas, breast cancers, liver cancers and some sarcomas. (Cohen et al., 2003; Davies et al., 2002; Kimura et al., 2003)

BRAF-activating missense point mutations in human cancer are clustered in the kinase domain in exons 11 and 15. The T1799A transversion mutation accounts for approximately 90% of the BRAF mutations in human cancer. This results in a valine to glutamate substitution at residue 600 (V600E) formally thought to be at residue 599. This substitution results in the constitutive activation of the BRAF kinase. Recent resolution of the crystal structure of the wild type and BRAF V600E kinase domains helped to elucidate the mechanism of mutational activation of the protein; this is illustrated in Figure 4.4. (Wan et al., 2004)

The mutation at V600E is thought to mimic phosphorylation in the activation segment of BRAF by inserting a negatively charged residue adjacent to an activating phosphorylation site at Ser 599. This causes the conversion of BRAF to a catalytically active form by disrupting the association of the activation segment with the ATP-binding P loop, which normally holds BRAF in an inactive form.

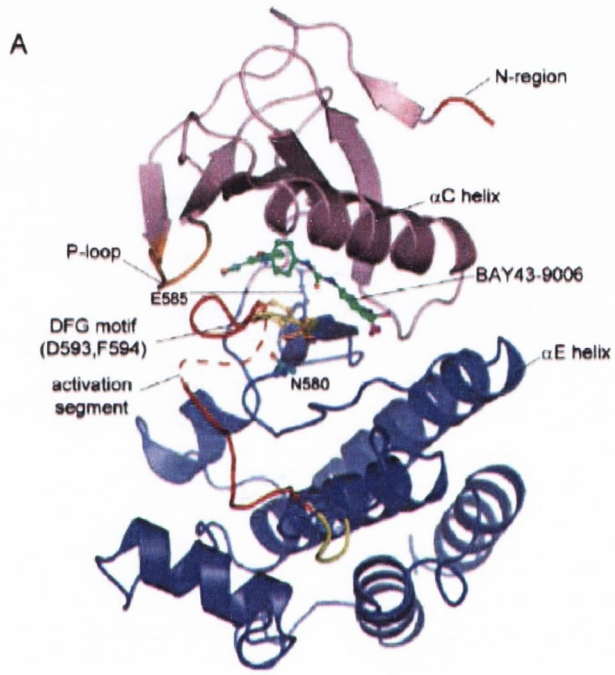

Figure 4.4 Structure of the ^{wt} B-RAF Kinase Domain.

The kinase inhibitor BAY43-9006 was used to obtained crystals suitable for analysis. The kinase domain of BRAF adopts bilobal architecture characteristic of protein kinases. The activation segment is adjacent to the DFG motif and in active conformation forms a β sheet interaction with the β6 strand. (Adapted from Wan et al, 2004).

Most BRAF mutants have elevated kinase activity compared to the wild type protein, however four cancer-derived mutants have reduced kinase activity. (Wan et al., 2004) Three of these mutants (BRAFG466E, BRAFG466V, and BRAFG596R) are capable of inducing ERK phosphorylation through heterodimerisation with CRAF (Figure 4.5) The fourth mutant (BRAFD594V) acts like a kinase-dead mutant and cannot bind CRAF. (Wan et al., 2004)

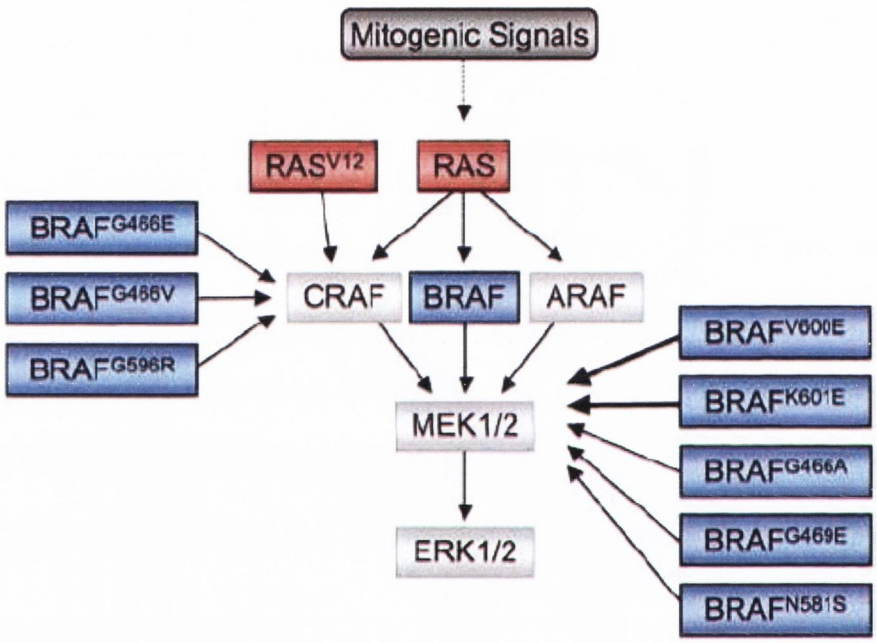

Figure 4.5 Oncogenic signaling by BRAF mutants through the RAS/RAF pathway. BRAF mutants activate MEK/ERK independently of mitogenic signals. Impaired activity mutants require CRAF for activation. (Michaloglou et al., 2008)

4.2.5.1 Oncogenic function of BRAFV600E in vitro and in xenograft models

Several studies have demonstrated the potential for BRAFV600E to act as an oncogene. BRAFV600E can transform NIH3T3 immortal fibroblasts and diploid fibroblasts (the latter through defined genetic lesions such as hTERT and disruption of the pRB and p53 pathways). (Davies et al., 2002; Hahn et al., 2002; Michaloglou et al., 2005) Over-expression of mutant BRAF in an immortal mouse melanocyte cell line (melan-a cells) induces constitutive MEK/ERK signaling and proliferation in the absence of TPA. BRAFV600E expressing melan-a cells grow anchorage independently and give rise to tumours when injected subcutaneously into immunodeficient mice. BRAFV600E over-expression in a well-differentiated rat cell line of thyroid origin induce DNA synthesis but also apoptosis. Thyroid specific genes are downregulated and chromosomal instability is induced. (Mitsutake et al., 2005) Related studies demonstrate a transformed phenotype of these cells through the ability to invade Matrigel due to upregulation of MMPs. (Mesa et al., 2006)

Treatment of cultured melanoma and thyroid cancer cell lines with either siRNA or shRNA targeting mutant or both wt and mutant BRAF leads to reduced phosphorylation of MEK and ERK (p-MEK and p-ERK). (Calipel et al., 2003; Hingorani et al., 2003; Salvatore et al., 2006) This leads to induction of cell cycle arrest, loss of anchorage independence and induction of apoptosis. The growth arrest triggers reduction in cyclin D1 and D3 (established effector proteins of the RAS/MEK/ERK pathway, Figure 4.5) which is associated with the accumulation of the hypophosphorylated form of pRB. (Rotolo et al., 2005)

BRAFV600E expression also regulates downstream effectors BRN2 and MITF. BRN2 is a transcription factor often overexpressed in melanoma. Loss of BRAFV600E leads to a reduction in BRN2 levels and decreased proliferation of melanoma cell lines. (Goodall et al.,

2004) BRAFV600E has also been shown to contribute to invasion. Its silencing inhibits Matrigel invasion that is accompanied by a reduction in MMP2 activity and a decline in β1-integrin protein levels in melanoma cells consistent with BRAFV600E overexpression promoting invasion. (Mesa et al., 2006)

The proliferative activity of melanoma cell lines is also highly dependant on BRAFV600E. Melanoma cells expressing shRNA targeting BRAF develop smaller tumours with fewer cycling cells in immunodeficient mice than in control mice. (Sumimoto et al., 2004) BRAFV600E silencing in an established tumour using shBRAF inhibits further tumour progression. (Hoeflich et al., 2006) In some cell lines, BRAFV600E silencing in an established tumour inhibits further tumour progression, through loss of proliferation, increased apoptosis and macrophage infiltration. Large tumours can even regress upon BRAF silencing however upon reversal there is rapid tumour relapse. (Hoeflich et al., 2006) BRAFV600E mutation can also block proliferation in primary cells and xenografted mice through induction of senescence and apoptosis through pathways mediated by the secreted protein IGFBP7.(Wajapeyee et al., 2008) All of these studies indicate that melanoma cell lines carrying mutant BRAF are addicted to it. (Weinstein, 2002) 'Oncogene addiction' denotes the dependency of the cancer cell on the mutated oncogene (or tumour suppressor), which makes BRAF a promising therapeutic target clinically.

4.2.5.2 BRAF mutations in malignant tumours

In human cancer, BRAF mutations are most common in melanoma although the prevalence of mutations varies substantially amongst the different subtypes. They are most common in cutaneous melanoma but rare in mucosal, acral and conjunctival melanomas and virtually absent from uveal melanoma. Furthermore, within the group of cutaneous melanomas BRAF mutations are found primarily in melanomas of intermittently sun-exposed skin rather than chronically sun-damaged skin. The latter group typically harbour wild-type BRAF. (Cohen et al., 2003; Curtin et al., 2005; Maldonado et al., 2003)

Mutations in the MAPK pathway components are frequently observed in melanoma; in cases with no BRAF mutation other oncogenic lesions affect proteins either upstream or downstream of BRAF. (Chin et al., 2006) NRAS mutations are frequently found in melanoma with a lower overall frequency than BRAF. (Curtin et al., 2005) Both mutations tend to be mutually exclusive. In addition, mutations in c-kit, amplification of CCND1 (encoding cyclin D1) and amplification of CDK4 have all been identified in the various melanoma subtypes, indicating that activation of the MAPK pathway is an important step in melanoma development. (Curtin et al., 2005; Errico et al., 2003; Willmore-Payne et al., 2006; Willmore-Payne et al., 2005)

In addition to genetic alterations in ret/PTC, NTRK1, PPARγ, HRAS and NRAS, mutations in BRAF represent the most oncogenic lesion found in thyroid cancer. (Ciampi and Nikiforov, 2005; Kondo et al., 2006; Trovisco et al., 2006; Xing, 2005) The BRAF mutation found in PTC is almost exclusively the BRAF ^{V600E} activating point mutation, and as in melanoma BRAF mutations are mutually exclusive with RAS mutations or ret/PTC rearrangements. BRAF mutations are thought to occur early in the development of PTC due to their presence in microscopic PTCs (a possible early precursor).

Numerous studies have shown a high prevalence of BRAF mutation in papillary thyroid cancer ranging from 29% - 69% of cases.(Fukushima et al., 2003; Namba et al., 2003; Soares et al., 2003; Xing, 2005; Xu et al., 2003) In addition, BRAF mutations have been described in approximately 13% of poorly differentiated thyroid carcinomas and 35% of anaplastic thyroid carcinomas arising from PTC. Follicular thyroid carcinomas and follicular adenomas tend to harbour RAS mutations rather than BRAF mutations.

Within the PTC group, BRAFV600E is most common in the conventional PTC and the tall cell variant (55-100%) compared to follicular-variant PTC (7-14%). (Kondo, 2006). It seems that BRAF mutations are specifically associated with distinctive papillary (classical) or mixed follicular-papillary morphology indicating that BRAF mutations are associated with distinct phenotypical and biological properties of papillary carcinomas.

BRAFV600E mutation seems to be associated with increased tumour aggressiveness, correlating with extra-thyroidal extension and cervical lymph node metastases. (Frasca et al., 2008; Wang et al., 2008) Moreover, BRAFV600E is observed in adult onset PTC as opposed to the rare paediatric PTC, which more often harbour ret/PTC rearrangements. However, a rare but interesting genetic alteration that can also cause constitutive activation of BRAF is the recently reported in vivo fusion of the BRAF gene with AKAP9 genes through a paracentric inversion of the long arm of chromosome 7. (Ciampi et al., 2005) This rearrangement was detected in a subset of thyroid tumours in children exposed to radiation after the Chernobyl accident. The chimeric protein displays similar kinase activity and transforming capacity as BRAFV600E, which probably accounts for its oncogenic role. In addition gains in chromosome 7 or BRAF amplification have been reported in PTC, indicating a third possible mechanism for BRAF activity in thyroid tumours.

Interestingly, PTCs with BRAF mutations have been found to have aggressive clinical features, notably presenting more often with extrathyroidal invasion and at a more advanced stage. (Fugazzola et al., 2006; Nikiforova et al., 2003; Riesco-Eizaguirre et al., 2006)

4.2.5.3 BRAF mutations in benign human lesions

Melanocytic naevi which are exceedingly common frequently harbour activating BRAF mutations (82%). (Pollock et al., 2003) In combination with the the prominent role of BRAFV600E in melanoma, this suggests that BRAF is already involved in the early stage of melanoma development, at least in those melanoma arising from a naevus. Although a large proportion of common acquired naevi harbour mutant BRAF, hardly any mutations have been identified in Spitz naevi, blue naevi and giant congenital naevi. (Bastian et al., 2000; De Raeve et al., 2006; Yazdi et al., 2003) Interestingly, BRAF mutations are also found in serrated polyps of the colon, benign epithelial neoplasms that are the precursors of some colorectal carcinoma. Both serrated polyps and colorectal carcinomas often carry BRAF mutations in association with DNA methylation and microsatellite instability. (Chan et al., 2003; Domingo et al., 2004; Kambara et al., 2004; Yang et al., 2004)

4.3 Aim

The aim of this study was to assess whether BRAF T1799A mutations are associated with the phenotypic expression of papillary morphology and to assess what role they may have in progression from well to poorly differentiated tumours.

4.4 Materials and Methods

Ethical approval for the study was obtained from the St. James's and Federation of Dublin Voluntary Hospitals Ethics committee.

4.4.1 Case selection

Papillary tumours were selected from archival formalin-fixed, paraffin-embedded tissue (FFPE), between the years 1991-2005 from St. James's Hospital and The Adelaide and Meath National Children's Hospital, Tallaght. The study cohort (n=57) included 15 primary peritoneal carcinoma, 10 serous carcinoma of the ovary (including 2 borderline tumours), 10 papillary renal cell carcinoma, 10 urothelial cell carcinoma, 5 serous carcinoma of the endometrium, and 7 carcinomas with mixed phenotypes (see chapter 3, Figure 3.5). Slides were reviewed blind by two histopathologists (RF&SF), original diagnoses confirmed, and representative sections chosen. The clinicopathological characteristics of the cases selected have been previously described in chapter 3 (Table 3.1).

4.4.2 Microdissection and DNA extraction

In order to accurately detect the BRAF mutant/wild type status of cases, it was necessary to acquire homogeneous cell populations of thyrocytes. 7μm sections were cut from each block, de-waxed and lightly stained with haematoxylin and eosin (H&E). Epithelial cells in each case were laser capture microdissected using the PixCell II™ System (Arcturus Engineering, Inc., CA, USA) for subsequent mutation analysis (see chapter 2.2). Following microdissection the Capsures™ were placed in sterile Eppendorf tubes and DNA extraction was performed using the PUREGENE® DNA Isolation Kit (Gentra Systems Inc., MN, USA) with modification of the protocol as previously described (chapter 2.4.2).

4.4.3 Agarose Gel Electrophoresis

The integrity and size distribution of total purified DNA was checked using denaturing agarose gel electrophoresis and ethidium bromide staining. A detailed protocol is described in chapter 2.6.

4.4.4 BRAF Mutation (T1799A) Detection

Taqman® SNP detection was used for mutation detection. The principle of the Taqman®/5' nuclease assay and its use in SNP detection is described in chapter 2.7.3. Briefly for allelic discrimination, two differentially labelled fluorescent (FAM and VIC) MGB-NFQ probes, differing by the one base pair T or A at the mutation site, competitively bind to target sequence between the forward and reverse primers. Mismatches between probe and target reduce hybridisation efficiency and DNA polymerase is more likely to displace mismatched probe than cleave it.

The appropriate probe(s) are cleaved by 5' nuclease activity on a perfectly matched probe/target duplex thereby generating fluorescence depending on the presence and abundance of target sequence(s). In this regard the assay functions as its own endogenous control as the wild-type allele would be detected even in the absence of mutant allele(s). Following thermal cycling, the fluorescence generated during PCR amplification can be read. By quantifying and comparing the fluorescent signals, it is then possible to determine the allelic content of each sample by comparison to known control samples.

Primers and probes used in this experiment were designed and used according to the Applied Biosystems (Foster City, CA, USA) Assays-by-Design^{SM} service. The primers/probes used were as follows: 5' CAT GAA GAC CTC ACA GTA AAA ATA GGT GAT 3' [BRAF-F], 5' GGA TCC AGA CAA CTG TTC AAA CTG A 3' [BRAF-R], VIC-5' CCA TCG AGA TTT CAC TGT AG 3' [BRAF-P^{WT}], and FAM-5' CCA TCG AGA TTT CTC TGT AG 3' [BRAF-P^{MUT}]. Amplification and analysis was performed on an ABI Prism 7000 Sequence Detection System (Applied Biosystems, CA, USA) for 40 cycles (92°C for 15sec, 60°C for 1min).

DNA from cell lines was used for control purposes. Controls were as follows; TPC-1 has wild type BRAF, B-CPAP homozygous for BRAF mutation and K-2 heterozygous for BRAF mutation. Control material had previously validated the method by sequencing. (Smyth et al., 2005) Four of each; no template controls (NTC), homozygous controls and heterozygous mutation controls were included in each run for control and allele calling purposes. All Nthy-BRAF DNA samples; rep 1, rep 2 and rep3, were analysed for BRAF mutation in duplicate. Allele calls were defined using the 7000 SDS software and the relative distances between unknowns and controls.

Cell line	Derived from	ret/PTC oncogene activation	BRAF allele status (HOM/HET/WT)
B-CPAP	PTC	none	HOM
K-2	PTC	none	HET
TPC-1	PTC	ret/PTC-1	WT

Table 4.1 Cell lines used as controls throughout the experiment

Abbreviations: HOM – homozygous, HET – heterozygous, WT – wild-type

Fluorescent signals from controls fell into clusters, which were used to form sectors, i.e. mutant, wild-type or heterozygous. Samples were called according to the sector in which they were located. Signals from NTCs (no template controls) formed the origin from which the sectors emanated. Signals greater than 0.5 fluorescent units from the NTCs were called according to the sector in which they were located (see Fig 4.6). Samples that did not reliably fall into a defined allele "sector" and those that displayed no amplification were subsequently re-extracted and/or reanalysed.

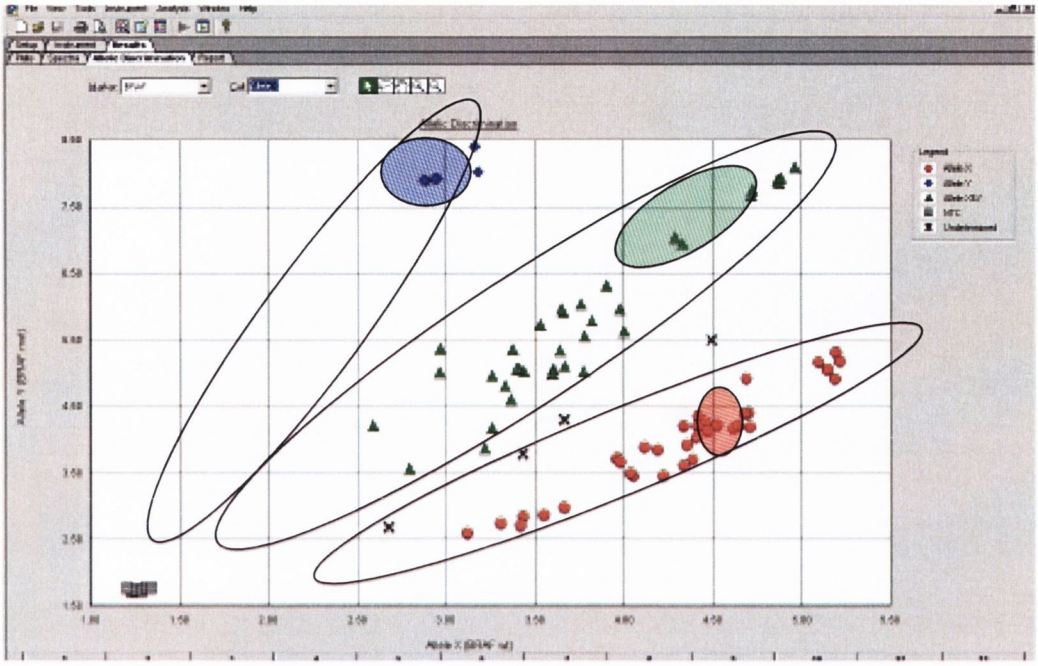

Figure 4.6 Sample output from an AD (allelic discrimination) assay

Figure shows clustering of the samples into 3 distinct groups depending on their respective levels of VIC/FAM fluorescence: homozygous T1799A mutation (◆), homozygous wild-type/normal (●) and heterozygous T1799 mutation (▲). Negative controls (■) and undetermined samples are also displayed (×). The locations of cell line controls are indicated by appropriate coloured shading. (adapted from Smyth et al)

4.5 Results

4.5.1 Integrity of Extracted DNA

The integrity of total purified DNA was checked using denaturing agarose gel electrophoresis and ethidium bromide staining. Good quality, non-degraded, DNA appeared as a smear (Figure 4.7 – lanes 4-7). Degraded DNA was discarded and samples were re-extracted.

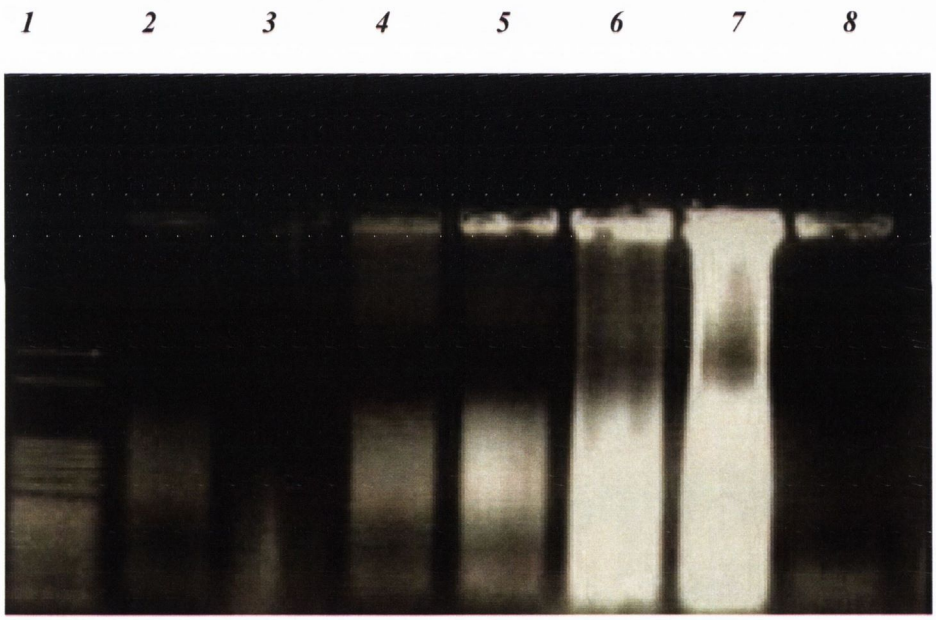

Figure 4.7 Solution phase genomic DNA electrophoresis on a 2% agarose gel containing ethidium bromide. Lane 1: DNA ladder, lanes 4-7: non-degraded genomic DNA, lanes 2, 3, 8: degraded DNA .

4.5.2 Allelic discrimination for BRAF Mutation (T1799A) Detection

BRAF T1799A mutation was not detected in any of the 55 tumours - all were homozygous for wild type *BRAF*. Figure 4.8 highlights an example of an output from an allelic discrimination plot.

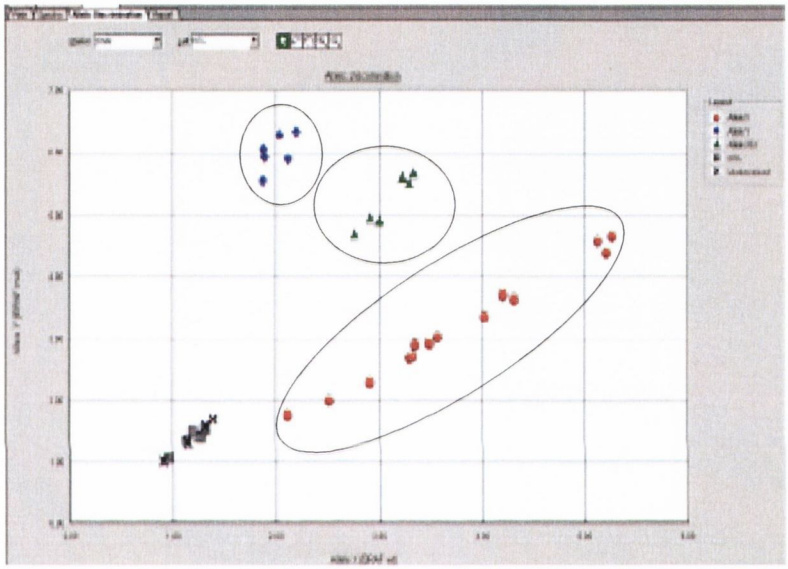

Figure 4.8 Example of the output from an AD (allelic discrimination) assay
Figure shows clustering of the samples into 3 distinct groups depending on their respective levels of VIC/FAM fluorescence: homozygous T1799A mutation (◆), homozygous wild-type/normal (●) and heterozygous T1799 mutation (▲). Negative controls (■) and undetermined samples are also displayed (×). The locations of cell line controls are indicated by appropriate coloured shading.
All samples are homozygous for wild type BRAF.

4.6 Discussion

BRAF mutations have been shown previously to be specifically associated with distinctive papillary (classical) or mixed follicular-papillary morphology in PTC. (Trovisco et al., 2004) Similarly, a recent cell culture model of serous borderline tumour of the ovary with BRAF mutation (a low-grade tumour) formed whorl-like epithelial colonies in culture, structures akin to formative papillae. (Woo et al., 2008) We hypothesised that BRAF mutations may be a key determinant in explaining the papillary phenotype which in theory may be mediated through downstream effects on the cytoskeleton via the ERK and the MAPK pathway. This study utilized a novel allelic discrimination assay for segregation of cases into wild type and mutant BRAF, as previously described. (Smyth et al., 2005) BRAF T1799A mutation found at exon 15 was chosen as it is responsible for over 80% of all BRAF mutations in several types of cancers. (Davies et al., 2002) BRAF T1799A mutation was not detected however in our cohort of papillary tumour samples.

Previous studies have examined the BRAF status in morphologically diverse tumour cohorts which have included samples with a papillary phenotype. Nagy et al. analyzed the BRAF locus on chromosome 7q34 with microsatellites for allelic changes and exons 11 and 15 of the BRAF with sequencing for mutations in 50 kidney cancers including 20 papillary, 15 conventional and 15 chromophobe renal cell carcinomas (RCC). Despite identifying allelic changes at the BRAF locus in 16 of 20 papillary RCC (renal cell carcinomas), 3 of 15 conventional RCC and 2 of 15 chromophobe RCC, sequencing failed to disclose mutations in exons 11 and 15 of the BRAF gene in any of the tumors. (Nagy et al., 2003) Even though it is not stated as to whether their study cohort included both type 1 and type 2 papillary RCC (unlike our study which included both), both sets of results reach the same conclusion.

Similarly, no BRAF T1796A mutations were detected in serous papillary endometrial carcinomas in two previous studies, (Feng et al., 2005; Mutch et al., 2004) albeit the number of papillary tumours included in both studies were small (1 and 12 respectively). It most be noted however, that 2/19 non-endometrioid samples in one of the studies had alternate BRAF mutations at exons 11 (A1412C) and 15 (C1840T), but it wasn't stated if these 2 cases had papillary morphology. (Feng et al., 2005) Cohen et al. found no BRAF T1796A (old annotation) mutation in 27 bladder tumours, however again the authors did not comment on the morphological appearance of these tumours. (Cohen et al., 2003) Our cohort included tumours from all areas of the urogenital tract and it is unlikely all of these tumours will express mutant BRAF, even bearing in mind that BRAF mutations tend to occur at a higher frequency in tumours that harbour RAS mutations. A small study of 28 pancreatic tumours that included 1 papillary tumour, had no detectable BRAF mutations; indeed the one papillary tumour included in the study had a detectable k-ras mutation (which can be found in up to 90% of pancreatic cancers). (Ishimura et al., 2003)

BRAF mutations however, have been detected in papillary tumours aside from PTC. These include tumours from the gallbladder, pancreas and serous papillary carcinomas of the ovary. 1/3 papillary tumours in a cohort of 21 gallbladder carcinomas had a demonstrable BRAF mutation at hotspot codon 599 of exon 15. (Saetta et al., 2004) These authors used PCR in combination with single-strand conformation polymorphism analysis (SSCP) and sequencing to detect mutated BRAF. The remaining 2 BRAF negative papillary tumours had alternate mutations in either K-RAS or p-53. Certainly, a result of one BRAF positive papillary tumour does not achieve statistical significance and of note, the authors in question used different BRAF forward and reverse primers to our group, together with different methodology in detecting the BRAF mutation.

Similarly, a low frequency of BRAF mutations were detected in intra-ductal papillary mucinous neoplasms of the pancreas (IPMN) in two separate studies, and seemed to be restricted to the intestinal type of mucosa. (Chadwick et al., 2008; Schonleben et al., 2008) Alternate mutations in genes such as K-ras, p53, PIK3CA seemed to be more prevalent suggesting alternate pathways for carcinogenesis between epithelial subtypes of IPMNs. Two separate studies both detected BRAF mutations only in low-grade forms of serous carcinoma of the ovary. (Davies et al., 2002; Singer et al., 2003) These results were further augmented by an extensive characterisation of BRAF mutations in the same tumour type by Sieben et al, who used a mini-sequencing technique, and found BRAF mutations in 33 of 91 low-grade tumours. (Sieben et al., 2004) No high grade tumours demonstrated BRAF mutations. None of our low-grade or high-grade serous carcinomas demonstrated BRAFT1799A mutation. The discrepancy in the sets of results (aside from methodological differences), may be that are numbers are too small (n=4) so no statistical inference can be drawn from our data. Tumour heterogeneity and geographical variations in the populations may be further explanatory factors.

As demonstrated by Davies et al (2002) BRAF mutation expression has spatial heterogeneity in terms of tissue distribution which is reflected in the morphological appearance of the tumour. For example a study on colorectal carcinomas found BRAF mutation in tumours with a mucinous (non-papillary) morphology [18], highlighting the phenotypic heterogeneity in terms of subsequent tumour morphology in BRAF positive tumours. (Li et al., 2006) BRAF mutations in this scenario may be contributing to the methylator phenotype. (Ang et al., 2008; Nagasaka et al., 2008)

Our results seem to indicate that BRAF T1799A mutation does not underpin the genotypic expression of the papillary phenotype, and similar to the results of other groups suggest that BRAF may not be a frequent target of mutations involved in the pathogenesis of human lung, breast, kidney, cervical, endometrial and ovarian carcinomas. (Ueda et al., 2008) It is possible that i) alternate BRAF mutations not examined may have a role; ii) akin to PTC, alternate oncogenes such as ras or ret/PTC, may be acting as key mediators in the RAS/RAF/ERK/MEK/ MAPK pathway to help induce papillary morphology or iii) it may be that there is activation of alternate pathways to MAPK to help induce papillary structures. (Soares et al., 2003) Future studies may have to look at alternate oncogene expression in papillary tumours or alternate pathways that have an influence on the cytoskeletal architecture (i.e. the WNT pathway) and at the role of cellular adhesion molecules such as the cadherin family.

4.7 Conclusion

In conclusion, BRAF (T1796A) mutations are restricted to certain subgroups of papillary tumours (PTC, low grade serous carcinoma of the ovary) and do not serve as a molecular link between tumours with a papillary phenotype.

4.8 References

Ang, P. W., W. Q. Li, R. Soong, and B. Iacopetta. 2008. BRAF mutation is associated with the CpG island methylator phenotype in colorectal cancer from young patients. Cancer Lett.

Barnier, J. V., C. Papin, A. Eychene, O. Lecoq, and G. Calothy. 1995. The mouse B-raf gene encodes multiple protein isoforms with tissue-specific expression. J Biol Chem 270:23381-9.

Bastian, B. C., P. E. LeBoit, and D. Pinkel. 2000. Mutations and copy number increase of HRAS in Spitz nevi with distinctive histopathological features. Am J Pathol 157:967-72.

Calipel, A., G. Lefevre, C. Pouponnot, F. Mouriaux, A. Eychene, and F. Mascarelli. 2003. Mutation of B-Raf in human choroidal melanoma cells mediates cell proliferation and transformation through the MEK/ERK pathway. J Biol Chem 278:42409-18.

Chadwick, B., C. Willmore-Payne, S. Tripp, L. J. Layfield, S. Hirschowitz, and J. Holden. 2008. Histologic, Immunohistochemical, and Molecular Classification of 52 IPMNs of the Pancreas. Appl Immunohistochem Mol Morphol.

Chan, T. L., W. Zhao, S. Y. Leung, and S. T. Yuen. 2003. BRAF and KRAS mutations in colorectal hyperplastic polyps and serrated adenomas. Cancer Res 63:4878-81.

Chin, L., L. A. Garraway, and D. E. Fisher. 2006. Malignant melanoma: genetics and therapeutics in the genomic era. Genes Dev 20:2149-82.

Ciampi, R., J. A. Knauf, R. Kerler, M. Gandhi, Z. Zhu, M. N. Nikiforova, H. M. Rabes, J. A. Fagin, and Y. E. Nikiforov. 2005. Oncogenic AKAP9-BRAF fusion is a novel mechanism of MAPK pathway activation in thyroid cancer. J Clin Invest 115:94-101.

Ciampi, R., and Y. E. Nikiforov. 2005. Alterations of the BRAF gene in thyroid tumors. Endocr Pathol 16:163-72.

Cohen, Y., M. Xing, E. Mambo, Z. Guo, G. Wu, B. Trink, U. Beller, W. H. Westra, P. W. Ladenson, and D. Sidransky. 2003. BRAF mutation in papillary thyroid carcinoma. J Natl Cancer Inst 95:625-7.

Curtin, J. A., J. Fridlyand, T. Kageshita, H. N. Patel, K. J. Busam, H. Kutzner, K. H. Cho, S. Aiba, E. B. Brocker, P. E. LeBoit, D. Pinkel, and B. C. Bastian. 2005. Distinct sets of genetic alterations in melanoma. N Engl J Med 353:2135-47.

Davies, H., G. R. Bignell, C. Cox, P. Stephens, S. Edkins, S. Clegg, J. Teague, H. Woffendin, M. J. Garnett, W. Bottomley, N. Davis, E. Dicks, R. Ewing, Y. Floyd, K. Gray, S. Hall, R. Hawes, J. Hughes, V. Kosmidou, A. Menzies, C. Mould, A. Parker, C. Stevens, S. Watt, S. Hooper, R. Wilson, H. Jayatilake, B. A. Gusterson, C. Cooper, J. Shipley, D. Hargrave, K. Pritchard-Jones, N. Maitland, G. Chenevix-Trench, G. J. Riggins, D. D. Bigner, G. Palmieri, A. Cossu, A. Flanagan, A. Nicholson, J. W. Ho, S. Y. Leung, S. T. Yuen, B. L. Weber, H. F. Seigler, T. L. Darrow, H. Paterson, R. Marais, C. J. Marshall, R. Wooster, M. R. Stratton, and P. A. Futreal. 2002. Mutations of the BRAF gene in human cancer. Nature 417:949-54.

De Raeve, L. E., A. Claes, D. J. Ruiter, G. N. van Muijen, D. Roseeuw, and L. C. van Kempen. 2006. Distinct phenotypic changes between the superficial and deep component of giant congenital melanocytic naevi: a rationale for curettage. Br J Dermatol 154:485-92.

Domingo, E., E. Espin, M. Armengol, C. Oliveira, M. Pinto, A. Duval, C. Brennetot, R. Seruca, R. Hamelin, H. Yamamoto, and S. Schwartz, Jr. 2004. Activated BRAF targets proximal colon tumors with mismatch repair deficiency and MLH1 inactivation. Genes Chromosomes Cancer 39:138-42.

Emuss, V., M. Garnett, C. Mason, and R. Marais. 2005. Mutations of C-RAF are rare in human cancer because C-RAF has a low basal kinase activity compared with B-RAF. Cancer Res 65:9719-26.

Errico, M. E., S. Staibano, F. Tranfa, G. Bonavolonta, L. Lo Muzio, P. Somma, A. Lucariello, G. Mansueto, A. D'Aponte, G. Ferrara, and G. De Rosa. 2003. Expression of cyclin-D1 in uveal malignant melanoma. Anticancer Res 23:2701-6.

Feng, Y. Z., T. Shiozawa, T. Miyamoto, H. Kashima, M. Kurai, A. Suzuki, and I. Konishi. 2005. BRAF mutation in endometrial carcinoma and hyperplasia: correlation with KRAS and p53 mutations and mismatch repair protein expression. Clin Cancer Res 11:6133-8.

Frasca, F., C. Nucera, G. Pellegriti, P. Gangemi, M. Attard, M. Stella, M. Loda, V. Vella, C. Giordano, F. Trimarchi, E. Mazzon, A. Belfiore, and R. Vigneri. 2008. BRAF(V600E) mutation and the biology of papillary thyroid cancer. Endocr Relat Cancer 15:191-205.

Fugazzola, L., E. Puxeddu, N. Avenia, C. Romei, V. Cirello, A. Cavaliere, P. Faviana, D. Mannavola, S. Moretti, S. Rossi, M. Sculli, V. Bottici, P. Beck-Peccoz, F. Pacini, A. Pinchera, F. Santeusanio, and R. Elisei. 2006. Correlation between B-RAFV600E mutation and clinico-pathologic parameters in papillary thyroid carcinoma: data from a multicentric Italian study and review of the literature. Endocr Relat Cancer 13:455-64.

Fukushima, T., S. Suzuki, M. Mashiko, T. Ohtake, Y. Endo, Y. Takebayashi, K. Sekikawa, K. Hagiwara, and S. Takenoshita. 2003. BRAF mutations in papillary carcinomas of the thyroid. Oncogene 22:6455-7.

Goodall, J., C. Wellbrock, T. J. Dexter, K. Roberts, R. Marais, and C. R. Goding. 2004. The Brn-2 transcription factor links activated BRAF to melanoma proliferation. Mol Cell Biol 24:2923-31.

Hahn, W. C., S. K. Dessain, M. W. Brooks, J. E. King, B. Elenbaas, D. M. Sabatini, J. A. DeCaprio, and R. A. Weinberg. 2002. Enumeration of the simian virus 40 early region elements necessary for human cell transformation. Mol Cell Biol 22:2111-23.

Hingorani, S. R., M. A. Jacobetz, G. P. Robertson, M. Herlyn, and D. A. Tuveson. 2003. Suppression of BRAF(V599E) in human melanoma abrogates transformation. Cancer Res 63:5198-202.

Hoeflich, K. P., D. C. Gray, M. T. Eby, J. Y. Tien, L. Wong, J. Bower, A. Gogineni, J. Zha, M. J. Cole, H. M. Stern, L. J. Murray, D. P. Davis, and S. Seshagiri. 2006. Oncogenic BRAF is required for tumor growth and maintenance in melanoma models. Cancer Res 66:999-1006.

Ishimura, N., K. Yamasawa, M. A. Karim Rumi, Y. Kadowaki, S. Ishihara, Y. Amano, Y. Nio, T. Higami, and Y. Kinoshita. 2003. BRAF and K-ras gene mutations in human pancreatic cancers. Cancer Lett 199:169-73.

Kambara, T., L. A. Simms, V. L. Whitehall, K. J. Spring, C. V. Wynter, M. D. Walsh, M. A. Barker, S. Arnold, A. McGivern, N. Matsubara, N. Tanaka, T. Higuchi, J. Young, J. R. Jass, and B. A. Leggett. 2004. BRAF mutation is associated with DNA methylation in serrated polyps and cancers of the colorectum. Gut 53:1137-44.

Kimura, E. T., M. N. Nikiforova, Z. Zhu, J. A. Knauf, Y. E. Nikiforov, and J. A. Fagin. 2003. High prevalence of BRAF mutations in thyroid cancer: genetic evidence for constitutive activation of the RET/PTC-RAS-BRAF signaling pathway in papillary thyroid carcinoma. Cancer Res 63:1454-7.

Knauf, J. A., X. Ma, E. P. Smith, L. Zhang, N. Mitsutake, X. H. Liao, S. Refetoff, Y. E. Nikiforov, and J. A. Fagin. 2005. Targeted expression of BRAFV600E in thyroid cells of transgenic mice results in papillary thyroid cancers that undergo dedifferentiation. Cancer Res 65:4238-45.

Kondo, T., S. Ezzat, and S. L. Asa. 2006. Pathogenetic mechanisms in thyroid follicular-cell neoplasia. Nat Rev Cancer 6:292-306.

Lee, J. W., Y. H. Soung, S. Y. Kim, W. S. Park, S. W. Nam, W. S. Min, S. H. Kim, J. Y. Lee, N. J. Yoo, and S. H. Lee. 2005. Mutational analysis of the ARAF gene in human cancers. Apmis 113:54-7.

Li, W. Q., K. Kawakami, A. Ruszkiewicz, G. Bennett, J. Moore, and B. Iacopetta. 2006. BRAF mutations are associated with distinctive clinical, pathological and molecular features of colorectal cancer independently of microsatellite instability status. Mol Cancer 5:2.

Maldonado, J. L., J. Fridlyand, H. Patel, A. N. Jain, K. Busam, T. Kageshita, T. Ono, D. G. Albertson, D. Pinkel, and B. C. Bastian. 2003. Determinants of BRAF mutations in primary melanomas. J Natl Cancer Inst 95:1878-90.

Marais, R., Y. Light, H. F. Paterson, C. S. Mason, and C. J. Marshall. 1997. Differential regulation of Raf-1, A-Raf, and B-Raf by oncogenic ras and tyrosine kinases. J Biol Chem 272:4378-83.

McPhillips, F., P. Mullen, K. G. MacLeod, J. M. Sewell, B. P. Monia, D. A. Cameron, J. F. Smyth, and S. P. Langdon. 2006. Raf-1 is the predominant Raf isoform that mediates growth factor-stimulated growth in ovarian cancer cells. Carcinogenesis 27:729-39.

Melillo, R. M., M. D. Castellone, V. Guarino, V. De Falco, A. M. Cirafici, G. Salvatore, F. Caiazzo, F. Basolo, R. Giannini, M. Kruhoffer, T. Orntoft, A. Fusco, and M. Santoro. 2005. The RET/PTC-RAS-BRAF linear signaling cascade mediates the motile and mitogenic phenotype of thyroid cancer cells. J Clin Invest 115:1068-81.

Mercer, K. E., and C. A. Pritchard. 2003. Raf proteins and cancer: B-Raf is identified as a mutational target. Biochim Biophys Acta 1653:25-40.

Mesa, C., Jr., M. Mirza, N. Mitsutake, M. Sartor, M. Medvedovic, C. Tomlinson, J. A. Knauf, G. F. Weber, and J. A. Fagin. 2006. Conditional activation of RET/PTC3 and BRAFV600E in thyroid cells is associated with gene expression profiles that predict a preferential role of BRAF in extracellular matrix remodeling. Cancer Res 66:6521-9.

Michaloglou, C., L. C. Vredeveld, W. J. Mooi, and D. S. Peeper. 2008. BRAF(E600) in benign and malignant human tumours. Oncogene 27:877-95.

Michaloglou, C., L. C. Vredeveld, M. S. Soengas, C. Denoyelle, T. Kuilman, C. M. van der Horst, D. M. Majoor, J. W. Shay, W. J. Mooi, and D. S. Peeper. 2005. BRAFE600-associated senescence-like cell cycle arrest of human naevi. Nature 436:720-4.

Mitsutake, N., J. A. Knauf, S. Mitsutake, C. Mesa, Jr., L. Zhang, and J. A. Fagin. 2005. Conditional BRAFV600E expression induces DNA synthesis, apoptosis, dedifferentiation, and chromosomal instability in thyroid PCCL3 cells. Cancer Res 65:2465-73.

Morice, C., F. Nothias, S. Konig, P. Vernier, M. Baccarini, J. D. Vincent, and J. V. Barnier. 1999. Raf-1 and B-Raf proteins have similar regional distributions but differential subcellular localization in adult rat brain. Eur J Neurosci 11:1995-2006.

Mutch, D. G., M. A. Powell, M. A. Mallon, and P. J. Goodfellow. 2004. RAS/RAF mutation and defective DNA mismatch repair in endometrial cancers. Am J Obstet Gynecol 190:935-42.

Nagasaka, T., M. Koi, M. Kloor, J. Gebert, A. Vilkin, N. Nishida, S. K. Shin, H. Sasamoto, N. Tanaka, N. Matsubara, C. R. Boland, and A. Goel. 2008. Mutations in both KRAS and BRAF may contribute to the methylator phenotype in colon cancer. Gastroenterology 134:1950-60, 1960 e1.

Nagy, A., I. Balint, and G. Kovacs. 2003. Frequent allelic changes at chromosome 7q34 but lack of mutation of the BRAF in papillary renal cell tumors. Int J Cancer 106:980-1.

Namba, H., M. Nakashima, T. Hayashi, N. Hayashida, S. Maeda, T. I. Rogounovitch, A. Ohtsuru, V. A. Saenko, T. Kanematsu, and S. Yamashita. 2003. Clinical implication of hot spot BRAF mutation, V599E, in papillary thyroid cancers. J Clin Endocrinol Metab 88:4393-7.

Nikiforova, M. N., E. T. Kimura, M. Gandhi, P. W. Biddinger, J. A. Knauf, F. Basolo, Z. Zhu, R. Giannini, G. Salvatore, A. Fusco, M. Santoro, J. A. Fagin, and Y. E. Nikiforov. 2003. BRAF mutations in thyroid tumors are restricted to papillary carcinomas and anaplastic or poorly differentiated carcinomas arising from papillary carcinomas. J Clin Endocrinol Metab 88:5399-404.

Park, J. I., C. J. Strock, D. W. Ball, and B. D. Nelkin. 2002. The ras/raf/mek extracellular signal-regulated kinase pathway induces autocrine-paracrine growth inhibition via the leukaemia inhibitory factor/JAK/STAT pathway. Mol Cell Biol 23:543-554.

Pollock, P. M., U. L. Harper, K. S. Hansen, L. M. Yudt, M. Stark, C. M. Robbins, T. Y. Moses, G. Hostetter, U. Wagner, J. Kakareka, G. Salem, T. Pohida, P. Heenan, P. Duray, O. Kallioniemi, N. K. Hayward, J. M. Trent, and P. S. Meltzer. 2003. High frequency of BRAF mutations in nevi. Nat Genet 33:19-20.

Rapp, U. R., and G. J. Todaro. 1980. Generation of oncogenic mouse type C viruses: in vitro selection of carcinoma-inducing variants. Proc Natl Acad Sci U S A 77:624-8.

Riesco-Eizaguirre, G., P. Gutierrez-Martinez, M. A. Garcia-Cabezas, M. Nistal, and P. Santisteban. 2006. The oncogene BRAF V600E is associated with a high risk of recurrence and less differentiated papillary thyroid carcinoma due to the impairment of Na+/I- targeting to the membrane. Endocr Relat Cancer 13:257-69.

Rotolo, S., R. Diotti, R. E. Gordon, R. F. Qiao, Z. Yao, R. G. Phelps, and J. Dong. 2005. Effects on proliferation and melanogenesis by inhibition of mutant BRAF and expression of wild-type INK4A in melanoma cells. Int J Cancer 115:164-9.

Saetta, A. A., P. Papanastasiou, N. V. Michalopoulos, F. Gigelou, P. Korkolopoulou, T. Bei, and E. Patsouris. 2004. Mutational analysis of BRAF in gallbladder carcinomas in association with K-ras and p53 mutations and microsatellite instability. Virchows Arch 445:179-82.

Salvatore, G., V. De Falco, P. Salerno, T. C. Nappi, S. Pepe, G. Troncone, F. Carlomagno, R. M. Melillo, S. M. Wilhelm, and M. Santoro. 2006. BRAF is a therapeutic target in aggressive thyroid carcinoma. Clin Cancer Res 12:1623-9.

Schonleben, F., J. D. Allendorf, W. Qiu, X. Li, D. J. Ho, N. T. Ciau, R. L. Fine, J. A. Chabot, H. E. Remotti, and G. H. Su. 2008. Mutational analyses of multiple oncogenic pathways in intraductal papillary mucinous neoplasms of the pancreas. Pancreas 36:168-72.

Sieben, N. L., P. Macropoulos, G. M. Roemen, S. M. Kolkman-Uljee, G. Jan Fleuren, R. Houmadi, T. Diss, B. Warren, M. Al Adnani, A. P. De Goeij, T. Krausz, and A. M. Flanagan. 2004. In ovarian neoplasms, BRAF, but not KRAS, mutations are restricted to low-grade serous tumours. J Pathol 202:336-40.

Singer, G., R. Oldt, 3rd, Y. Cohen, B. G. Wang, D. Sidransky, R. J. Kurman, and M. Shih Ie. 2003. Mutations in BRAF and KRAS characterize the development of low-grade ovarian serous carcinoma. J Natl Cancer Inst 95:484-6.

Smyth, P., S. Finn, S. Cahill, E. O'Regan, R. Flavin, J. J. O'Leary, and O. Sheils. 2005. ret/PTC and BRAF act as distinct molecular, time-dependant triggers in a sporadic Irish cohort of papillary thyroid carcinoma. Int J Surg Pathol 13:1-8.

Soares, P., V. Trovisco, A. S. Rocha, J. Lima, P. Castro, A. Preto, V. Maximo, T. Botelho, R. Seruca, and M. Sobrinho-Simoes. 2003. BRAF mutations and RET/PTC rearrangements are alternative events in the etiopathogenesis of PTC. Oncogene 22:4578-80.

Sumimoto, H., M. Miyagishi, H. Miyoshi, S. Yamagata, A. Shimizu, K. Taira, and Y. Kawakami. 2004. Inhibition of growth and invasive ability of melanoma by inactivation of mutated BRAF with lentivirus-mediated RNA interference. Oncogene 23:6031-9.

Trovisco, V., P. Soares, and M. Sobrinho-Simoes. 2006. B-RAF mutations in the etiopathogenesis, diagnosis, and prognosis of thyroid carcinomas. Hum Pathol 37:781-6.

Trovisco, V., I. Vieira de Castro, P. Soares, V. Maximo, P. Silva, J. Magalhaes, A. Abrosimov, X. M. Guiu, and M. Sobrinho-Simoes. 2004. BRAF mutations are associated with some histological types of papillary thyroid carcinoma. J Pathol 202:247-51.

Ueda, M., E. Toji, O. Nunobiki, S. Izuma, Y. Okamoto, K. Torii, and S. Noda. 2008. Mutational analysis of the BRAF gene in human tumor cells. Hum Cell 21:13-7.

Wajapeyee, N., R. W. Serra, X. Zhu, M. Mahalingam, and M. R. Green. 2008. Oncogenic BRAF induces senescence and apoptosis through pathways mediated by the secreted protein IGFBP7. Cell 132:363-74.

Wan, P. T., M. J. Garnett, S. M. Roe, S. Lee, D. Niculescu-Duvaz, V. M. Good, C. M. Jones, C. J. Marshall, C. J. Springer, D. Barford, and R. Marais. 2004. Mechanism of activation of the RAF-ERK signaling pathway by oncogenic mutations of B-RAF. Cell 116:855-67.

Wang, H. G., U. R. Rapp, and J. C. Reed. 1996. Bcl-2 targets the protein kinase Raf-1 to mitochondria. Cell 87:629-38.

Wang, Y., M. Ji, W. Wang, Z. Miao, P. Hou, X. Chen, F. Xu, G. Zhu, X. Sun, Y. Li, S. Condouris, D. Liu, S. Yan, J. Pan, and M. Xing. 2008. Association of the T1799A BRAF mutation with tumor extrathyroidal invasion, higher peripheral platelet counts, and over-expression of platelet-derived growth factor-B in papillary thyroid cancer. Endocr Relat Cancer 15:183-90.

Weinstein, I. B. 2002. Cancer. Addiction to oncogenes--the Achilles heal of cancer. Science 297:63-4.

Willmore-Payne, C., J. A. Holden, S. Hirschowitz, and L. J. Layfield. 2006. BRAF and c-kit gene copy number in mutation-positive malignant melanoma. Hum Pathol 37:520-7.

Willmore-Payne, C., J. A. Holden, S. Tripp, and L. J. Layfield. 2005. Human malignant melanoma: detection of BRAF- and c-kit-activating mutations by high-resolution amplicon melting analysis. Hum Pathol 36:486-93.

Woo, M. M., C. M. Salamanca, M. Miller, J. Symowicz, P. C. Leung, C. Oliveira, T. G. Ehlen, C. B. Gilks, D. Huntsman, and N. Auersperg. 2008. Serous borderline ovarian tumors in long-term culture: phenotypic and genotypic distinction from invasive ovarian carcinomas. Int J Gynecol Cancer.

Xing, M. 2005. BRAF mutation in thyroid cancer. Endocr Relat Cancer 12:245-62.

Xu, X., R. M. Quiros, P. Gattuso, K. B. Ain, and R. A. Prinz. 2003. High prevalence of BRAF gene mutation in papillary thyroid carcinomas and thyroid tumor cell lines. Cancer Res 63:4561-7.

Yang, S., F. A. Farraye, C. Mack, O. Posnik, and M. J. O'Brien. 2004. BRAF and KRAS Mutations in hyperplastic polyps and serrated adenomas of the colorectum: relationship to histology and CpG island methylation status. Am J Surg Pathol 28:1452-9.

Yazdi, A. S., G. Palmedo, M. J. Flaig, U. Puchta, A. Reckwerth, A. Rutten, T. Mentzel, H. Hugel, M. Hantschke, M. H. Schmid-Wendtner, H. Kutzner, and C. A. Sander. 2003. Mutations of the BRAF gene in benign and malignant melanocytic lesions. J Invest Dermatol 121:1160-2.

Yuryev, A., M. Ono, S. A. Goff, F. Macaluso, and L. P. Wennogle. 2000. Isoform-specific localization of A-RAF in mitochondria. Mol Cell Biol 20:4870-8.

Zebisch, A., P. B. Staber, A. Delavar, C. Bodner, K. Hiden, K. Fischereder, M. Janakiraman, W. Linkesch, H. W. Auner, W. Emberger, C. Windpassinger, M. G. Schimek, G. Hoefler, J. Troppmair, and H. Sill. 2006. Two transforming C-RAF germ-line mutations identified in patients with therapy-related acute myeloid leukemia. Cancer Res 66:3401-8.

Chapter 5

General Discussion

5.1 General Discussion of Results

Undoubtedly the interest in ret and it's association with papillary thyroid carcinoma (PTC) was fuelled by the Chernobyl disaster in 1986. Santoro's initial well-powered study of ret/PTC arrangements in non-thyroid tumours seemed to solidify ret activation as the exclusive reserve of PTC; despite technical limitations and sampling issues (which have already been discussed in Chapter 3). More recent reports however, have challenged the validity of RET/PTC as a tumour marker and its specificity for PTC. One of these studies had emanated from our research group when we demonstrated the presence of ret/PTC-1 rearrangement in Hashimoto's thyroiditis. (Sheils et al., 2002) Though controversial at the time, these results were later validated by work carried out by Tallini's group. They used interphase FISH to demonstrate the presence of low-level ret/PTC rearrangements in non-neoplastic follicular cells of Hashimoto's thyroiditis. (Rhoden et al., 2006) Further work has identified ret/PTC activation in other thyroid tumour histotypes such as oncocytic adenomas and carcinomas, (Cheung et al., 2000) and non-neoplastic entities such as hyperplastic nodules (Elisei et al., 2001; Ishizaka et al., 1991).

In parallel with these studies, ret rearrangements were found to be associated with radiation-induced PTC and ret/PTC-3 was strongly associated with the morphologically distinct solid variant occurring in Chernobyl fallout children. (Klugbauer et al., 2000; Klugbauer et al., 1995; Nikiforov et al., 1997) The association between ret activation and tumour morphology was noted by our group and subsequently we established a relationship between ret/PTC-1 activation and the cell adhesion molecules E-cadherin and β and γ-catenin. (Smyth et al., 2003; Smyth et al., 2001) Indeed, comparison of the morphological features of PTC with specific ret rearrangements, helped identify ret/PTC-3 as being exclusively associated with the follicular

variant of PTC. (Finn et al., 2003) ***The former study seemed to indicate to us a possible mechanism of how ret activation may influence epithelial morphology and the latter study firmly established the association between ret rearrangements and tumour morphology.*** Indeed, as an adjunct we established that mutant BRAF V600E was seen almost exclusively in PTC with a classic or papillary morphology, findings which were confirmed by Trovisco et al. (Smyth et al., 2005; Trovisco et al., 2004) This prompted the question as to whether ret/PTC rearrangements and BRAF V600E mutation were associated with papillary morphology per se and it is this hypothesis that formed the basis of this thesis.

In chapter 3 we demonstrated that a small subset of non-thyroid papillary tumours had detectable ret/PTC-1 rearrangements (i.e. primary peritoneal carcinoma and papillary renal cell carcinoma). The number of tumours with rearranged ret is small and a larger powered study (to include fresh frozen samples with high quality RNA) will be needed to definitively assess the role of ret rearrangements in the development or maintenance of a papillary phenotype. In chapter 4 we demonstrated that all 57 papillary tumours were homozygous for wild type BRAF. Though disappointing, the latter set of results are not wholly surprising. As discussed in chapter 4 BRAF mutations are seen in a morphologically diverse set of tumours which includes a large number of tumours with a non-papillary phenotype. What the ret study does do however is highlight the poignant fact that biological systems rarely obey an 'all or nothing law' and seem to operate somewhere in a middle ground. Our findings however lead us to the following logical questions: Why is ret activation occurring in these tumours? What is its role (if any) in the genesis of these tumours? How does it contribute in part to the tumour ('papillary') phenotype?

The first question was dealt with in the discussion in chapter 3 where we highlighted the possible role of inflammation and X-ray irradiation in inducing the ret/PTC-1 rearrangement. As to the potential role of activated ret in the genesis of these tumours recent literature suggests that ret/PTC rearrangements may be secondary non-clonal or sub-clonal events even in Chernobyl PTCs. Somatic mutations in cancer have been called driver when they are positively selected and causally related to tumour development and passenger when not directly implicated with tumour growth. (Davies et al., 2005) *ret/PTC* rearrangements in our study can hardly be considered as driver mutations in tumours with minimal levels of detectable fusion gene. These rearrangements may reflect *RET* instability in epithelial cells and point to the existence of secondary cell subclones, which are unlikely to be of any pathological consequence in determining biological behaviour. Our group has noted previously that ret/PTC-3 transcripts are transiently expressed at low levels by a minority of cells irradiated with γ-rays, findings consistent with this viewpoint. (Finn et al., 2004) Indeed, Unger et al have also found that ret rearrangements are heterogenous in their distribution within PTCs a finding which further corroborates the impression that ret activation is a secondary event in PTC tumourigenesis. (Unger et al., 2004)

To our last question: how does ret activation contribute in part, to the adaptation of papillary morphology? To elaborate on our discussion in chapter 3, one of the clues may lie in previous work carried out by our group. Smyth et al. demonstrated variable down-regulation of E-cadherin among thyroid carcinomas with a gradual reduction in expression from normal to well-differentiated carcinomas to its absence in anaplastic lesions. (Smyth et al., 2001) We can elaborate from this that solid ('structure less') anaplastic tumours have reduced E-cadherin compared to classical PTC which displays the geometric orderliness of papillary morphology.

Similarly, E-cadherin expression has been described in ovarian serous carcinomas, with maintenance of expression in primary disease and decrease in expression in metastatic disease. (Marques et al., 2004; Peralta Soler et al., 1997; Sundfeldt et al., 1997) Importantly, most primary lesions maintain their papillary architecture whilst metastatic disease assumes a more solid morphology.

We speculated at the time that down-regulation of E-cadherin expression is an ultimate consequence of the aberrant kinase signaling of ret/PTC. The relationship between tyrosine kinase signaling and reduced cellular adhesion is well known. Studies such as Behrens et al. have shown that disturbance of intercellular adhesion and induction of in vitro invasion of MDCK cells by tyrosine kinases such as v-src is accomplished by tyrosine phosphorylation of the E-cadherin/catenin complex. (Behrens et al., 1993) Due to the fact that ret/PTC is also a tyrosine kinase, the tyrosine phosphorylation-dependent checkpoints that regulate cell adhesion, locomotion and tissue morphogenesis in the thyroid are likely to be important factors that contribute to converting the aberrant expression of a tyrosine kinase into the pathological phenotype of PTC. Yap et al. showed that E-cadherin is essential for initial thyroid cell adhesion and follicular reorganisation. (Yap et al., 1995) During thyroid follicular morphogenesis, E-cadherin mediates cell-cell adhesion and recruits other specialised proteins to the cell surface such as ZO-1 and Na^+/K^+-ATPase. Machado et al. suggested that inactivation of E-cadherin may be responsible for the characteristic growth pattern of diffuse gastric carcinomas. (Machado et al., 1999) It may be therefore fair to say that in human cancers such as thyroid or ovary that E-cadherin expression is directly related to histological features as well as invasion and metastasis. Could this imply that the ret/PTC oncogene influences tumour morphology to the extent of the

distinctive characteristics of papillary morphology indirectly via E-cadherin? It is possible and perhaps even more so due to the fact that the study also revealed significantly different E-cadherin expression levels between PTC and FTC with the latter being much lower.

But what is the link so (however indirect) between ret/PTC activation, the E-cadherin complex and subsequent tissue/epithelial morphology? Tissue morphogenesis is a complex interplay between intrinsic forces that drive cell shape and external interactions with basement membrane (BM) and extra-cellular matrix (ECM) directing biochemical and biomechanical cues to regulate epithelial development. Adhesion complexes which include the cadherin-catenin complex have a role in regulating actin filaments within the cell (Figure 5.1) and hence in directing cell shape.

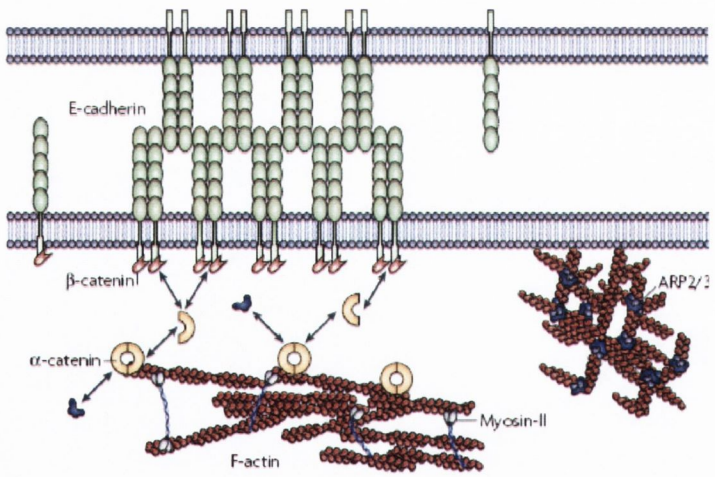

Figure 5.1 Interplay between the cadherin-catenin complex and actin-myosin complex. (Lecuit and Lenne, 2007)

Indeed the development of epithelial tissues is tightly coupled to the production of basement membrane and interstitial matrix at all stages of development ranging from the newly formed embyronic endoderm and ectoderm to the remodelled gland in the adult.

As epithelial cells proliferate and differentiate they remodel the BM and interstitial matrix to facilitate proper development and orientation in a process called ***dynamic reciprocity***. (Lopez et al., 2008) ECM components also modulate cell phenotype by generating tensional forces within the interstitum and through spatial orientation of matrix fibrils. Cells in turn respond to external forces through cytoskeletal remodelling and actomyosin contractility by a process called ***mechanoreciprocity***. (Lopez et al., 2008) Intracellular forces are transmitted into biochemical signals via integrins and actin molecules acting through signal transducers ERK and ROCK (Figure 5.2).

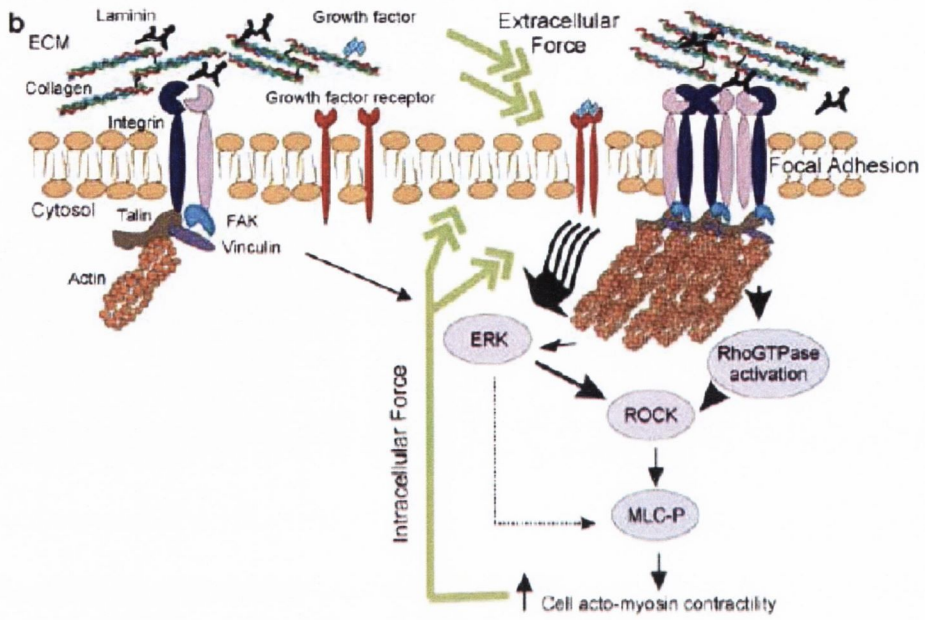

Figure 5.2 Mechanism of transmission of extra-cellular forces into biochemical signals . (Lopez et al., 2008)

Of consequence is that ERK is a known substrate of the classical MAPK pathway (Figure 5.3) and as such provides a second possible link (aside from E-cadherin) between ret activation and cytoskeletal remodelling.

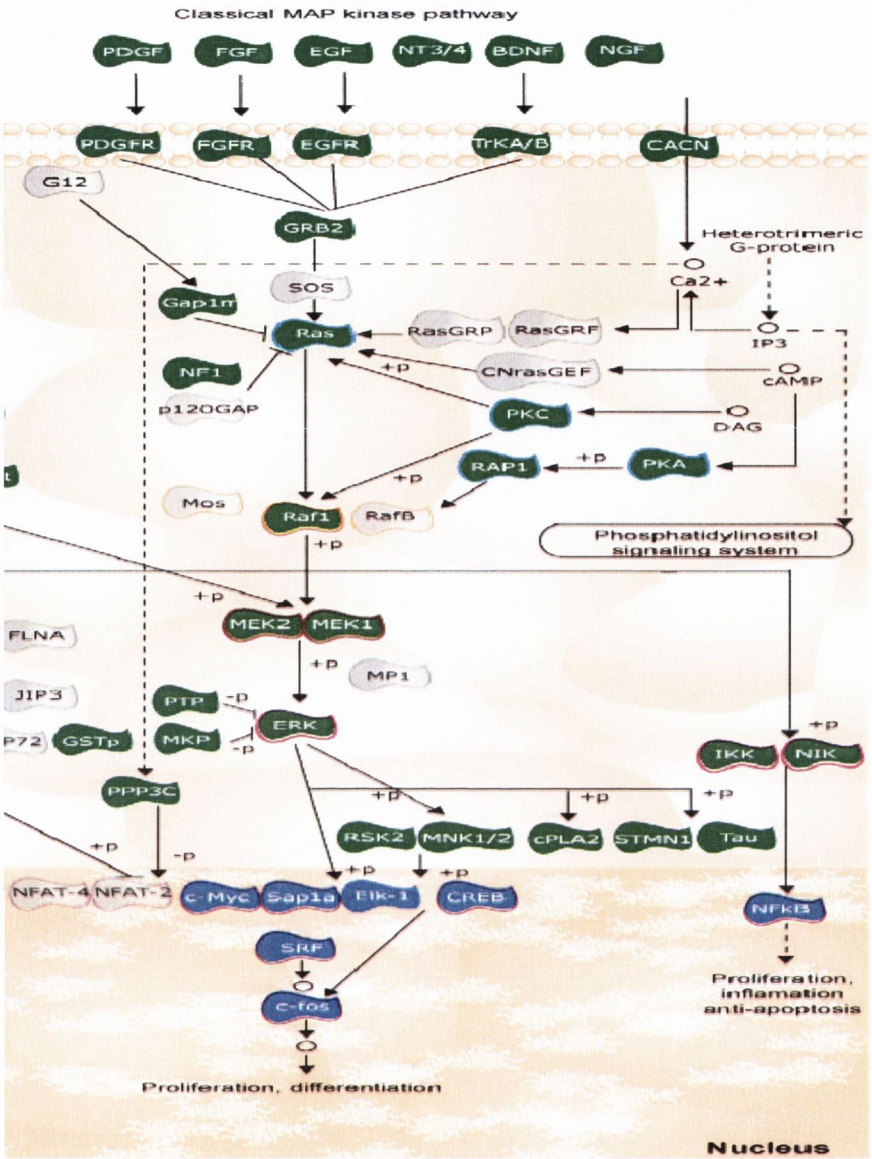

Figure 5.3 Classical MAPK signaling pathway. Note ERK is a central effector molecule of the pathway.

We have so far discussed how ret may influence papillary morphology in thyroid and ovarian tumours. But how is this of relevance to PRCC? It is possible that a different mechanism maybe at play. Many organs in the body are made up of a network of branched tubules. Cells are responsive to positional signals from their local cellular microenvironment that govern where and when branches are formed.

The ret receptor tyrosine kinase is activated by GDNF and controls outgrowth and invasion of the ureteric bud in the developing kidney. In renal epithelia activation of ret results in chemotaxis as ret expressing cells invade the surrounding GDNF expressing tissue. The PI3K/PTEN axis has a critical role in shaping the epithelial branches in the developing kidney in response to ret activation. (Kim and Dressler, 2007) PTEN helps regulate cellular chemotaxis by antagonising the PI3K signalling pathway. Of note, PTEN mutations have been described in human primary renal cell carcinomas, (Kondo et al., 2001) with reduction in PTEN protein occurring in papillary RCC. (He et al., 2007) It is interesting to hypothesis that this in turn may lead to loss of PTEN mediated suppression of ret induced cell migration and hence the adoption of a papillary morphology.

5.2 Future Work: 'The RET Effect'

To address the question as to why ret activation occurs in PPC and PRCC, future work will look at the cellular and transcriptome effects of X-ray irradiation and inflammation on primary cell cultures of primary peritoneal and papillary renal cell carcinoma. Specifically we will look for the induction of the ret/PTC-1 chimera and the downstream pathway effects through a pan-genomic approach using microarray technology. To assess the ret effect on tumour morphology, we will employ a 3D culture system to accurately study ret activated (and ret deactivated using siRNA technology) epithelial cell morphogenesis in vitro (to recapitulate the in vivo 3D environment). 3D models involve embedding a single type of cell in a biocompatible scaffold which provide cells with a prefabricated ECM, which is often modifiable by the embedded cells. Moreover, we will assess the overlapping transcriptome and miRNAome profiles of papillary tumours to get a more global 'holistic' view of the multiple regulator checkpoints involved in determining the papillary phenotype.

5.3 Magic Bullets

To date we have just discussed the molecular implications of ret activation occurring in tumours outside of the thyroid gland, and the clinical implications have largely been ignored. Primary peritoneal carcinoma is a devastating disease and as eluded to in chapter 1, patients with this disease have a very poor prognosis. Why is this so? Primary peritoneal carcinoma is histologically identical to ovarian serous carcinoma and as such is classified and treated similarly. The majority of these cancers only present at advanced stages (III or IV) and are treated by surgery and systemic chemotherapy.

Despite an initial 70-80% response rate, current therapy is frequently followed by recurrence which is often resistant to chemotherapy, as demonstrated by 5-20% long-term survivors. (Kikkawa et al., 2006) As such there is an urgent need to develop newer treatment modalities. The description of ret activation in primary peritoneal carcinoma in this study, if validated, may offer a more novel therapeutic strategy for oncologists in the form of the newly developed ret kinase inhibitors.

At the time of writing targeted treatment for RET-driven cancers is not clinically available in current therapy. Though not licensed for non-thyroid malignancy, small molecule tyrosine kinase inhibitors, including sorafenib, sunitinib, motesanib and vandetanib, which have already shown efficacy against other neoplastic diseases, are being evaluated in clinical trials for treatment of thyroid carcinomas. (Lanzi et al., 2008) Most of them, also described as Ret inhibitors, are multi-kinase inhibitors with antiangiogenic activity related to inhibition of receptor tyrosine kinases, such as the vascular endothelial growth factor receptors.

Preclinical evidence supports the relevance of ret oncoproteins as therapeutic targets for a subset of thyroid neoplastic diseases and, although targeting the original causal genetic change may not be sufficient to control the disease efficiently, the available knowledge outlines therapeutic opportunities for exploiting ret inhibition.

5.4 References

Behrens, J., L. Vakaet, R. Friis, E. Winterhager, F. Van Roy, M. M. Mareel, and W. Birchmeier. 1993. Loss of epithelial differentiation and gain of invasiveness correlates with tyrosine phosphorylation of the E-cadherin/beta-catenin complex in cells transformed with a temperature-sensitive v-SRC gene. J Cell Biol 120:757-66.

Cheung, C. C., S. Ezzat, L. Ramyar, J. L. Freeman, and S. L. Asa. 2000. Molecular basis of Hurtle cell papillary thyroid carcinoma. J Clin Endocrinol Metab 85:878-82.

Davies, H., C. Hunter, R. Smith, P. Stephens, C. Greenman, G. Bignell, J. Teague, A. Butler, S. Edkins, C. Stevens, A. Parker, S. O'Meara, T. Avis, S. Barthorpe, L. Brackenbury, G. Buck, J. Clements, J. Cole, E. Dicks, K. Edwards, S. Forbes, M. Gorton, K. Gray, K. Halliday, R. Harrison, K. Hills, J. Hinton, D. Jones, V. Kosmidou, R. Laman, R. Lugg, A. Menzies, J. Perry, R. Petty, K. Raine, R. Shepherd, A. Small, H. Solomon, Y. Stephens, C. Tofts, J. Varian, A. Webb, S. West, S. Widaa, A. Yates, F. Brasseur, C. S. Cooper, A. M. Flanagan, A. Green, M. Knowles, S. Y. Leung, L. H. Looijenga, B. Malkowicz, M. A. Pierotti, B. T. Teh, S. T. Yuen, S. R. Lakhani, D. F. Easton, B. L. Weber, P. Goldstraw, A. G. Nicholson, R. Wooster, M. R. Stratton, and P. A. Futreal. 2005. Somatic mutations of the protein kinase gene family in human lung cancer. Cancer Res 65:7591-5.

Elisei, R., C. Romei, T. Vorontsova, B. Cosci, V. Veremeychik, E. Kuchinskaya, F. Basolo, E. P. Demidchik, P. Miccoli, A. Pinchera, and F. Pacini. 2001. RET/PTC rearrangements in thyroid nodules: studies in irradiated and not irradiated, malignant and benign thyroid lesions in children and adults. J Clin Endocrinol Metab 86:3211-6.

Finn, S. P., P. Smyth, J. O'Leary, E. C. Sweeney, and O. Sheils. 2003. Ret/PTC chimeric transcripts in an Irish cohort of sporadic papillary thyroid carcinoma. J Clin Endocrinol Metab 88:938-41.

Finn, S. P., P. Smyth, E. O'Regan, S. Cahill, R. Flavin, J. O'Leary, and O. Sheils. 2004. Array comparative genomic hybridisation analysis of gamma-irradiated human thyrocytes. Virchows Arch 445:396-404.

He, L., C. Fan, A. Gillis, X. Feng, M. Sanatani, S. Hotte, A. Kapoor, and D. Tang. 2007. Co-existence of high levels of the PTEN protein with enhanced Akt activation in renal cell carcinoma. Biochim Biophys Acta 1772:1134-42.

Ishizaka, Y., S. Kobayashi, T. Ushijima, S. Hirohashi, T. Sugimura, and M. Nagao. 1991. Detection of ret/PTC transcripts in thyroid adenomas and adenomatous goiter by an RT-PCR method. Oncogene 6:1667-72.

Kikkawa, F., A. Nawa, K. Ino, K. Shibata, H. Kajiyama, and S. Nomura. 2006. Advances in treatment of epithelial ovarian cancer. Nagoya J Med Sci 68:19-26.

Kim, D., and G. R. Dressler. 2007. PTEN modulates GDNF/RET mediated chemotaxis and branching morphogenesis in the developing kidney. Dev Biol 307:290-9.

Klugbauer, S., A. Jauch, E. Lengfelder, E. Demidchik, and H. M. Rabes. 2000. A novel type of RET rearrangement (PTC8) in childhood papillary thyroid carcinomas and characterization of the involved gene (RFG8). Cancer Res 60:7028-32.

Klugbauer, S., E. Lengfelder, E. P. Demidchik, and H. M. Rabes. 1995. High prevalence of RET rearrangement in thyroid tumors of children from Belarus after the Chernobyl reactor accident. Oncogene 11:2459-67.

Kondo, K., M. Yao, K. Kobayashi, S. Ota, M. Yoshida, S. Kaneko, M. Baba, N. Sakai, T. Kishida, S. Kawakami, H. Uemura, Y. Nagashima, Y. Nakatani, and M. Hosaka. 2001. PTEN/MMAC1/TEP1 mutations in human primary renal-cell carcinomas and renal carcinoma cell lines. Int J Cancer 91:219-24.

Lanzi, C., G. Cassinelli, V. Nicolini, and F. Zunino. 2008. Targeting RET for thyroid cancer therapy. Biochem Pharmacol.

Lecuit, T., and P. F. Lenne. 2007. Cell surface mechanics and the control of cell shape, tissue patterns and morphogenesis. Nat Rev Mol Cell Biol 8:633-44.

Lopez, J. L., J. K. Mouw, and V. M. Weaver. 2008. Biomechanical regulation of cell orientation and fate. Oncogene 27:6981-6993.

Machado, J. C., P. Soares, F. Carneiro, A. Rocha, S. Beck, N. Blin, G. Berx, and M. Sobrinho-Simoes. 1999. E-cadherin gene mutations provide a genetic basis for the phenotypic divergence of mixed gastric carcinomas. Lab Invest 79:459-65.

Marques, F. R., G. A. Fonsechi-Carvasan, L. A. De Angelo Andrade, and F. Bottcher-Luiz. 2004. Immunohistochemical patterns for alpha- and beta-catenin, E- and N-cadherin expression in ovarian epithelial tumors. Gynecol Oncol 94:16-24.

Nikiforov, Y. E., J. M. Rowland, K. E. Bove, H. Monforte-Munoz, and J. A. Fagin. 1997. Distinct pattern of ret oncogene rearrangements in morphological variants of radiation-induced and sporadic thyroid papillary carcinomas in children. Cancer Res 57:1690-4.

Peralta Soler, A., K. A. Knudsen, A. Tecson-Miguel, F. X. McBrearty, A. C. Han, and H. Salazar. 1997. Expression of E-cadherin and N-cadherin in surface epithelial-stromal tumors of the ovary distinguishes mucinous from serous and endometrioid tumors. Hum Pathol 28:734-9.

Rhoden, K. J., K. Unger, G. Salvatore, Y. Yilmaz, V. Vovk, G. Chiappetta, M. B. Qumsiyeh, J. L. Rothstein, A. Fusco, M. Santoro, H. Zitzelsberger, and G. Tallini. 2006. RET/papillary thyroid cancer rearrangement in nonneoplastic thyrocytes: follicular cells of Hashimoto's thyroiditis share low-level recombination events with a subset of papillary carcinoma. J Clin Endocrinol Metab 91:2414-23.

Sheils, O., P. Smyth, S. Finn, E. C. Sweeney, and J. J. O'Leary. 2002. RET/PTC rearrangements in Hashimoto's thyroiditis. Int J Surg Pathol 10:167-8; author reply 168-9.

Smyth, P., S. Finn, S. Cahill, E. O'Regan, R. Flavin, J. J. O'Leary, and O. Sheils. 2005. ret/PTC and BRAF act as distinct molecular, time-dependant triggers in a sporadic Irish cohort of papillary thyroid carcinoma. Int J Surg Pathol 13:1-8.

Smyth, P., S. Finn, J. O'Leary, and O. Sheils. 2003. Real-time analysis of beta- and gamma-catenin mRNA expression in ret/PTC-1 activated and nonactivated thyroid tissues. Diagn Mol Pathol 12:44-9.

Smyth, P., O. Sheils, S. Finn, C. Martin, J. O'Leary, and E. C. Sweeney. 2001. Real-time quantitative analysis of E-cadherin expression in ret/PTC-1-activated thyroid neoplasms. Int J Surg Pathol 9:265-72.

Sundfeldt, K., Y. Piontkewitz, K. Ivarsson, O. Nilsson, P. Hellberg, M. Brannstrom, P. O. Janson, S. Enerback, and L. Hedin. 1997. E-cadherin expression in human epithelial ovarian cancer and normal ovary. Int J Cancer 74:275-80.

Trovisco, V., I. Vieira de Castro, P. Soares, V. Maximo, P. Silva, J. Magalhaes, A. Abrosimov, X. M. Guiu, and M. Sobrinho-Simoes. 2004. BRAF mutations are associated with some histological types of papillary thyroid carcinoma. J Pathol 202:247-51.

Unger, K., H. Zitzelsberger, G. Salvatore, M. Santoro, T. Bogdanova, H. Braselmann, P. Kastner, L. Zurnadzhy, N. Tronko, P. Hutzler, and G. Thomas. 2004. Heterogeneity in the distribution of RET/PTC rearrangements within individual post-Chernobyl papillary thyroid carcinomas. J Clin Endocrinol Metab 89:4272-9.

Yap, A. S., B. R. Stevenson, J. R. Keast, and S. W. Manley. 1995. Cadherin-mediated adhesion and apical membrane assembly define distinct steps during thyroid epithelial polarization and lumen formation. Endocrinology 136:4672-80.